# Study of modulation of immune function of dendritic cells by *Vibrio cholerae* outer membrane protein OmpU

**VINICA DHAR**

***A thesis submitted for the partial fulfillment of the degree of***

***Doctor of Philosophy***

**Department of Biological Sciences**

**Indian Institute of Science Education and Research (IISER) Mohali**

**Sector 81, Knowledge City, SAS Nagar, Manauli PO, Mohali,140306**

**Punjab, India**

**November 2022**

I dedicate this thesis to my parents Sh. Kuldeep Dhar and Smt. Rajni Dhar for their immense support and love.

# Declaration

The work presented in this thesis has been carried out by me under the guidance of Dr. Arunika Mukhopadhaya at the Indian Institute of Science Education and Research, Mohali. This work has not been submitted in part or in full for a degree, diploma, or fellowship to any other university or institute. Whenever contributions of others are involved, every effort has been made to indicate this clearly, with due acknowledgement of collaborative research and discussions. This thesis is a bonafide record of original work done by me, and all sources listed within have been detailed in the bibliography

Vinica Dhar

In my capacity as a supervisor of the candidate's Ph.D. thesis work, I certify that the above statements by the candidate are true to the best of my knowledge.

Dr. Arunika Mukhopadhaya

Associate Professor

Department of Biological Sciences

Indian Institute of Science Education and Research Mohali

# Acknowledgements

First and foremost, I would like to express my deep and sincere gratitude to my supervisor Dr. Arunika Mukhopadhaya for giving me the opportunity to do research and providing invaluable guidance throughout my PhD. Her immense knowledge and plentiful experience have encouraged and inspired me in academic life. I sincerely thank her for helping me in carrying out the research work and refining my scientific writing.

I am grateful to my thesis committee members Dr. Kausik Chattopadhyay and Dr. Rachna Chaba for their continuous suggestions and insightful comments which have helped me in improving my research work. I am extremely thankful to Dr. Kausik Chattopadhyay for allowing me to use his lab resources.

I express my heartfelt thanks to all my lab mates, without them this journey would not have been possible. I sincerely thank my senior Dr. Sanica who guided me and helped me during the beginning of my PhD. I would like to thank my senior Dr. Krishna who has been a constant support, for his encouragement and help in my work. I thank my seniors Dr. Shelly, Dr. Aakanksha, Dr. Deepinder and post doc Dr. Ritam for their guidance and invigorating discussions which helped in shaping me as a better researcher. I would like to appreciate my present lab mates Arpita, Shraddha, Yogesh, Shashi, Dwipjyoti, Sanjeev, Sougata, Tanya, Riya, MS thesis student Pranav and post doc in our lab Dr. Vidushi for being great friends and making lab work lively and exciting. They have always helped me whenever I needed them and working with each of them has been a great experience. I would specially like to thank Arpita and Shashi who have been great companions and have literally stood by me ‘in sickness and in health’. I express my gratitude to Shraddha and Dwipjyoti for their sincere help with my experiments and sharing their knowledge with me. I would like to acknowledge the previous MS thesis students in our lab Raminder, Rhythm, Mohit, Shivansh, Shubham, Shreya and Aavani. Their thoughts and inputs have deeply affected me.

I would like to sincerely thank Dr. Kausik’s past and present lab members Dr. Anand, Dr. Barkha, Dr. Nidhi, Dr. Reema, Dr. Anish, Pratima, Kusum, Mahendra, Shamaita, Sindhoora, Aakanksha, Koyel, Sunil and post doc Dr. Reena for being great friends and sharing the workspace. My PhD has been a cumulative effort and journey shared with each of them and I cannot thank them enough for this.

I would like to express gratitude to my fellow batchmate Dr. Aditya who has been a great friend and immense support. I express thanks to my dear friends Archana and Parul for being there and always inspiring me.

I am forever deeply grateful to my parents and sister for their love, care and constant support. They have been my pillars of strength and it is their encouragement and patience which has made everything possible.

I would like to acknowledge the Department of Biotechnology (DBT) and IISER Mohali for providing me the infrastructure and fellowship to carry out the research work.

Life was meant to be lived, and

Curiosity must be kept alive.

-Eleanor Roosevelt

# List of Illustrations

# List of Figures

# List of Tables

# Abbreviations

TCP: Toxin-coregulated pilus

CTX: Cholera toxin

ZOT: Zonna occludens toxin

ACE: Accessory cholera toxin

MARTX: Multifunctional auto-processing repeats-in-toxin

VCC: *Vibrio cholerae* cytolysin

Omps: Outer membrane proteins

OmpU: Outer membrane protein U

LPS: Lipopolysaccharide

AMPs: Anti-microbial peptides

PAMP: Pathogen-associated molecular pattern

TLR: Toll-like receptor

DC: Dendritic cell

MMP: Mitochondrial membrane potential

AIF: Apoptosis-inducing factor

MAPK: Mitogen-activated protein kinase

IL-6: Interleukin-6

TNFα: Tumour necrosis factor α

NO: Nitric oxide

MyD88: Myeloid differentiation factor 88

NOX: NADPH oxidase

JNK: c-Jun N-terminal kinase

PRR: Pattern recognition receptor

DAMP: Damage-associated molecular pattern

CLR: C-type lectin receptor

RLR: RIG-I-like receptor

NLR: Nucleotide-binding and oligomerization domain (NOD)-like receptor

APCs: Antigen-presenting cells

MHC: Major histocompatibility complex

ROS: Reactive oxygen species

IKK: IκB kinase

PI3K: Phosphoinositide-3-kinase

PKC: Protein kinase C

NFκB: Nuclear factor κB

IFN: Interferon

TGF: Transforming growth factor

ERK: Extracellular signal-regulated kinase

ELISA: Enzyme-linked immunosorbent assay

BMDC: Bone-marrow derived dendritic cell

PMA: Phorbol myristate acetate

ASC: Apoptosis-associated speck-like protein containing CARD domain

AIF: Apoptosis inducing factor

NOX: NADPH oxidase complex

ETC: Electron transport chain

mitoROS: Mitochondrial reactive oxygen species

DCFDA: Dichlorofluorescein diacetate

# Contents

# I. Introduction

# It is often said that 'Trust your gut; if you feel something is wrong, there usually something is'

# *Vibrio cholerae* is one such organism which can make your gut sick.

## 1.1 *Vibrio cholerae,* the causal organism of cholera

*Vibrio cholerae* is a motile Gram-negative, flagellated comma-shaped bacterium responsible for the human diarrhoeal disease cholera [1]. In 1853, John Snow, one of the founders of modern epidemiology, first time described that cholera, one of the most deadly disease for centuries, spreads through contaminated water [2]. Filippo Pacini, an Italian anatomist, in 1854 examined that a vibrion is associated with the intestines and stools of cholera affected individuals and also described the disease as an enormous loss of electrolytes from the intestines [3]. Later, Robert Koch first isolated the bacterium *Vibrio cholerae* in 1884 [4].

*V. cholerae* thrives in aquatic environment and the mode of transmission is mainly through contaminated food and water [5]. There are over 200 serogroups of *Vibrio cholerae* but only serogroups O1 and newly emerged O139 are found to be associated with pandemics and cholera disease [6]. *V. cholerae* serogroup O1 is further divided into biotypes 'classical' and 'El Tor' based on the susceptibility to Polymyxin B, phage resistance and other phenotypic properties [7].

Scientific Classification:

Species: *Vibrio cholerae*

Genus: *Vibrio*

Family: Vibrionaceae

Order: Vibrionales

Class: Gammaproteobacteria

Phylum: Proteobacteria

## 1.2 Pathogenesis of cholera

*V. cholerae* infection spreads through contaminated food and water mainly due to improper sanitation and disseminates through the faecal-oral route [8]. Infection starts by ingestion

of contaminated food or water by oral route [9]. Following ingestion, the bacteria must survive the acidic pH of the stomach and then colonize in the intestinal epithelia by penetrating the mucus lining that coats the epithelium [10]. *V. cholerae* biofilms harbour resistance to acid in the stomach and thus require low infection doses [9, 11]. The adherence of bacteria to the intestinal epithelia precedes the multiplication and colonization of bacteria in the gut [12]. Simultaneously, several factors are released from the bacteria which mediate these colonization events, and eventually, lead to formation of microcolonies in the villi and crypts of intestines [13]. Following the formation of microcolonies in the gut, *V. cholerae* secretes various toxins which manifest the disease symptoms leading to acute diarrhoea [14, 15]. Finally, the bacteria detach and disseminate throughout the small intestines [9, 10].

The suckling mouse and the adult rabbit model of the cholera disease have shown the importance of various *V. cholerae* gene products in the pathogenesis of cholera including the differential expression of 524 genes in the classical and El Tor strains [16-18]. Several *V. cholerae* virulence factors have been studied including Toxin-coregulated pilus (TCP), cholera toxin (CTX), zona occludens toxin (ZOT), accessory cholera toxin (ACE), multifunctional auto-processing repeats-in-toxin (MARTX), *V. cholerae* cytolysin (VCC) and many more, which facilitate the pathogenesis of *V. cholerae* [19-26]. Additionally, various outer membrane proteins of *V. cholerae* can function as virulence factors playing crucial roles in bacterial adhesion and infection.

### 1.3 Outer membrane proteins of *Vibrio cholerae*

In addition to the virulence factors and toxins, *V. cholerae* harbours several outer membrane proteins which facilitate the survival of bacterium and also aid in infection in certain cases. So far, 15 outer membrane proteins have been reported in *V. cholerae* and their role in bacteria is highlighted in table 1.

**Table 1: Outer membrane proteins of *V. cholerae***

| **Outer membrane proteins (Omps)** | **Function** |
|---|---|
| OmpA | Heat modifiable protein [27] |
| OmpH | Unfolded protein binding [28] |

| | |
|---|---|
| OmpF-like protein | Porin activity [29] |
| OmpK | Porin; nucleoside transmembrane transporter activity; receptor for broad-host range virbiophage [30] |
| OmpW | Transports small hydrophobic molecules and iron; confers salt tolerance and helps in osmoadaptation [31-33] |
| OmpS | Maltoporin; inducible by maltose and trehalose; λ phage receptor [34, 35] |
| OmpV | Porin; heat-shock protein; immunogenic; protein binding and bridging [34, 36] |
| OmpR | Transcriptional regulator; forms hydrophobic channels; osmolarity sensor [37, 38] |
| EnvZ | Transcriptional regulator; osmolarity sensor; histidine kinase/phosphatase [38, 39] |
| OmpX | Osmo-regulated; non porin; helps in adhesion; iron homeostasis [34] |
| OmpU | General diffusive porin; upregulated in the presence of glucose, bile, acid stress; immunogenic, could be a potential virulence factor [40, 41] |
| OmpT | Porin activity; upregulated in the presence of iron; virulence factor [40, 41] |
| TolC | Porin activity; VP3 phage receptor; efflux transmembrane transporter activity; bile resistance [42-44] |
| IrgA | Porin; iron-regulated; virulence protein [44] |
| VCA1008 | Anion-selective porin [45, 46] |

### 1.4 Role of porins in bacterial pathogenesis and their immunological role

As evident from the list of outer-membrane proteins of *V. cholerae*, quite a few of them are porin in nature. Porins are one of the major class of proteins in the outer-membrane of

Gram-negative bacteria. The bacterial outer membrane consists of lipopolysaccharide (LPS), phospholipids, outer membrane proteins and porins as shown in illustration 1.

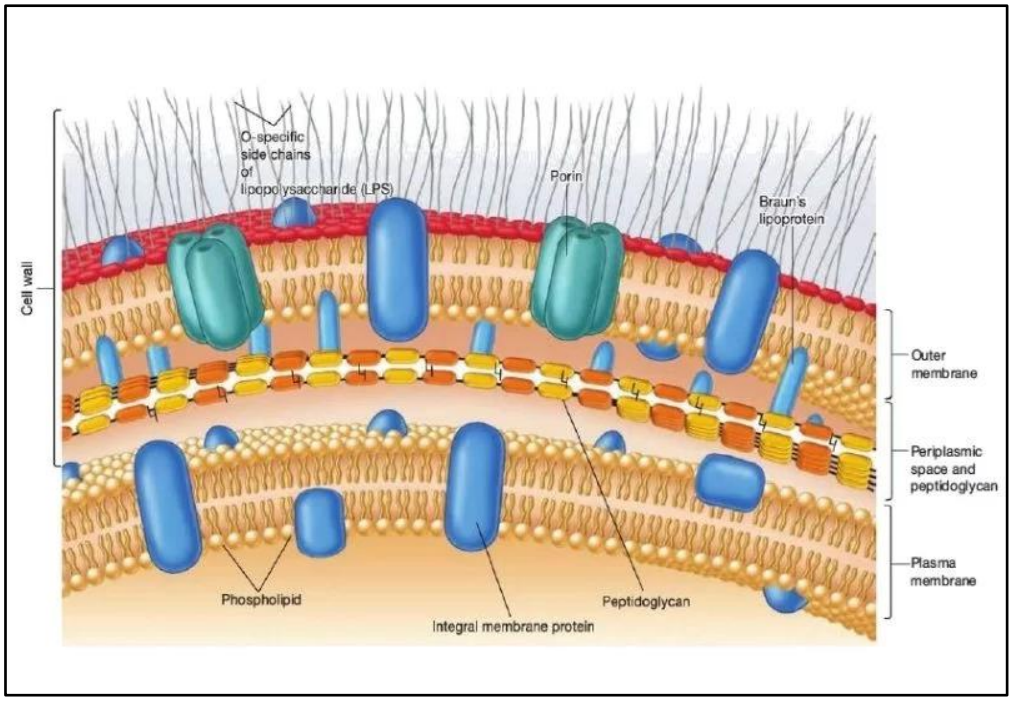


**Illustration 1: Gram-negative bacterial cell envelope**

***(Source: www.microbiologynote.com)***

*The Gram-negative bacterial outer membrane harbours several membrane proteins, lipopolysaccharide (LPS) and lipoproteins. Porins (shown in green) form a major part of the outer membrane proteins.*

Porins are membrane spanning hydrophilic channels with around 1 nm pore size which allow non-specific or specific diffusional movement of molecules across the membrane. They generally are monomeric or trimeric structures depending on their conformation and physicochemical properties with each monomer containing 16 or 18 β-sheets forming the barrel [47]. A prototypic porin structure contains an eyelet region in the middle of the β-barrel formed by the loop inserted into the lumen as shown in illustration 2. This region forms a constriction and restricts the passage of molecules [48].

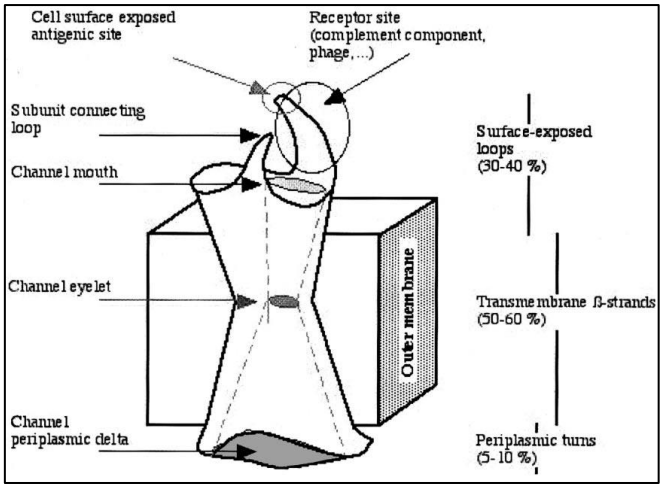


**Illustration 2: Representation of monomeric subunit of prototype porin**

***(Source: W. Achouak et al. / FEMS Microbiology Letters 199 (2001))***

*The structure of outer membrane porin is formed by β-barrel which forms the channel and a constriction in the middle of channel called eyelet region.*

In addition to acting as channels, porins assist in bacterial pathogenesis by helping in adhesion and modulating the host cell responses. *Klebsiella* porin OmpK35 confers resistance against AMPs to the bacteria and aid in survival [49]. Moreover, *E. coli* porins OmpF, OmpC and TolC, and PorB from *N. gonorrhoeae* and *N. meningitidis* have been studied to impart the bacteria with resistance to different antibiotics and assist in infection [50-54]. OmpA porin from different Gram-negative bacteria such as *Klebsiella, Neisseria and E. coli* help the bacteria in adhering to various epithelial and immune cells leading to invasion into the host [55-57].

Several porins from *Neisseria* and *Salmonella* have shown host immunomodulatory properties. PorB (*Neisseria*), OmpC and OmpF (*Salmonella*) porins act as PAMPs and were recognized by TLRs [58, 59]. These porins further induced the expression of co-stimulatory molecules and assisted in maturation of dendritic cells (DCs) [59, 60]. OmpC and OmpF *Salmonella* porins also generated antibody titre in mice model [61]. Also, porins from *Shigella* were shown to be recognized by TLR2, induced pro-inflammatory cytokine production and further, polarized the T-cells towards Th1-type profile [62].

In addition to immune responses, some porins contribute to cell death and cytotoxic responses which further mediate the infection and pathogenesis. *Neisserial* porin PorB induced apoptosis in the host cells via disruption of mitochondrial membrane potential (MMP) whereas

*Acinetobacter* porin OmpA was reported to induce the apoptosis inducing factor (AIF) and caspase-dependent apoptosis in host cells [63-65]. These studies suggest that porins are critical in bacterial infections and affect the host immune responses as well.

### 1.5 OmpU: Role in *Vibrio species*

OmpU is one of the major conserved outer membrane proteins present across several pathogenic *Vibrio* species [34]. It plays diverse functions ranging from having porin activity to acting as an immunogen in different host organisms.

OmpU has been characterized as a key virulence factor in several aquatic pathogenic *Vibrio* species. In *V. splendidus* (LGP32), OmpU conferred resistance to oyster cationic anti-microbial peptides (AMPs), and further helped the pathogen to attach and invade the oyster immune cells [66].

In *V. alginolyticus*, OmpU was also reported to play a role in iron metabolism in the bacteria [67]. Further, in *V. mimicus*, OmpU was found to function as an adhesin in host cells [68].

OmpU from several *Vibrio* species can also act as pathogen-associated molecular pattern (PAMP) and induce immune responses. OmpU from *V. alginolyticus* and *V. harveyi* showed antibody response against the pathogenic infection in fish *Lutjanus erythropterus* and *Scophthalmus maximus,* respectively showing potential as a vaccine candidate [69, 70]. A subunit OmpU vaccine also generated a strong antibody response against *V. mimicus* in yellow catfish [71]. These studies highlight the importance of OmpU as a crucial determinant of pathogenicity in the aquatic fauna and as a potential vaccine candidate against several pathogenic *Vibrio* species.

Moreover, there are several studies suggesting the role of OmpU in the pathogenesis of human pathogenic *Vibrio* species. *V. vulnificus* OmpU helps in adhesion to the host cells via fibronectin and aids in cytotoxic responses of the bacteria and further, immunization with OmpU lead to the generation of IgM and IgG antibody responses in mice model [72, 73]. Gulati et al, from our laboratory reported that *V. parahaemolyticus* OmpU acts as a PAMP for the host immune cells (monocytes and macrophages) and activates MyD88-IRAK1-MAPK-dependent signalling leading to the activation of NFκB and AP-1 transcription factors [74]. Additionally, the authors have showed that *V. parahaemolyticus* OmpU was recognised by TLR1/2 and TLR2/6 in macrophages while in monocytes by TLR1/2 only [74]. The role of OmpU from

different human pathogenic *Vibrio* species such as, *V. cholerae*, *V. parahaemolyticus* and *V. vulnificus* are summarised in table 2.

**Table 2: Role of OmpU in the pathogenesis of human pathogenic *Vibrios***

| **OmpU** | | |
|---|---|---|
| ***V. cholerae*** | ***V. vulnificus*** | ***V. parahaemolyticus*** |
| Aids in bile and AMP resistance [75, 76] | Functions as an adhesin helping in bacterial pathogenesis [72] | Acts as a PAMP and activates monocytes and macrophages [74] |
| Recognized as a PAMP by monocytes and macrophages [77, 78] | Generates protective antibody response in murine model [73] | Single domain antibodies generated showing immunotherapeutic potential [79] |
| Induces caspase-independent cell death in the host cells [80] | | |
| Characterized as a biomarker for the epidemic *V. cholerae* strains [81] | | |

### 1.6 Host immunomodulation by *Vibrio cholerae* OmpU

*V. cholerae* OmpU is a 38 kDa outer membrane porin protein which exists as an oligomeric homotrimer (mol. wt-114 kDa). It has a 16 transmembrane β-sheet structure with a non-canonical N-terminal coil penetrating the pore lumen further acting as a gate in the constriction region and making the pore more restrictive to small molecules [82, 83]. The expression of OmpU is under the control of ToxR regulon which is the major transcriptional activator for most of the *V. cholerae* virulence factors. In the salt free environment, OmpU constitutes 60% of the total outer membrane proteins and its expression increases in the presence of bile, thus, underlining its role in bacterial pathogenesis [34]. So far, it is known

that OmpU help in the survival of the bacteria in the gut by helping in bile and AMP resistance [75, 76].

As previously discussed, OmpU from *Vibrio* species such as *V. mimicus*, *V. parahaemolyticus* and *V. vulnificus* were reported to activate different cells of the immune system and augment the production of various inflammatory mediators. Our laboratory has shown that *V. cholerae* OmpU induces the activation of monocytes and macrophages leading to the production of pro-inflammatory mediators such as IL-6, TNFα and nitric oxide (NO) [77]. Further, OmpU is recognized by TLR1/2 heterodimer in these innate immune cells and activates MyD88-dependent signalling. This signalling leads to the activation and translocation of p65 sub-unit of NFκB transcription factor to the nucleus which results in the transcription of the genes important for pro-inflammatory responses [84]. In contrast, OmpU also induces LPS tolerance by attenuating the LPS-mediated TLR signalling and up-regulating the expression of negative regulators of TLR signalling upon LPS stimulation [85]. We have also shown that besides TLR signalling, the scavenger receptor CD36 also recognizes OmpU as a PAMP and leads to the NADPH oxidase (NOX)-mediated ROS generation in macrophages. Further, NOX-mediated ROS leads to the activation of c-Jun N-terminal kinases (JNK) which contributes to the inflammatory cytokine production [78].

Furthermore, our laboratory also established that *V. cholerae* OmpU induces a pathway of cell death in the host. OmpU translocates to the mitochondria of the host cells disrupting the mitochondrial membrane potential (MMP) and prompting the release of AIF. Further, AIF translocate to the nucleus and mediates caspase-independent programmed host cell death [80]. These observations indicated that OmpU plays a pivotal role in host immunomodulation during *V. cholerae* infection.

## 1.7 Role of inflammation in host immune responses

Inflammation is the first line of defence of the innate immune system against any pathogenic encounter to avert or control the infection. Innate immune system employs numerous ways to deter the microbial invasion from the early onset (0-12 h) via the epithelial barriers, killing by phagocytes such as neutrophils, macrophages, dendritic cells and natural killer cells (NK cells), neutralization or killing by complement proteins and further recognition by pattern recognition receptors (PRRs) [86, 87].

At the tissue level, the process of inflammation starts at the site of entry of the pathogen or injury leading to the cardinal signs of inflammation- pain, swelling, redness, heat and loss of function [88]. These signs are a result of certain cellular events which mediate pathogen clearance or cueing the activation of adaptive immune response. The cellular events in inflammation (in intestinal region) involves following:

**i) Disruption of anatomical barriers**

The pathogen or injury can disrupt/cross the anatomical barriers (physical, chemical or biological) of the innate immune system. Epithelial surfaces present at all the entry points are highly effective as protective barriers and are specialised in recognising the foreign microbes or particles. As the pathogen disrupts the epithelial barrier it is detected by various tissue-resident innate immune cells (macrophages or mast cells or DCs) which either sense the pathogen-associated molecular patterns (PAMPs) or damage-associated molecular patterns (DAMPs) through PRRs or phagocytose the pathogen [89]. The damaged host cells along with the tissue-resident immune cells release various mediators of inflammation for example, histamines, leukotrienes, kinins and many more which help in both limiting the pathogen and recruitment of specialised cells to the site of infection [90].

**ii) Vasodilation and increased vascular permeability**

For the recruitment of different leukocytes from blood vessels to the site of infection the endothelial lining of the blood vessels gets dilated and the blood flow is increased due to the action of pro-inflammatory mediators (various chemokines and cytokines) which leads to redness and swelling of the tissue [91]. Cytokines secreted by the tissue resident innate immune cells and intestinal epithelial cells cause vasodilatation.

**iii) Leukocyte extravasation and transmigration**

The leukocytes e.g., neutrophils adhere to the endothelial lining using vascular cell adhesion molecules e.g., VCAM-1, then insert pseudopods into the vasculature and through diapedesis migrate out of the blood vessels [92].

**iv) Chemotaxis and pathogen killing**

After transmigration into the interstitial fluid, leukocytes migrate towards the site of infection or injury following a chemical gradient, that is, chemotaxis. These chemo-attractants are chemokines produced from the cells in the vicinity of infection. These leukocytes mediate pathogen killing via phagocytic uptake of the

pathogen or degranulation (releasing pre-formed granules containing histamines, proteases and proteoglycans) [92, 93].

All these events of inflammation attempt to control or kill the pathogen. Cytokines and chemokines play a major role in these inflammatory responses. Different PRRs on the immune cells recognise different PAMPs and mediate the downstream signalling which leads to activation of different effector cells and production of an array of pro-inflammatory mediators [90]. PRRs are a set of receptors present on or within the cells which recognize specific conserved patterns or microbial components (PAMPs) and initiate definite signalling pathways leading to the distinct immune response against pathogen [89]. PRRs are categorized into different types such as Toll-like receptors (TLRs), C-type lectin receptors (CLRs), RIG-I like receptors (RLRs) and NOD-like receptors (NLRs). Based on their structure, they recognise different categories of PAMPs and they activate distinct signalling cascades. The stimulation of inflammatory pathways by PRRs culminate in the activation of several transcription factors e.g., NFκB and AP-1 which transcribe the genes involved in the cytokine/chemokine production, molecules responsible for effector cell activation and production of other pro-inflammatory mediators [94]. These pro-inflammatory signals result in acute inflammation leading to pathogen clearance and further activate the adaptive immune system, if the infection persists.

### 1.8 Dendritic cells: Intermediaries between innate and adaptive immune system

Dendritic cells (DCs) are specialized antigen-presenting cells (APCs) derived from bone-marrow precursors which home to different tissues and in the steady state reside as immature DC with high antigen capture ability [95]. Immature DCs capture the antigen while circulating in the blood stream or in specific tissues as tissue-resident DCs. While capturing and processing the antigen DC undergoes maturation. Signals through innate receptors are important for DC maturation. Mature DCs help in induction of T cell immune responses ultimately leading to generation of immunologic memory [96]. The phenotypic features of immature and mature DCs are highlighted in illustration 3. The mature DCs migrate to the draining lymph node/secondary lymphoid organs to present the antigen to the effector cells e.g., T-cells, B-cells which further initiate the adaptive responses. DCs also can also induce T cell tolerance [95]. Thus, DCs act as critical link between the innate and adaptive immune responses.

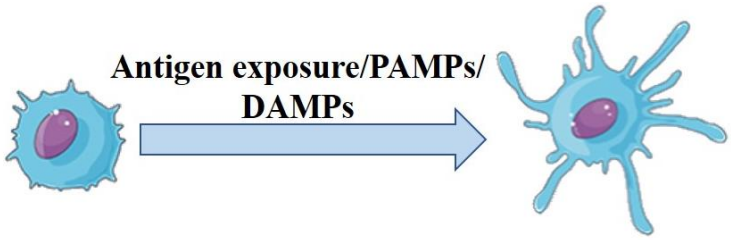


**Immature DC**

Antigen uptake/processing

- High endocytic receptors
- High Fc receptors
- High CD68
- Low MHC II
- Low CD40, CD80 CD86

**Mature DC**

Antigen presentation

- Low endocytic receptors
- Low Fc receptors
- High MHC II
- High IL-12
- High CD40, CD80 CD86

**Illustration 3: Molecules involved in DC maturation.**

*The maturation of DCs involves high expression of receptors such as MHC II, CD40, CD80 and CD86 on the cell surface, and increased antigen presentation capability of DCs.*

DCs harbour several receptors which aid in capturing the antigen in the immature state and help in the activation of effector cells in the mature state. These can be categorized as endocytic receptors e.g., DEC-205, PRRs e.g., TLRs, CLRs and scavenger receptors (CD36); Fcγ receptors e.g., CD32, CD64; and various complement receptors e.g., CD11b and CD88 [97, 98]. These receptors play distinct functions that assist in DC heterogeneity and induction of discrete immune responses as shown in table 3.

**Table 3: Receptors on DCs and their functions**

| DC receptors | Functions |
|---|---|
| Endocytic receptors (DEC-205, Dectin-1, CD206) | Antigen uptake, processing of the antigen and activation of signalling mediators [99, 100] |
| PRRs (TLRs and CLRs) | Antigen uptake, induction of immune responses, antigen processing and upregulation of molecules for antigen presentation (e.g., cytokines and co-stimulatory molecules) [100, 101] |
| Co-stimulatory receptors (B7 family) | Providing the 'second signal' for survival during antigen presentation [97] |

| | |
|---|---|
| Fcγ receptors (CD64, CD16a) | Antigen internalization, processing and aid in presentation to $CD4^+$ T-cells [98] |
| Complement receptors (CR3, CR4) | Antigen opsonisation for internalization and processing [100, 102] |

### 1.9 Objectives of the study

As highlighted in the previous sections, OmpU plays a role in the pro-inflammatory responses in innate immune cells such as monocytes and macrophages. Further, as DCs are crucial for the activation of host adaptive responses, therefore, based on this knowledge our overall objective is to understand how OmpU modulates DC-mediated immune responses. Under this objective we have following three aims:

**AIM 1:** To probe whether and how OmpU induces the activation of DCs.

**AIM 2:** To explore whether inflammasome complex is involved in DC activation.

**AIM 3:** To investigate whether there is any role of ROS in OmpU-mediated DC activation.

#### AIM 1: To probe whether and how OmpU induces the activation of DCs

Under the aim 1 we have two specific aims:

**Specific aim 1:** Whether OmpU act as a PAMP and activate PRR to induce DC activation?

**Specific aim 2:** To understand the signalling molecules involved in OmpU-mediated activation of DCs.

#### AIM 2: To explore whether inflammasome complex is involved in OmpU-mediated DC activation.

Under the aim 2 we have two specific aims:

**Specific aim 1:** Whether and which inflammasome complex is involved in OmpU-mediated DC activation?

**Specific aim 2:** How the inflammasome complex is activated in DCs in response to OmpU?

**AIM 3: To investigate whether there is any role of ROS in OmpU-mediated DC activation.**

Under the aim 3 we have two specific aims:

**Specific aim 1:** Whether OmpU-induces ROS generation in OmpU-activated DCs and whether ROS play any role in activation of DCs?

**Specific aim 2:** To understand the signalling mechanism underlying ROS generation.

# II. Materials and Methods

### 2.1 Purification of recombinant OmpU from *E. coli*

OmpU was purified from *E. coli* origami cells as previously described by Khan et al [103]. Briefly, the OmpU gene was cloned in pET-14b vector (EMD Millipore, USA) and transformed into *E. coli* origami cells. The ampicillin-resistant transformed colonies were inoculated (2%) in Luria broth (#M575 HiMedia, India) and grown at 37 $^{o}$C till $O.D_{600}$ reached 0.5-0.6. The culture was induced by adding 1mM IPTG (#BC0168 BR Biochem, India) and incubated for 3 h at 37 $^{o}$C. The bacterial cells were further pelleted at 2000 x g for 30 min at 4 $^{o}$C and lysed using lysis buffer (50 mM Tris, 50 mM NaCl, 0.1% Triton-X, pH 7.5) containing bacterial protease inhibitor cocktail (#P8465, Sigma Aldrich, USA) (1 litre bacterial culture resuspended in 10 ml lysis buffer and 100 µl of bacterial protease inhibitor cocktail). The cell suspension was sonicated using Misonix sonicator (QSonica, Newton, USA) at 25-30 A for 15-20 min with 15 sec on-20 sec off pulse and then centrifuged at 18000 x g for 30 min at 4 $^{o}$C in Oakridge tubes to obtain the inclusion bodies. The inclusion bodies were further washed using phosphate-buffered saline (PBS- 137 mM NaCl, 2.7 mM KCl, 10 mM $Na_2HPO_4$, 1.8mM $KH_2PO_4$ pH-7.4) with 100 mM NaCl at 18000 x g for 15 min at 4 $^{o}$C. The pelleted inclusion bodies were solubilized in 8 M urea (10 ml 8 M urea for 1 litre bacterial culture) and incubated for 30-40 min at room temperature. Subsequently, the solubilized inclusion bodies were centrifuged at 18000 x g for 10 min at 4 $^{o}$C to remove the insoluble debris.

The solubilized supernatant containing the recombinant OmpU protein was further purified by Nickel-NTA affinity chromatography. Ni-NTA resin (Profinity$^{TM}$ IMAC resin, Bio-Rad, USA) (5 ml) was packed in a column and washed using PBS. The column was equilibrated with 10 ml of 8 M urea in PBS and then loaded with the solubilized inclusion bodies. After incubation for 30 min at room temperature, the flowthrough was collected and column was further washed using 20 ml of 8 M urea in PBS with 20 mM imidazole (#RM1864 HiMedia, India). The bound protein was eluted using 300 mM imidazole in 8 M urea in PBS and four fractions including one of volume 5 ml followed by three fractions of 1 ml each were collected. The denatured OmpU protein in the fractions was further refolded in refolding buffer (10% glycerol, 0.5% LDAO (#40231 Sigma Aldrich) in PBS) using the rapid dilution method. 1 ml of denatured OmpU protein was added to 10 ml of refolding buffer in 50 µl instalments and was incubated overnight at 4 $^{o}$C. The refolded protein was centrifuged at 18000 x g for 15 min at 4 $^{o}$C to remove the aggregates if any and concentrated using 10 kDa centrifugal filters (Amicon, MerckMillipore, USA) (10 ml protein was concentrated to 2 ml).

The refolded concentrated protein was further purified using size exclusion chromatography. Sephacryl S-200 prepacked column (GE Life Sciences, USA) (1.6*60 cm, bed volume-120 ml) was equilibrated with 120 ml of buffer (10 mM Tris, 10 mM NaCl, 0.5% LDAO, pH 8) and loaded with the protein sample at a flow rate of 1 ml/min. 2 ml fractions of final eluted protein were collected. The protein concentration was estimated using Bradford assay and aliquots were stored in -20 $^{o}$C.

### 2.2 Bradford's Assay for estimation of protein concentration

The Bradford's protein assay is a spectroscopic colorimetric method to measure the concentration of a protein in solution. The binding of protein with the Coomassie dye present in the Bradford's reagent under acidic conditions leads to a change in colour from brown to blue. Protein standards for Bradford's assay were prepared by serially diluting 2 mg/ml of Bovine serum albumin (BSA) (#MB063 HiMedia, India) in Tris buffer (10 mM Tris, 10 mM NaCl, 0.5% LDAO, pH-8).

For estimation, 5 µl of protein sample (standard or test) was added to 95 µl of Bradford's reagent and incubated in dark for 10 min. The absorbance was measured at 595 nm using iMark Microplate Absorbance Reader (Bio-Rad, USA) and a standard curve was obtained by plotting the absorbance on y-axis and the standard concentrations of BSA on the x-axis. The protein concentration of the test samples was calculated relative to the absorbance of BSA obtained from the curve.

### 2.3 Sodium dodecyl sulphate-Polyacrylamide gel electrophoresis (SDS-PAGE) for protein separation

Discontinuous SDS-PAGE was used to separate the proteins based on their molecular weights ranging from 5-250 kDa. The following components were used in SDS-PAGE:

1) 30% acrylamide solution (Solution A)- 29.2 g of acrylamide and 0.8 g of bis-acrylamide were mixed in 50 ml of Milli-Q water and allowed to dissolve on a magnetic stirrer followed by volume make up to 100 ml.
2) Resolving gel buffer (Solution B)- 1.5 M Tris-Cl, 0.4% SDS, pH-8.8
3) Stacking gel buffer (Solution C)- 0.5 M Tris-Cl, 0.4% SDS, pH-6.8

4) Running Buffer- 25 mM Tris, 192 mM glycine, 0.1% SDS, pH-8.3
5) 5x sample loading dye- 250 mM Tris-Cl pH 6.8, 10% SDS, 30% glycerol, 5% 2-mercaptoethanol, 0.02% bromophenol blue

**Table 4: Volumes of Buffers used for SDS-PAGE.**

| Components | Stacking (ml) | Resolving (10%) (ml) | Resolving (12.5%) (ml) |
|---|---|---|---|
| Solution A | 0.45 | 3 | 3.75 |
| Solution B | - | 2.25 | 2.25 |
| Solution C | 0.75 | - | - |
| Milli-Q water | 1.8 | 3.75 | 3 |
| 10% ammonium persulphate (APS) | 0.05 | 0.05 | 0.05 |
| TEMED | 0.005 | 0.005 | 0.005 |

These buffers were mixed according to the volumes mentioned in table 4 to obtain different percentages of gels. 1x sample loading dye was added to the protein samples and incubated at 65 $^{o}$C for 10 min. This was followed by loading the samples into the wells of SDS-PAGE and the protein bands were resolved by applying voltage of 90 V.

### 2.4 Primary cells and culture conditions

All the cells were cultured in a 5% $CO_2$ humidified incubator (#CO170R-230-1000, Eppendorf, Germany) at 37 $^{o}$C. Mouse bone marrow-derived dendritic cells (BMDCs) were cultured in RPMI 1640 (#31800-022 Life Technologies, USA) medium supplemented with 10% (v/v) heat-inactivated foetal bovine serum (FBS) (#16000044, Life Technologies, USA), 1.5 mM L-glutamine, 100 U/ml penicillin, 100 U/ml streptomycin (#17-602E Lonza, Switzerland), that is, complete RPMI media, supplemented with 1% β-mercaptoethanol (#M3148 Sigma Aldrich), 0.1 mM non-essential amino acids (NEAA) (#11140-050 Life Technologies) and

1mM sodium pyruvate (#11360-070 Life Technologies) (**Supplemented complete RPMI media**).

### 2.5 Isolation of bone marrow cells from mouse

6-8 weeks old male or female BALB/c or C57BL/6 (The Jackson laboratory) mice were obtained from the Small Animal Facility for Experimentation (SAFE), IISER Mohali after the approval from our Institutional Animal Ethics Committee (IISERM/SAFE/PRT/2016-2022/004, 005, 010, 001, 015, 016, 012, 011, 013, 018, 021). The mice were euthanized by cervical dislocation and the femur/tibia bones were cut from the hip joint. Muscles attached to the bones were removed and femur was dislocated slightly to break the knee joint. Both femur and tibia were cleaned and washed using 1x PBS followed by sterilization in 70% ethanol. Then, the bones were once washed using sterile 1x PBS and transferred in sterile supplemented RPMI media on ice. Finally, the epiphyses of the bones were cut and the bone marrow cells were flushed out using a syringe. The media containing bone marrow cells was centrifuged at 1100 x g at 4 $^{o}$C to pellet the cells. The pellet was subjected to RBC lysis by using ACK lysis buffer (2-3 ml) for 5 min at room temperature followed by addition of RPMI media to stop the lysis. Then the cells were pelleted, resuspended in supplemented complete RPMI media and plated according to the experiment.

### 2.6 Differentiation of bone marrow cells into BMDCs

The bone marrow cells plated in supplemented complete RPMI were differentiated to bone marrow-derived DCs (BMDCs) using murine granulocyte-macrophage colony stimulating factor (GM-CSF) (#AF-315-03 Peprotech, USA). The cells were supplemented with 10 ng/ml GM-CSF and kept at 37 $^{o}$C in a 5% $CO_2$ environment. After every 2 days, the floating cells were removed and fresh supplemented complete RPMI with GM-CSF was added to the cells. At the 7$^{th}$ day of differentiation, the cells were suspended in fresh supplemented RPMI media and analysed for the expression of differentiation marker CD11c as in illustration 4. Increased CD11c expression in GM-CSF treated cells was observed compared to the untreated cells indicating differentiation into BMDCs and used for further experiments.

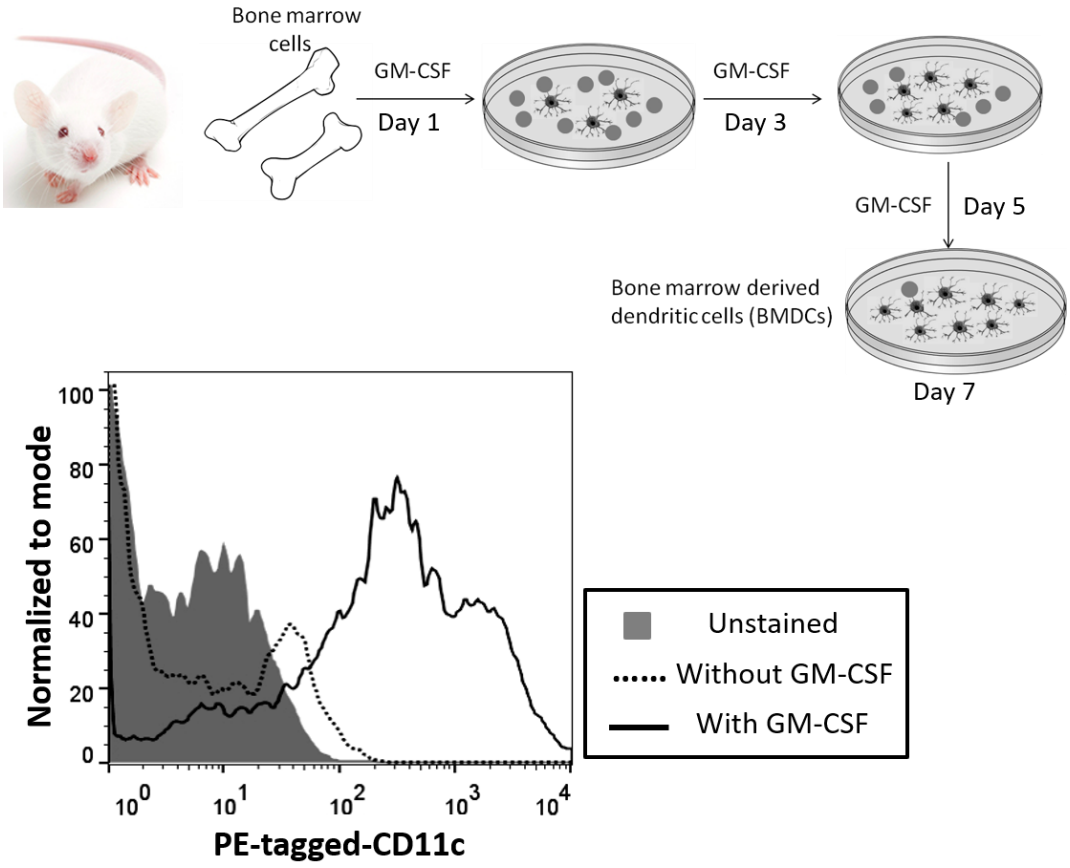


**Illustration 4: Differentiation protocol for mouse bone marrow derived dendritic cells and the CD11c levels obtained.**

*The bone marrow cells were differentiated into DCs using GM-CSF (Granulocyte monocyte-colony stimulating factor) for 7 days, supplementing the media with GM-CSF on alternate days. After 7 days, the cells were stained for surface expression of CD11c and analysed by flow cytometry to check the population of differentiated cells (CD11c+ cells).*

### 2.7 Isolation of Splenic DCs from mouse

Spleen was isolated from mouse and ballooned with 400 U/ml Collagenase D (#11088866001, Roche Diagnostics, Switzerland) in 5 ml calcium-magnesium free HBSS (#14175-095, ThermoFisher Scientific, USA). Cells were incubated at 37 °C for 25 min. The reaction was stopped by adding 100 µl of 0.5 M EDTA to the cells and incubating at 37 °C for 5 min. The cells were harvested by flushing and the cell suspension was then passed through a 0.45 µm filter into 5 ml cold RPMI media to obtain a single-cell suspension. Cells were washed with cold 1x PBS and centrifuged at 1500 rpm for 5 min at 4 °C to obtain a pellet. The pellet was resuspended in 3 ml 30% BSA (#A9576, Sigma Aldrich), and 1 ml 1x PBS was carefully

layered on top. Cells were centrifuged at 620 x g, at 12 °C without a break for 30 min. $CD11c^+$ enriched cells at the interface of BSA and PBS were collected and washed with 1x PBS. Further, purified splenic DCs were isolated by positive selection method using an anti-$CD11c^+$ mouse dendritic cell MACS purification kit (#130-097-059, Miltenyi Biotec, Germany).

According to the kit, $10^7$ cells were resuspended in 40 µl of MACS buffer (0.5% FBS and 2 mM EDTA in 1x PBS) and 5 µl of anti-$cD11c^+$ microbeads were added to it followed by incubation at 4 °C for 20 min. Cells were washed with MACS buffer and then resuspended in 500 µl of MACS buffer. MS MACS column was prepared for loading the cells by washing the column with MACS buffer placed on a magnetic stand. Following loading the cells onto the column, the cells were washed using 500 µl of MACS buffer thrice and removed from the magnetic stand. The cells were suspended in 2.5 ml of MACS buffer and eluted from the column using plunger in a 15 ml tube. The eluted cells were washed using MACS buffer and suspended in supplemented complete RPMI media and plated according to the experiment.

### 2.8 Whole cell lysate preparation

BMDCs were harvested and washed using cold 1x PBS. The cells were centrifuged at 1100 x g for 5 min at 4 $^oC$ and resuspended in 80 µl lysis buffer (150 mM Tris HCl pH 8, 150 mM NaCl, 0.1% SDS, 0.1% Triton X-100) containing mammalian protease inhibitor (1:100). The cells were sonicated at 10 A with three 4 sec pulses followed by centrifugation at 13000 x g for 30 min at 4 $^oC$. The supernatant was collected as the whole-cell lysate and the protein content was estimated using Bradford's reagent. It was stored at -80 $^oC$ for further use.

### 2.9 Immunoblotting for the detection of desired proteins

The samples were resolved on a 10% or 12.5% SDS-PAGE gel and the separated proteins were transferred onto polyvinylidene fluoride membrane (PVDF) (#SVFX8301XXXX101 MDI Membrane Technologies, India) at 80 V for 80 min. The membrane blot was blocked with 5 % bovine serum albumin (BSA) in TBST buffer (20 mM Tris, 150 mM NaCl, 0.1% Tween-20, pH 7.6) for 1 h on shaking. The blot was subsequently probed for the desired proteins using different primary antibodies. The blot was incubated in the primary antibody diluted in TBST buffer for 3 h at RT on shaking or overnight at 4 $^oC$ followed by washing for 1 h using the TBST buffer. Then the HRP-conjugated secondary antibody diluted in TBST was added to the

blot and incubated for 1 h at RT. Following washing for 1 h, the blot was developed using Clarity$^{TM}$ Western ECL chemiluminescent HRP substrate (#170-5060 BioRad) and visualized in ImageQuant LAS4000 (GE Healthcare Bio-Sciences, Sweden). The same blot was used to probe for different proteins by stripping off the bound antibodies using warm stripping buffer (15 g glycine, 1 g SDS, 10 ml Tween 20 in 1 L MiliQ water, pH 2.2) for 1 h changing the buffer 4 times. This was followed by washing with 1x PBS for 10 min and then with TBST for 10 min. The blot was then probed for other proteins by repeating the above-mentioned procedure.

### 2.10 Enzyme-linked immunosorbent assay (ELISA)

The levels of different cytokines in the cell supernatant were estimated using sandwich ELISA. For this, 96-well immunosorbent plates (#442404 Nunc, USA) were coated with 100 µl of coating antibody diluted in coating buffer (Set B buffer: 0.1 M sodium carbonate buffer, pH 9.5 or Set A buffer: 0.2 M sodium phosphate buffer, pH 6.5) and incubated overnight at 4 $^{o}$C. Next day, the coated wells were washed using 200 µl wash buffer (1x PBS with 0.05% Tween-20) thrice and blocked with 200 µl blocking buffer (3% or 1% BSA in PBS or 10% FBS in PBS) for 1 h at RT. The wells were again washed using 200 µl wash buffer thrice and 100 µl samples or standards in blocking buffer were added to the wells for 2 h at RT. Subsequently, washing was done 4-5 times followed by addition of 100 µl biotin-conjugated detection antibody and streptavidin-conjugated HRP mixture diluted in blocking buffer. After incubation for 1 h, the wells were washed 4-5 times and finally 100 µl of the substrate solution mixture [1 mg/ml O-phenyldiamine (#78412 Sigma Aldrich) + 0.2% hydrogen peroxide (#7722-841, Merck, USA) in citric acid buffer pH 4.5] was added to the wells and incubated at RT till the yellow colour developed. The reaction was stopped using 100 µl of stop solution (2 N $H_2SO_4$) and the absorbance was measured at 490 nm using iMark microplate reader (BioRad). The concentration of antigen (cytokine) in the sample was calculated from linear equation obtained by plotting the absorbance of the standards. The kits and antibodies used in ELISA are mentioned in table 5.

**Table 5: List of kits and antibodies used in ELISA.**

| Cytokine | ELISA kit/antibodies | Company |
|---|---|---|
| Mouse IL-6 | Capture Ab: #554400 | Becton Dickinson (BD) |

| | | |
|---|---|---|
| | Detection Ab: #554402 | |
| Mouse TNFα | Capture Ab: #551225<br>Detection Ab: #554415 | Becton Dickinson (BD) |
| Mouse IL-1β | BD OptEIA mouse IL-1β ELISA set (#559603)<br>Or<br>DuoSet mouse IL-1β (DY401-05) | Becton Dickinson (BD)<br>Or<br>R&D systems |
| Streptavidin-HRP | #5554066 | Becton Dickinson (BD) |

### 2.11 Determination of surface expression of MHC II and co-stimulatory molecules

BMDCs ($5 \times 10^5$) were treated with OmpU for 24 h to detect CD80 levels and for 8 h to detect MHC II and CD86 levels. Then, the cells were harvested and washed with flow cytometry buffer (1x PBS with 1% FBS and 0.05% sodium azide). This was followed by incubation with mouse Fc block (#553142, BD Biosciences) for 15 min on ice. Cells were then incubated with FITC-conjugated anti-MHC II (#553547), FITC-conjugated anti-CD80 (#553768) and PE-conjugated anti-CD86 antibodies (#553692) (BD Biosciences) for 45 min. Cells were then washed with flow cytometry buffer and analysed using FACSCalibur (BD Biosciences).

### 2.12 Determination of calcium flux using Fluo-4 AM

The intracellular calcium levels were assessed using Fluo-4 (AM) dye (Ex.480 nm/Em.525 nm) (#F14201 Invitrogen Life Technologies), a cell-permeant fluorescent calcium indicator, and measured by flow cytometry in a time-dependent manner (illustration 5) [104]. The cells ($5 \times 10^5$) were loaded with 1.5 µM Fluo-4 (AM) dye in 20% Pluronic acid in HBSS without calcium and magnesium (ThermoFisher Scientific) along with 2 mM probenecid (Sigma-Aldrich) for 1 h at 37 $^{o}$C. Subsequently, the cells were washed using warm 1x PBS and

harvested in HBSS with calcium and magnesium, followed by the treatments just before acquisition of the cells using FACSCalibur.

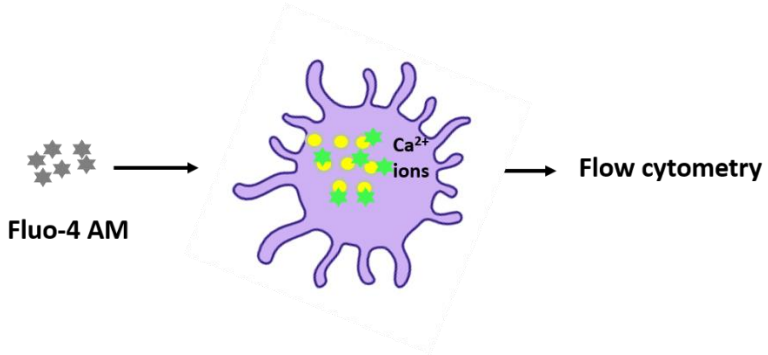


**Illustration 5: Detection of calcium ions by Fluo-4 AM in cells.**

*Fluo-4 AM (Ex.480 nm/Em.525 nm) binds to intracellular calcium ions emitting fluorescence detectable in the green channel in flow cytometer.*

### 2.13 MitoROS detection using MitoSOX dye

Mitochondrial ROS was measured using MitoSOX Red dye (Ex.510 nm/Em.580 nm) (#M36008 Invitrogen Life Technologies) (illustration 6) [105]. BMDCs ($1 \times 10^5$) were grown on coverslips and loaded with 2.5 µM MitoSOX dye diluted in warm RPMI without FBS. Cells were incubated for 20 min at 37 $^{o}$C and then rinsed with warm 1x PBS. Fresh complete RPMI was added to the cells, followed by OmpU treatment for 30 min. Buffer or Antimycin A (10 µM) (Sigma-Aldrich) treated cells were used as negative and positive controls, respectively. Antimycin A inhibits the mitochondrial electron transport chain by disrupting the electron transport between the cytochrome *b* and *c* complexes. This inhibition leads to disruption of proton gradient across the inner membrane of mitochondria and results in generation of superoxide radicals, that is, mitoROS. Following incubation, the cells were washed with 1x PBS and detected using microscopy or flow cytometry.

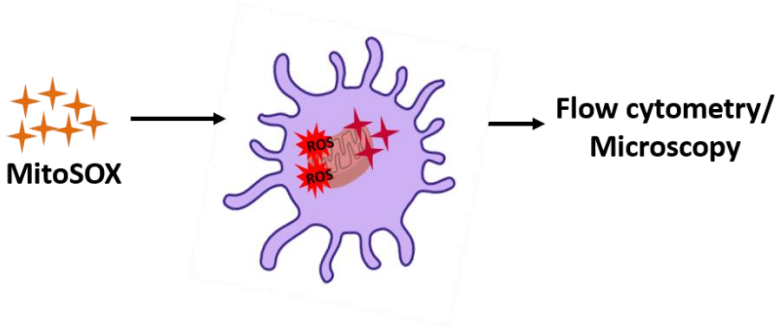


**Illustration 6: Detection of mitoROS by MitoSOX dye in cells.**

*MitoSOX (Ex.510 nm/Em.580 nm) accumulates in the mitochondria based on its positive charge and detects mitochondrial superoxide producing fluorescence in the red channel in flow cytometer or fluorescence microscope.*

### 2.14 Image acquisition and analysis for mitoROS detection

Imaging for mitoROS detection was done using EVOS Life Technologies FL fluorescence microscope (ThermoFisher Scientific) (for mitoROS generation and BAPTA-AM inhibition experiments) and Zeiss Axio Observer Z1 inverted microscope (Zeiss) using a 63x oil immersion objective (for Cytochalasin D inhibition of mitoROS). In each experiment 10-15 images were acquired using identical conditions. The experiment was repeated 3-4 times to obtain a total of 30-40 images which were further analysed using ImageJ software (National Institutes of Health, NIH) using identical values of brightness and contrast.

For flow cytometric analysis, the cells were washed using 1x PBS after treatment, harvested in 1x PBS and acquired in FACSCalibur flow cytometer.

### 2.15 Confocal microscopy for determining colocalization of proteins

Cells ($2 \times 10^5$) were grown on coverslips and treated with buffer or OmpU for 30 min. Following treatment, the cells were washed with 1x PBS, fixed using 4% PFA for 30 min on ice and then permeabilised with 0.1% saponin in 1x PBS. Subsequently, cells were incubated with 3% BSA in 1x PBS for 1 h at room temperature for blocking. This was followed by incubation with primary antibodies at room temperature. The cells were then washed with 1x PBS and incubated with secondary antibodies for 1 h at room temperature. Post-incubation, the cells were washed with 1x PBS, and the coverslips were mounted onto glass slides using

fluoromount mounting medium (#F4680 Sigma-Aldrich). The details of antibodies used are mentioned in table 6.

### 2.16 Image acquisition and analysis for confocal microscopy

The imaging was done using Leica confocal microscope (Leica) and Olympus confocal microscope (Zeiss). Each experiment was repeated at least three or more times to obtain a total of 30-45 images for every treatment. The images were analysed using ImageJ software using identical brightness and contrast values. For colocalization studies, Mander's coefficient was calculated by analysing in the ImageJ software.

### 2.17 Quantification and analysis of the flow cytometry data

The flow cytometry data was analysed in FlowJo software to obtain the mean fluorescence intensity (MFI) values for each sample. The MFI values for buffer-treated samples were considered baseline, that is, one and corresponding to it, the fold change of treated samples was calculated. For calcium detection experiments, the Fluo-4 (AM) fluorescence was measured per sec for 1000 sec to obtain a time kinetics, and a histogram was obtained by plotting the MFI obtained for the total duration.

### 2.18 Detection of intracellular ROS using dichlorofluorescein diacetate (DCFDA) dye

Intracellular ROS was measured using a cell-permeant fluorogenic dye DCFDA (Ex.485 nm/Em.535 nm) which detects the hydroxyl, peroxyl and other reactive oxygen species within the cell [106]. Upon deacetylation by cellular esterases, DCFDA further undergoes oxidation in presence of reactive oxygen species to emit fluorescence. The cells were loaded with 10-15 μM DCFDA in RPMI without FBS 30-45 min prior to the completion of incubation period of the treatments. After 30-45 min, the cells were washed with 1x PBS twice, harvested in 500 μl of 1x PBS and acquired in FACSCalibur flow cytometer. The emission of DCFDA occurs around 527 nm and is detected in the FL-1 channel in FACSCalibur. Further, the data obtained was analysed in the FlowJo software (FlowJo LLC, USA).

**Table 6: List of antibodies used in the study.**

| Antibody | Catalogue no. | Company |
|---|---|---|
| Caspase-1 | Sc-56036 | Santa Cruz Biotechnology |
| NLRP3 | 15101S | Cell Signaling Technology |
| β-actin | Sc-81178 | Santa Cruz Biotechnology |
| OmpU (polyclonal serum) | generated | Bangalore Genei |
| TIM23 | 611223 | Becton Dickinson |
| GAPDH | Sc-32233 | Santa Cruz Biotechnology |
| LAMP-1 | MA1-164 | ThermoFisher Scientific |
| p-PI3K | 4228T | Cell Signaling Technology |
| PI3K | 4257T | Cell Signaling Technology |
| p-AKT | 4060T | Cell Signaling Technology |
| AKT | 4691T | Cell Signaling Technology |
| p-PKC | 9379S | Cell Signaling Technology |
| PKC | Ab19031 | Abcam |
| p-p38 | 4511S | Cell Signaling Technology |
| p38 | 8690S | Cell Signaling Technology |
| p-JNK | 9251S | Cell Signaling Technology |
| JNK | 9252S | Cell Signaling Technology |
| p-ERK | 4370S | Cell Signaling Technology |
| ERK | 4695S | Cell Signaling Technology |
| IκBα | Sc-1643 | Santa Cruz Biotechnology |
| TLR2 | 13744 | Cell Signaling Technology |

| | | |
|---|---|---|
| CD36 | AF2519 | R & D systems |
| p47 | Sc-7660R | Santa Cruz Biotechnology |
| $Na^+$-$K^+$ ATPase | Ab7671 | Abcam |
| TLR2 neutralizing antibody | 121802 | BioLegend |
| TLR2 isotype control | 400102 | BioLegend |
| TLR4 neutralizing antibody | 117608 | BioLegend |
| TLR4 isotype control | 400516 | BioLegend |
| Alexa 488 anti-rabbit | A11034 | Molecular probes |
| Alexa 568 anti-mouse | A11004 | Molecular probes |
| Anti-rabbit IgG HRP | A0545 | Sigma Aldrich |
| Anti-mouse IgG HRP | A9044 | Sigma Aldrich |
| Anti-goat IgG HRP | 81-1620 | ThermoFisher Scientific |

### 2.19 Experimental Designs:

Cells were treated with 3 μg/ml OmpU and buffer (Tris-HCl pH 7.6 diluted in PBS containing 0.5% LDAO) for 24 h for cytokine-related experiments unless otherwise indicated. In each experimental set-up, the cells were treated with 10 μg/ml Polymyxin B Sulphate (Sigma-Aldrich) for 30 min prior to OmpU treatment to neutralise the responses against endotoxin in the purified OmpU if any.

#### 2.19.1 Assessment of the role of MyD88, TLR2 and NLRP3 in OmpU-mediated cytokine responses using MyD88$^{-/-}$, TLR2$^{-/-}$ and NLRP3$^{-/-}$ BMDCs.

BMDCs from C57BL/6 (WT), MyD88$^{-/-}$, TLR2$^{-/-}$ and NLRP3$^{-/-}$ mice were plated at a density of 1 x $10^6$ cells/ml in a 24-well plate followed by buffer and OmpU treatments. After 24 h incubation, the supernatant from the cells was collected and assayed for the levels of TNFα,

IL-6 and IL-1β cytokines for MyD88$^{-/-}$ and TLR2$^{-/-}$ BMDCs and for IL-1β levels in case of NLRP3$^{-/-}$ BMDCs using sandwich ELISA.

### 2.19.2 Estimation of the effect of different inhibitors on the cytokine levels in response to OmpU treatment.

BMDCs were plated at a density of 1 x $10^6$ cells/ml in a 24-well plate. The cells were pre-treated with various chemical inhibitors followed by OmpU treatment for 24 h. The pre-treatment time and the concentrations of various inhibitors used are summarised in the table 7. The supernatant was assayed for IL-6 or IL-1β levels by sandwich ELISA.

**Table 7: List of inhibitors used in the study.**

| Inhibitor | Catalogue no. and company | Concentration used | Pre-treatment |
|---|---|---|---|
| BAPTA-AM | B1205<br>Invitrogen | 5 μM & 10 μM (for calcium flux experiments<br>2 μM & 4 μM (for mitoROS experiments) | 1 h (for calcium flux experiments)<br>30 min (for mitoROS) |
| MitoTEMPO | SML0737<br>Sigma Aldrich | 5 μM | 2 h |
| Cytochalasin D | C8273<br>Sigma Aldrich | 5 μM & 10 μM | 30 min |
| LY294002 | L9908<br>Sigma Aldrich | 10 μM & 20 μM | 1 h |
| GDC-0941 | 5.09226.0001 | 1 μM | 1 h |

| | | | |
|---|---|---|---|
| | Merck Life science | | |
| SAR 405 | 5.33063.0001<br>Merck Life science | 200 nM | 1 h |
| AKT VIII | 124018<br>Merck Life science | 8 μM | 1 h |
| BIM IV | B3306<br>Sigma Aldrich | 1 μM & 2 μM | 1 h |
| HBDDE | 372770<br>Merck Life science | 50 μM | 1 h |
| PD184352 | PZ0181<br>Sigma Aldrich | 500 nM & 1 μM | 1 h |
| N-acetylcystine (NAC) | A9165<br>Sigma Aldrich | 10 mM | 2 h |
| Diphenyleneiodonium chloride (DPI) | D2926<br>Sigma Aldrich | 100 nM | 1 h |
| PP2 | P0042<br>Sigma Aldrich | 5 μM | 1 h |
| SP600125 | S5567<br>Sigma Aldrich | 25 μM | 1 h |
| SB202190 | S7067<br>Sigma Aldrich | 10 μM | 1 h |
| PS-1145 | P6624<br>Sigma Aldrich | 2.5 μM | 1 h |

### 2.19.3 Estimation of the effect of neutralization of TLR2 or TLR4 on the IL-6 cytokine levels in response to OmpU treatment.

BMDCs were plated at a density of 1 x $10^6$ cells/ml in a 24-well plate and pre-treated with 5 μg/ml anti-TLR2 or anti-TLR4 or isotype control antibodies (BioLegend) for 1 h followed by OmpU treatment for 24 h. After incubation the supernatant was collected and analysed for IL-6 production using sandwich ELISA.

### 2.19.4 Checking the levels of phosphoinositide-3-kinases (PI3Ks), protein kinase C (PKC), MAPKs, IκBα, caspase-1 and NLRP3 in OmpU-treated BMDCs.

BMDCs were plated at a density of 1 x $10^6$ cells/ml in 60 mm petri-dish. For checking caspase-1 activation and NLRP3 levels, the cells were treated with OmpU for 2 h and 3 h respectively, otherwise the cells were treated with OmpU for various time points 30 min, 60 min and 120 min. Further, the cells were rinsed with 1x PBS and whole-cell lysate was prepared as described previously. The whole-cell lysate was probed for p-PI3K, PI3K, p-PKC, PKC, p-p38, p38, p-JNK, JNK, p-ERK 1/2, ERK, IκBα, caspase-1 and NLRP3 using western blotting. GAPDH or β-actin were used as loading controls.

### 2.19.5 *In vivo* OmpU studies and checking the gene expression levels of pro-inflammatory cytokines.

Two mice each of C57BL/6 (wildtype) and TLR2$^{-/-}$ background were immunized intraperitoneally (I.P.) with 100 μg of OmpU. Two C57BL/6 mice administered I.P. with buffer were kept as controls. 6 h post-immunization spleens were isolated from the OmpU and buffer-treated mice followed by isolation of splenic DCs. The cells from two mice for each treatment were pooled together and proceeded for RNA isolation.

### 2.19.5 (a) RNA isolation using TRIzol reagent

For isolation of total RNA from the splenic DCs, the cells were lysed in 500 μl of TRIzol reagent (#15596018 Ambion, Life Technologies, USA) followed by incubation at room temperature for 5 min. Then 100 μl of chloroform was added to the samples, followed by

vigorous shaking. After incubation at RT for 2-3 min, the samples were centrifuged at 12,000 x g for 15 min for phase separation. The aqueous phase containing the RNA was collected into a fresh tube, and 500 µl of 100% isopropanol (#I9030 Sigma-Aldrich) was added. Followed by incubation at RT for 10 min, the samples were centrifuged at 12,000 × g for 10 min. The precipitated RNA samples were then washed twice using 75% ethanol (Merck) and pelleted at 7500 x g for 5 min. The RNA was then air-dried for 10 min and resuspended in Milli-Q water. RNA in each sample was quantified by a nanodrop.

### 2.19.5 (b) cDNA synthesis

0.5-1 µg of the isolated RNA from each sample was used for cDNA synthesis following the manufacturer's instructions of the Verso cDNA synthesis kit (#AB1453A ThermoFisher Scientific). The reaction mixture prepared for each sample is as shown in the table 8.

**Table 8: cDNA reaction mixture.**

| Components | Concentration | Volume (µl) |
|---|---|---|
| 5x cDNA synthesis buffer | 1x | 4 |
| dNTPs | 500 µM | 2 |
| RNA primer | 0.5-2 µM | 1 |
| RT enhancer | - | 1 |
| Verso enzyme mix | - | 1 |
| Template RNA | 0.5-1 µg | 1-5 |
| Nuclease-free water | - | Make up to 20 |
| Total | - | 20 |

The PCR cycle program was one cycle at 42 $^{o}$C for 30 min and one cycle at 95 $^{o}$C for 2 min carried out using MyCycler thermocycler (Biorad). The 20 µl cDNA samples obtained were diluted two-folds in nuclease-free water for further use.

### 2.19.5 (c) Semi-quantitative real-time PCR (RT-qPCR)

The cDNA samples were used as a template for the RT-qPCR reaction (volume-10 µl) performed using Maxima SYBR green qPCR master mix (#K0252, ThermoFisher Scientific) and Eppendorf Mastercycler EP Realplex Thermal Cycler (Eppendorf, Germany) according to the manufacturer's protocol. The RT-qPCR was performed for 40 cycles. The primer sequences were obtained from the Harvard primer bank and were synthesized by IDT Technologies (USA). The relative TNFα and IL-6 gene expression was expressed as a mean fold change over the buffer-treated cells. All the sample values were normalised with the values of housekeeping control genes *Hprt* or *18srrna*. The primer sequences used in the study are mentioned in the table 9.

**Table 9: Primer sequences used in the study.**

| Primer name | Sequence 5'-3' |
|---|---|
| TNFα | Forward sequence: CCCTCACACTCAGATCATCTTCT<br>Reverse sequence: GCTACGACGTGGGCTACAG |
| IL-6 | Forward sequence: TAGTCCTTCCTACCCCAATTTCC<br>Reverse sequence: TTGGTCCTTAGCCACTCCTTC |
| Hprt | Forward sequence: TCAGTCAACGGGGGACATAAA<br>Reverse sequence: GGGGCTGTACTGCTTAACCAG |
| 18srRNA | Forward sequence: AAGGAGACTCTGGCATGCTAAC<br>Reverse sequence: CAGACATCTAAGGGCATCACAGAC |

### 2.19.6 Assessment of the role of potassium efflux on NLRP3 activation.

BMDCs were plated at a density of 1 x $10^6$ cells/ml in a 24-well plate and pre-treated with 50 mM KCl for 30 min. Then the cells were treated with OmpU or buffer for 24 h. Cells primed with LPS (50 ng/ml) for 3 h followed by ATP (5 mM) treatment for 30 min were used as

positive control [107]. The cell supernatant was analysed for IL-1β production using ELISA post-incubation.

### 2.19.7 Estimation of the calcium flux in BMDCs and effect of BAPTA-AM on OmpU-induced calcium influx.

BMDCs were plated at a density of 1 x $10^6$ cells/ml in a 24-well plate and pre-treated with BAPTA-AM for 1 h. The cells were washed with warm 1x PBS and then added with Fluo-4 AM dye mixture as mentioned before. Following by washing with 1x PBS, the cells were harvested in 1x PBS and treated with buffer or OmpU (5 μg/ml) or PMA+Ionomycin (1 μg/ml) just before acquisition in flow cytometer.

### 2.19.8 Checking the translocation of OmpU to mitochondria of BMDCs and the effect of cytochalasin D on OmpU translocation.

BMDCs were plated at a density of 1 x $10^6$ cells/ml in 100 mm petri-dish. The cells were pre-treated with cytochalasin D (cyt. D) for 30 min and then treated with buffer or OmpU (5 μg/ml) for 30 min. The enriched mitochondrial fractions were isolated from the cells using mitochondrial isolation kit (#MITOISO2-1KT, Sigma-Aldrich). Briefly, the cells were harvested and washed with 1x PBS. To the cell pellet, 150-200 μl of lysis buffer [1x extraction buffer with detergent (1:200) and mammalian protease inhibitor (1:100)] was added followed by vortexing 5 times with an interval of 1 min. Then, to the lysed cells, double the volume of 1x extraction buffer (300-400 μl) was added and incubated on ice for 10 min. The mixture was then subjected to centrifugation at 850 x g at 4 ºC for 10 min twice to get rid of the cell debris. The supernatant was collected and centrifuged at 6000 x g for 10 min at 4 ºC. The pellet obtained was enriched in the mitochondrial fraction and was dissolved in 40-50 μl of CelLytic M buffer (#C2978, Sigma-Aldrich). Subsequently, the mitochondrial lysates were immunoblotted to check the presence of OmpU and control proteins such as TIM23, GAPDH or LAMP-1.

### 2.19.9 Probing the co-immunoprecipitation of OmpU with TLR2 and CD36 in BMDCs.

BMDCs were plated at a density of 1 x $10^6$ cells/ml in 100 mm petri-dish. The cells were treated with buffer or OmpU (5 μg/ml) for 15 min followed by preparation of whole cell lysate as mentioned before. The whole cell lysate was added with 1 μg of anti-TLR2 or anti-CD36 antibodies and rotated in a rotospin at 4 $^oC$ for 3 h. Then 20 μl of protein A/G agarose beads (#SC2003, Santa Cruz Biotechnology) were added to the lysate and incubated overnight in a rotospin. Next day, the lysate was centrifuged at 6000 x g for 5 min at 4 $^oC$ and the supernatant was discarded. The beads were then washed using whole cell lysis buffer thrice. Finally, the proteins from the beads were eluted using 40-60 μl of SDS loading dye, boiled for 10-15 min and run on SDS-PAGE for immunoblotting TLR2 or CD36 and OmpU.

### 2.19.10 Determining the colocalization of NLRP3 and mitochondrial marker TIM23 using confocal microscopy.

Cells (2 × $10^5$) were grown on coverslips and treated with buffer or OmpU (5 μg/ml) for 30 min. Following treatment, the cells were washed with 1x PBS, fixed using 4% PFA on ice and then permeabilised with 0.1% saponin in 1x PBS. Subsequently, cells were incubated with 3% BSA in 1x PBS for 1 h at room temperature for blocking. This was followed by incubation with mouse anti-TIM23 (BD Biosciences) and rabbit anti-NLRP3 antibodies for 4 h at room temperature. The cells were then washed with 1x PBS and incubated with Alexa 568-conjugated anti-mouse IgG (for TIM23) and Alexa 488-conjugated anti-rabbit IgG secondary antibodies (for NLRP3) (Invitrogen Life Technologies) for 1 h at room temperature. Subsequently, the cells were washed with 1x PBS, and the coverslips were mounted onto glass slides using fluoromount. The imaging was done using Olympus confocal microscope.

### 2.19.11 Estimation of mitochondrial ROS in OmpU-treated BMDCs and the effect of inhibitors MitoTEMPO, cytochalasin D and BAPTA-AM on the mitoROS levels.

BMDCs (1 × $10^5$) were grown on coverslips for fluorescence microscopy studies and 5 × $10^5$ cells were plated for flow cytometric analysis. The cells were pre-treated with MitoTEMPO for 2 h [108] while cytochalasin D and BAPTA-AM were incubated for 30 min [109].

Following inhibitor pre-treatment, the cells were stained with MitoSOX Red dye as described before.

For fluorescence microscopic analysis, following treatment the cells were washed with 1x PBS, fixed using 2% paraformaldehyde (PFA) (w/v) for 15 min on ice and the coverslips were mounted onto glass slides using fluoromount mounting medium and analysed using fluorescent microscopy for mitoROS detection.

For flow cytometric analysis, the cells were washed using 1x PBS after treatment, harvested in 1x PBS and acquired in FACSCalibur flow cytometer.

### 2.19.12 Confocal microscopy for determining co-localization of OmpU and mitochondrial marker TOM20.

BMDCs ($2 \times 10^5$) were grown on coverslips and treated with buffer or OmpU (5 μg/ml) for 30 min. Following treatment, the cells were washed with 1x PBS, fixed using 4% PFA at room temperature and then permeabilised with 0.1% saponin in 1x PBS for 30 min on ice. Subsequently, cells were washed with 1x PBS and incubated with blocking buffer (3% BSA + FBS in 1 x PBS) for 1 h at room temperature. This was followed by incubation with 1:400 rabbit anti-TOM20 (Sigma-Aldrich) and 1:600 mouse anti-OmpU (generated) antibodies for 1 h at room temperature. The cells were then washed with 1x PBS and incubated with Alexa 568- conjugated anti-mouse IgG (for OmpU) and Alexa 488-conjugated anti-rabbit IgG secondary antibodies (for TOM20) (Invitrogen Life Technologies) for 1 h at room temperature. Subsequently, the cells were washed with 1x PBS, and incubated with DAPI for 5 min. Finally, the coverslips were mounted onto glass slides using fluoromount. The imaging was done using Leica confocal microscope.

### 2.19.13 Checking the ROS generation in response to OmpU at different time points.

$5 \times 10^5$ BMDCs were grown in a 24-well plate and treated with OmpU (3 μg/ml) for different time periods 4 h, 8 h, 12 h and 24 h. Buffer-treated cells served as negative control. The cells were then incubated with DCFDA dye mixture for 30 min and following washing with 1x PBS twice, the cells were acquired in FACSCalibur flow cytometer.

### 2.19.14 Effect of ROS inhibitors on OmpU-induced ROS generation and cytokine production.

$5 \times 10^5$ BMDCs were grown and pre-treated with different inhibitors. OmpU or buffer was added to the cells for 8 h and then the cells were stained with DCFDA and acquired in FACSCalibur.

For estimating the cytokine production, following the pre-treatment with inhibitors, the cells were treated with OmpU for 24 h. After incubation, the cell supernatant was collected and IL-6 levels were assessed in them using ELISA.

### 2.19.15 Determining the co-localization of $p47_{phox}$ and plasma membrane marker $Na^+$-$K^+$ ATPase using confocal microscopy.

Cells ($2 \times 10^5$) were grown on coverslips and treated with buffer or OmpU (3 μg/ml) for 4 h. Following treatment, the cells were washed with 1x PBS, fixed using 4% PFA and then permeabilised with 0.2% saponin in 1x PBS for 30 min on ice. Subsequently, cells were incubated on RT with 3% BSA in 1x PBS for 1 h for blocking. This was followed by incubation with rabbit anti-$p47_{phox}$ (Santa Cruz Biotechnology) and mouse anti-$Na^+$-$K^+$ ATPase (Abcam) antibodies for 4 h at room temperature. The cells were then washed with 1x PBS and incubated with Alexa 568- conjugated anti-mouse IgG (for $Na^+$-$K^+$ ATPase) and Alexa 488-conjugated anti-rabbit IgG secondary antibodies (for $p47_{phox}$) (Invitrogen Life Technologies) for 1 h at room temperature. Subsequently, the cells were washed with 1x PBS, and DAPI was added to the coverslips for 5 min. Then the coverslips were mounted onto glass slides using fluoromount. The imaging was done using Olympus confocal microscope.

### 2.20 Data and statistical analysis

Data were represented as mean ± SD. Statistical analysis was performed using Graphpad/quickcalcs and the comparisons were performed using Student's two-sided *t*-test. The *p*-values obtained less than 0.05 were considered significant.

# III. Results

**Aim 1:** To probe whether and how OmpU induces the activation of DCs.

**Specific aim 1:** Whether OmpU acts as a PAMP and activates PRRs to induce DC activation?

**Specific aim 2:** To understand the signalling molecules involved in OmpU-mediated activation of DCs.

# Aim 1: To probe whether and how OmpU induces the activation of DCs.

## 3.1 Role of DCs in host immune responses

DCs are a unique subset of immune cells that recognise the danger signals or patterns on the pathogen, capture the pathogen by using various innate and endocytic receptors present on them, secrete pro-inflammatory mediators to prompt other innate cells and assist in shaping the adaptive immune responses. DCs possess potent immunostimulatory capacity as they process the antigen and migrate to the neighbouring lymphoid organs to present the antigen to naïve T cells [97]. The pro-inflammatory mediators, such as cytokines, chemokines and reactive oxygen species, produced by DCs in response to antigen communicate the signal to the innate as well as the adaptive immune cells and decide the fate of the immune responses. The activation of T cells by DCs is the key to adaptive immunity [96].

DCs reside in an immature state scouring the tissues and lymphatic system until they encounter an antigen that induces certain phenotypic changes in the DCs, leading to maturation. DCs can be myeloid or lymphoid in origin, which differs in their ontogenic and phenotypic characteristics, such as conventional DCs (cDCs), plasmacytoid DCs (pDCs) and monocyte-derived DCs (MoDCs) [96, 110]. The cDCs commonly used for *in vitro* studies are believed to be myeloid in origin and are generated using GM-CSF and IL-4 to differentiate the murine bone-marrow progenitor cells [111]. The cDCs undergo various intermediate stages during differentiation, as shown in the illustration 7.

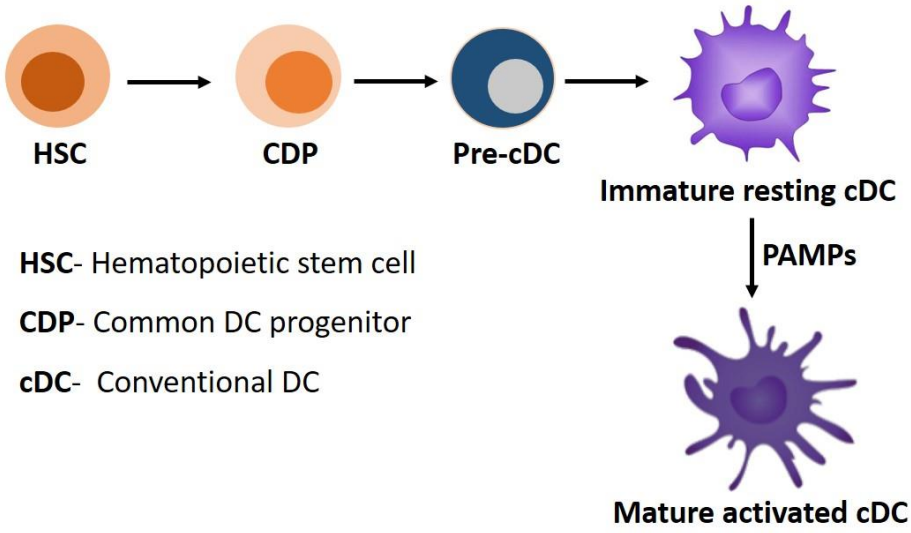


**Illustration 7: Differentiation of cDCs.**

*The conventional DCs (cDCs) undergo different stages while differentiation from hematopoietic stem cells (HSCs). HSCs first differentiate into common DC progenitor (CDP) followed by pre-cDC and then into immature cDCs. The immature cDCs when stimulated by pathogen-associated molecular patterns (PAMPs) terminally differentiate into mature cDCs.*

### 3.1.1 DC maturation and T cell activation

DC maturation is important for antigen presentation and T cell activation. The maturation of DCs is a complex process which involves upregulation of MHC II and co-stimulatory molecules such as CD80, CD86 and CD40, enhanced antigen processing and presentation capabilities and low phagocytic capacity [96]. The mature DCs also exhibit migratory properties and produce various cytokines and chemokines necessary for T cell stimulation and clonal expansion. The cytokines produced by mature DCs play a critical role in differentiation of T cells into antigen-specific effector T cells and promote the activation of other immune cells [112].

The activation of T cells by DCs requires three signals; the first is interaction of the MHC II-peptide complex on DCs to the T-cell receptor (TCR); the second is through the co-stimulatory molecules on the DCs, and the third signal is via the cytokines secreted by the DCs. All of these signals together assure the activation of adaptive immunity [112].

## 3.2 TLR signalling in DCs

DCs harbour various PRRs, which upon engagement with the different microbial ligands/PAMPs, initiate signalling pathways that lead to the expression of molecules involved in distinct immune responses. The efficiency of priming the naïve T cells, as well as the decision to promote T cell anergy, depends on the specific ligand-PRR interaction [113]. TLRs are one of the major PRRs expressed on the DCs [114]. They are transmembrane receptors containing leucine-rich repeat (LRR) ectodomain and cytoplasmic Toll/IL-1R homology (TIR) domain. The TIR domain recruits TIR domain-containing adaptor proteins such as myeloid differentiation protein 88 (MyD88), which mediate the signalling pathway. MyD88 is the major adaptor protein for all TLRs except TLR3, which signals through Toll/IL-1R domain-containing adaptor inducing IFN-β (TRIF), while TLR4 signals via both MyD88 and TRIF [115]. TLRs can be present on the cell surface, such as TLR1, TLR2, TLR4, TLR5, TLR6 or in the intracellular region (in the endosomal compartments) such as TLR3, TLR7, TLR8 and

TLR9 [116]. TLR signalling through different adaptor molecules and various kinases result in the activation of transcription factors, such as NFκB and AP-1, which leads to the inflammatory cytokine production, induction of co-stimulatory molecules (CD80, CD86 and CD83) and eventually, DC maturation [114].

Signalling via TLRs is initiated upon recognition of PAMPs, such as LPS, peptidoglycan, flagellin and many more. TLRs generally signal as hetero- or homo-dimer upon ligand binding. Among the surface TLRs, TLR2 heterodimerises with TLR1 or TLR6 and mainly recognises bacterial proteins and lipoproteins as PAMPs. TLR4 generally forms a homo-dimer and predominantly recognises LPS as PAMP. TLR5 forms a homodimer and recognises flagellar protein. The intracellular TLRs such as TLR3, 7, 8 and 9 also act as homodimers and are majorly involved in recognising viral and bacterial nucleic acids as PAMPs [117, 118].

TLRs activate a cascade of signalling mediators, such as IκB kinase (IKK), mitogen-activated protein kinases (MAPKs), phosphoinositide-3-kinases (PI3Ks), protein kinase C (PKC) and src kinases among many others and culminate in the activation of transcription factors, such as NFκB and AP-1 and the production of pro-inflammatory/anti-inflammatory cytokines, such as IL-1β, IL-6, IL-4, IL-2, IL-10, TGF-β, TNFα, IL-12, IL-21, IL-23 depending on the PAMP that the DC has encountered (Table 10) [119, 120].

**Table 10: Major cytokines secreted by DCs on encountering different PAMPs.**

| ***S. no.*** | ***PAMPs*** | ***Cytokines secreted by DCs*** | ***References*** |
|---|---|---|---|
| 1 | Bacterial (Intracellular) | IFN (α, β)<br>IL-12 | [121, 122] |
| 2 | Bacterial (Extracellular) | IL-6<br>TGF-β<br>IL-21<br>IL-23 | [122] |
| 3 | Viral | IFN (α, β)<br>IL-12 | [121, 122] |
| 4 | Fungal | IL-6 | [121] |

| | | | |
|---|---|---|---|
| | | TGF-β<br>IL-1<br>IL-23 | |
| 5 | Parasitic | IL-4 | [121, 122] |

### 3.3 MAP kinases activated in inflammatory pathways

TLR activation in response to various PAMPs and DAMPs leads to the initiation of a signalling cascade and several protein kinases act as intermediates in this signalling, which following activation by phosphorylation by the upstream molecules, phosphorylate their downstream targets. MAP kinase pathway is a three-tiered evolutionarily conserved signal transduction pathway. It involves the phosphorylation of an upstream MAP3K (MAP kinase kinase kinase), which then phosphorylates and activates MAP2K (MAP kinase kinase). MAP2Ks directly activate MAPKs (MAP kinase), which can regulate the gene expression of various transcription factors. There are mainly three MAPKs identified in the inflammatory processes: ERK (extracellular stress-regulated kinases), p38 and JNK (c-Jun N-terminal kinase) [123].

ERK has two isoforms, ERK1/2, which mediate activation of cellular processes such as proliferation, innate immunity and inflammation. p38 has four isoforms: p38α, p38β, p38γ and p38δ involved in cell differentiation, apoptosis, and inflammatory signalling. JNK has three isoforms JNK1/2/3 which are primarily activated in response to various stress stimuli and induce pro-inflammatory signals [123].

### 3.4 PI3K-AKT signalling in inflammation

Phosphoinositide-3-kinases (PI3Ks) are plasma membrane-bound enzymes that lead to the phosphorylation of different phospholipids and induce downstream signalling via various second messengers. They are involved in various cellular pathways such as growth, survival, differentiation, metabolism and inflammatory signalling. There are eight isoforms of PI3K divided into three families: four class I isoforms, three class II isoforms and one class III isoform. Upon receiving the activation signal, the class I PI3Ks convert phosphatidylinositol-3,4-biphosphate ($PIP_2$) to phosphatidylinositol-3,4,5-trisphosphate ($PIP_3$) [124].

Further, AKT binds to $PIP_3$, allowing PDK1 to phosphorylate and activate AKT. AKT acts on various target substrates, including IKKs and upstream MAPKKs, which can regulate inflammatory responses [125].

PI3Ks are also reported to play a role in the activation of proteins such as src kinases, PKC and Rac, which mediate different inflammatory pathways [126]. In addition, PI3K signalling aids in ROS generation in neutrophils, *in vivo* migration of DCs, phagosome maturation and T cell functioning [124, 127].

### 3.5 Calcium signalling and PKC activation in inflammatory responses

The conversion of PIP2 to PIP3 by PI3Ks on the plasma membrane can recruit another enzyme called phospholipase Cγ (PLCγ). PLCγ also acts on PIP2 and leads to the production of diacylglycerol (DAG) and Inositol- 1,4,5, -triphosphate (IP3). IP3 acts as a second messenger and prompts the release of calcium from organelles such as endoplasmic reticulum (ER). The influx of calcium ion in the cytosol and DAG further mediates the activation of various signalling molecules, such as protein kinase C (PKC) [128].

Therefore, the activation of PI3Ks and calcium signalling could be a prerequisite for the phosphorylation and activation of the PKC. PKC are a family of serine/threonine kinases which induce the activation of signalling molecules involved in various inflammatory signalling cascades. PKC comprises of three sub-families: conventional isoforms (PKC α, βI, βII and γ) which require calcium, DAG and phosphatidylserine; novel isoforms (PKC δ, ε, η and θ) require DAG and phosphatidylserine; while the atypical isoforms (PKC ζ and ι/λ) require only phosphatidylserine. Different isoforms are active in different cell types and respond to varied stimuli. Upon stimulation, PKC activation downstream to the TLR signalling pathway has been shown to activate MAPKs and TAK1, leading to the activation of NFκB and AP-1 transcription factors, inducing the production of pro-inflammatory cytokines [129].

DCs are crucial cells for establishing immune responses upon PAMP recognition. As discussed so far, they release various mediators, and there is upregulation in the expression of various surface markers signifying their activation and maturation. Based on this idea we formulated our specific aims:

### 3.6 Specific aim 1: Whether OmpU acts as a PAMP and activates PRRs to induce DC activation?

From our lab, we have already reported that OmpU activates the innate immune cells such as macrophages and monocytes via the TLR1/2 pathway triggering the production of pro-inflammatory cytokines. Further, we wanted to check whether OmpU could act as a PAMP for DCs as well and induce DC activation.

**Background data**

In our laboratory, my senior, Dr. Sanica C. Sakharwade, observed that OmpU could activate DCs leading to the production of pro-inflammatory cytokines such as TNFα, IL-6 and IL-1β (Fig. 1A-C). These observations indicate that DCs probably recognise OmpU as a PAMP.

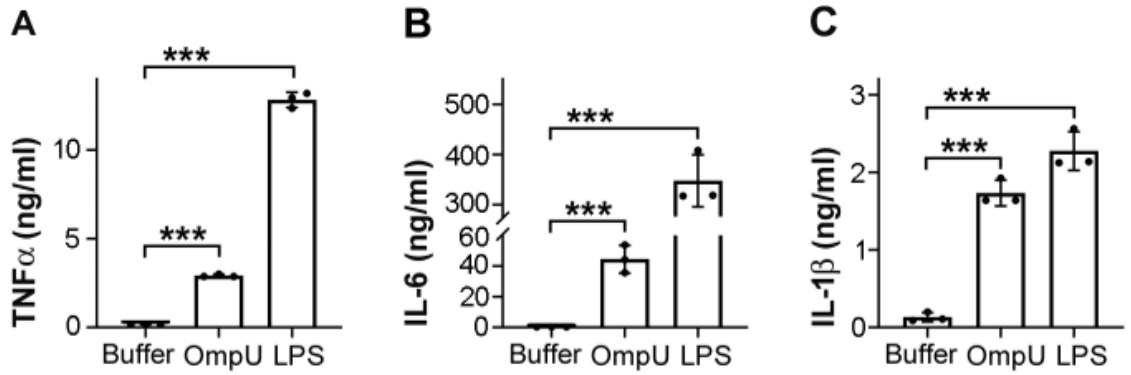


**Figure 1: OmpU induces the production of pro-inflammatory cytokines in DCs. (shown by Dr. Sanica C. Sakharwade)**

*(A-C) Significant production of (A) TNFα, (B) IL-6 and (C) IL-1β was observed in OmpU-treated DCs. BMDCs were treated with 2 μg/ml of OmpU and incubated for 24 h. Buffer-treated and LPS-treated cells (1 μg/ml) served as negative and positive controls, respectively. Following incubation, supernatants were collected and assessed for cytokine production by ELISA. Results are expressed as mean ± SD and represent the average of three independent experiments. Statistical analysis was done using student's two-sided t-test. *p< 0.05, **p< 0.01, ***p < 0.001 versus buffer-treated cells.*

**Based on this background data, I have further carried out the detailed characterization.**

#### 3.6.1 DC activation and maturation by *V. cholerae* OmpU

Further, we have looked at the surface expression of MHC II and co-stimulatory molecules CD80 and CD86 in OmpU-activated DCs. We observed that there is a considerable increase in

the expression of all the three markers, suggesting that OmpU can induce maturation in DCs (Fig. 2).

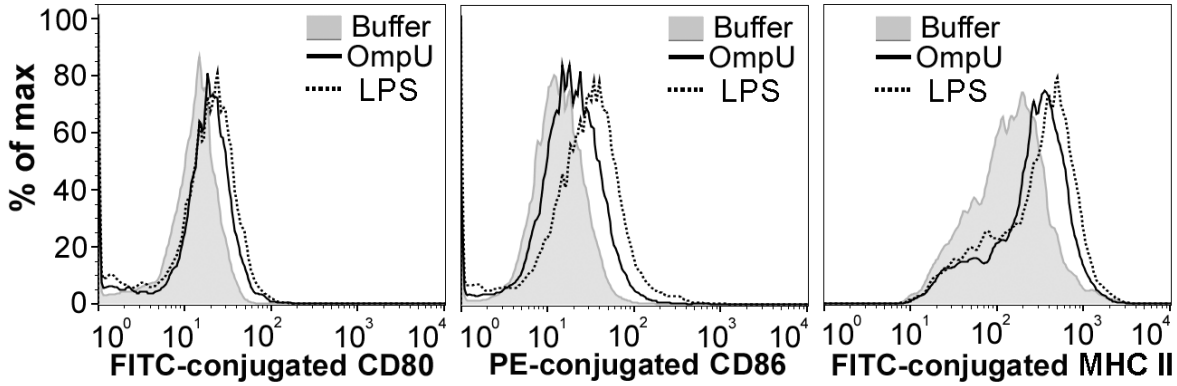


**Figure 2: OmpU induces the expression of MHC II and co-stimulatory markers.**

*Increment in CD80, CD86 and MHC II surface expression in OmpU-treated DCs. BMDCs were treated with OmpU (3 μg/ml) or LPS (2 μg/ml) and incubated for 24 h for CD80 expression. BMDCs were treated with OmpU (3 μg/ml) or LPS (1 μg/ml) and incubated for 8 h for CD86 and MHC II expression. Following incubation, cells were collected and analysed for surface expression by flow cytometry. Histograms are representative of three independent experiments.*

### 3.6.2 OmpU induces DC activation via MyD88 adaptor molecule

As we observed that OmpU could induce DC activation and maturation, we wanted to check the PRR through which OmpU induces its activation signal. Towards this, we first wanted to understand whether TLRs play any role in OmpU-induced signalling. As MyD88 is majorly involved in TLR-mediated signalling, we checked OmpU activation in the presence and absence of MyD88. We have used BMDCs from wildtype (Wt) and MyD88$^{-/-}$ mice, treated them with OmpU and analysed the supernatant for pro-inflammatory cytokines, such as TNFα, IL-6 and IL-1β. We observed that the production of TNFα, IL-6 and IL-1β was significantly reduced in the BMDCs from MyD88$^{-/-}$ mice indicating that MyD88 plays a role in OmpU-mediated signalling in DCs (Fig. 3A-C).

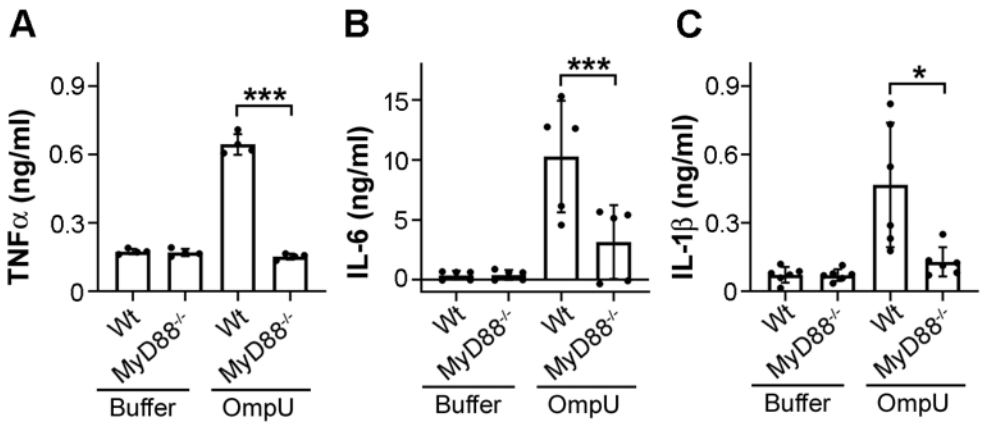


**Figure 3: MyD88 is involved in OmpU-mediated cytokine production in DCs.**

*Significant decrease in cytokine levels in OmpU-treated DCs in the absence of MyD88. BMDCs from Wt (wild type) and MyD88$^{-/-}$ mice were treated with OmpU (3 μg/ml) or buffer and incubated for 24 h. Levels of (A) TNFα, (B) IL-6 and (C) IL-1β were measured by ELISA in culture supernatants. Results are expressed as mean ± SD and represent the average of five independent experiments. Statistical analysis was done using student's two-sided t-test. *p< 0.05, ***p < 0.001 versus OmpU-treated Wt BMDCs.*

### 3.6.3 TLR2 is involved in OmpU-mediated DC activation

The involvement of MyD88 in OmpU-induced DC activation implied that TLRs are playing a role in OmpU-mediated signalling. As the surface TLRs are the probable candidates and among them TLR5 is majorly known to recognise flagellin and TLR1 and TLR6 require the cooperation of TLR2 to induce signalling; to further investigate which TLR is involved in OmpU-mediated signaling, we first probed for TLR2 and TLR4 using respective neutralising antibodies. We have pre-treated BMDCs with neutralising antibodies and the corresponding isotype controls. Following incubation, we treated the cells with OmpU for 24 h and collected the culture supernatants. We analysed the supernatants for the levels of IL-6 using ELISA. We observed that IL-6 production was significantly decreased in the cells pre-treated with TLR2 neutralising antibody but not with TLR4 neutralising antibody, suggesting that TLR2, but not TLR4, probably plays a role in OmpU-mediated DC activation (Fig. 4A).

Further, to confirm the role of TLR2, we cultured the BMDCs from TLR2$^{-/-}$ mice and treated them with OmpU for 24 h. We performed ELISA to check the levels of pro-inflammatory cytokines in the culture supernatants of OmpU-treated Wt and TLR2$^{-/-}$ BMDCs and found that the cytokines were significantly reduced in BMDCs from TLR2$^{-/-}$ mice compared to the Wt

(Fig. 4B-D). Therefore, our *ex vivo* results confirmed that TLR2 is involved in OmpU-mediated activation of DCs.

Further, we wanted to check whether TLR2 plays a role in response to OmpU *in vivo* and could be responsible for the generation of pro-inflammatory responses in DCs in mice. To check that we administered OmpU in Wt and TLR2$^{-/-}$ mice via the intraperitoneal (I.P.) route and isolated the splenic DCs 6 h post-I.P. We extracted total RNA from the isolated splenic DCs and assessed for the TNFα and IL-6 gene expression levels using semi-quantitative PCR. We observed a considerable reduction in the TNFα and IL-6 gene expression levels in splenic DCs from TLR2$^{-/-}$ mice compared to the splenic DCs from Wt mice. Therefore, from our experiments, we concluded that TLR2 is involved in triggering the OmpU-mediated pro-inflammatory responses in DCs both in *ex vivo* and *in vivo* conditions (Fig. 4E, F).

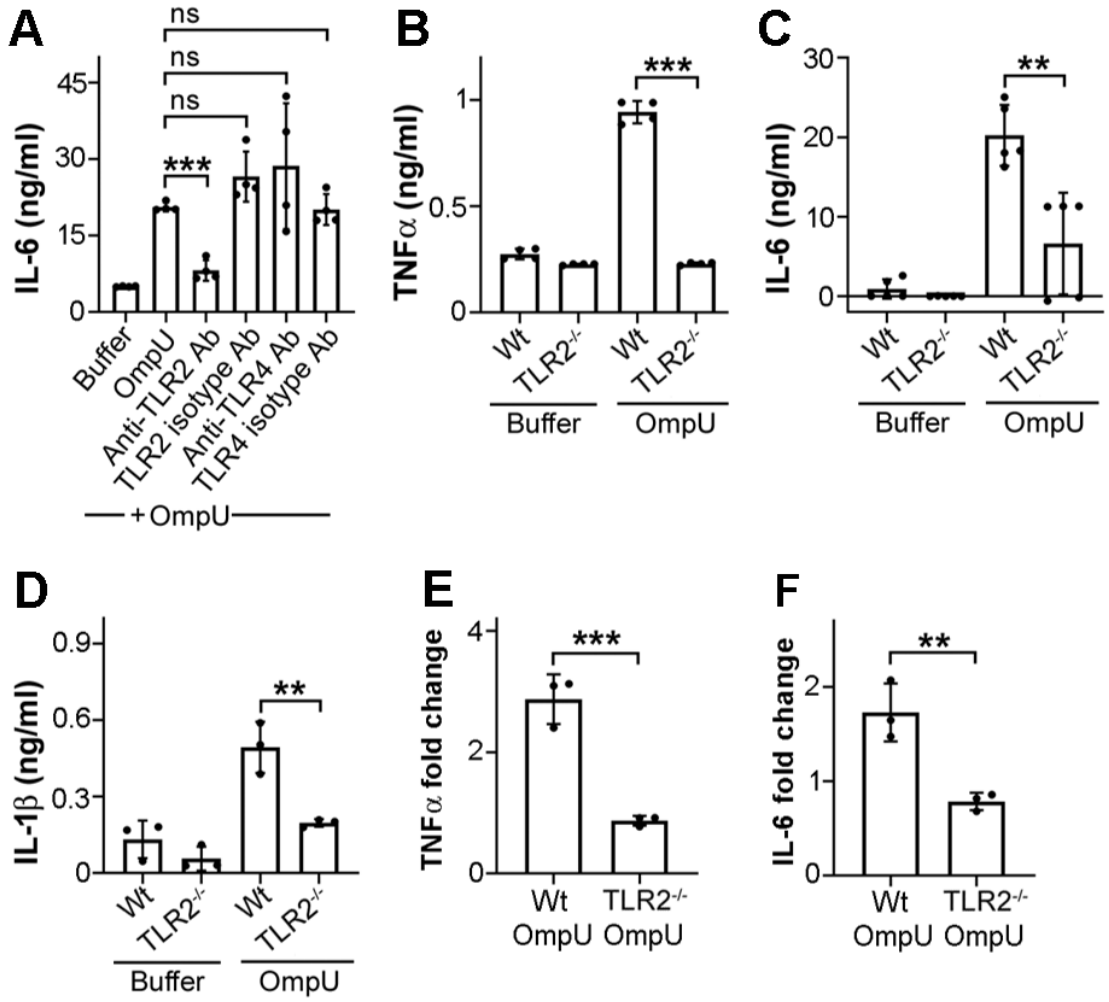


**Figure 4: OmpU induces pro-inflammatory cytokine production in DCs via TLR2.**

*(A) Significant decrease in IL-6 levels in OmpU-treated DCs upon TLR2 neutralisation but not with TLR4 neutralisation. BMDCs were pre-treated with anti-TLR2 or anti-TLR4 neutralising antibody for 1 h. Following incubation, cells were treated with OmpU (3 μg/ml) and incubated for 24 h. Cells pre-treated with isotype antibody and buffer-treated cells served as controls. Collected supernatants were analysed for IL-6 production by ELISA. Results are expressed as mean ± SD and represent the average of four independent experiments. ***p < 0.001, ns denotes non-significant versus OmpU-treated BMDCs.*

*(B, C, D) Significant decrease in cytokine levels in OmpU-treated BMDCs in the absence of TLR2. BMDCs from Wt (wildtype) and TLR2$^{-/-}$ mice were treated with OmpU (3 μg/ml) or buffer for 24 h. Levels of (B) TNFα, (C) IL-6 and (D) IL-1β were measured by ELISA in culture supernatants. Results are expressed as mean ± SD and represent the average of three to five independent experiments. **p< 0.01, ***p < 0.001 versus OmpU-treated Wt BMDCs.*

*(E, F) TNFα and IL-6 gene expression was significantly decreased in splenic DCs isolated from OmpU I.P. TLR2$^{-/-}$ mice. Wt (Wildtype) and TLR2$^{-/-}$ mice were injected with 100 μg OmpU I.P. and splenic DCs were isolated 6 h post-I.P., and total RNA was extracted, followed by relative (E) TNFα and (F) IL-6 gene expression analysis by semi-quantitative real-time PCR. Results are expressed as mean ± SD and represent the average of three independent experiments. Statistical analysis was done using student's two-sided t-test. **p< 0.01, ***p < 0.001 versus OmpU I.P. Wt mice.*

## 3.7 Specific aim 2: To understand the signalling molecules involved in OmpU-mediated activation of DCs.

As we observed, OmpU mediates the activation of DCs via the induction of TLR2; we further investigated the downstream signalling mediators activated in response to OmpU.

### 3.7.1 OmpU activates IKK and induces NFκB activation in DCs

TLR signalling is known to induce several mediators and transcription factors and NFκB is a typical transcription factor involved in promoting the gene expression for inflammatory processes. Therefore, we next questioned if OmpU induces NFκB activation for the generation of pro-inflammatory responses. In the steady-state condition, the NFκB protein is sequestered in the cytoplasm by the IκB family protein members, and upon stimulation, the IκB is degraded by IκB kinase (IKK) complex proteins via phosphorylation which leads to the translocation of NFκB proteins into the nucleus for pro-inflammatory gene expression [130].

Towards understanding whether OmpU is able to activate NFκB in DCs, we first wanted to check whether IKK is involved in OmpU-mediated DC activation. We observed a significant inhibition of IL-6 responses in OmpU-induced BMDCs in the presence of pharmacological

inhibitor of IKK (PS-1145) indicating that IKK is involved and therefore NFκB might be involved in OmpU-mediated signalling (Fig. 5A).

To confirm the role of NFκB, we further probed for the levels of IκBα, a typical IκB family protein, upon OmpU treatment by western blotting. We observed that IκBα levels decreased with OmpU treatment in the BMDCs compared to buffer-treated cells indicating degradation of IκBα and activation of NFκB in response to OmpU stimulation (Fig. 5B).

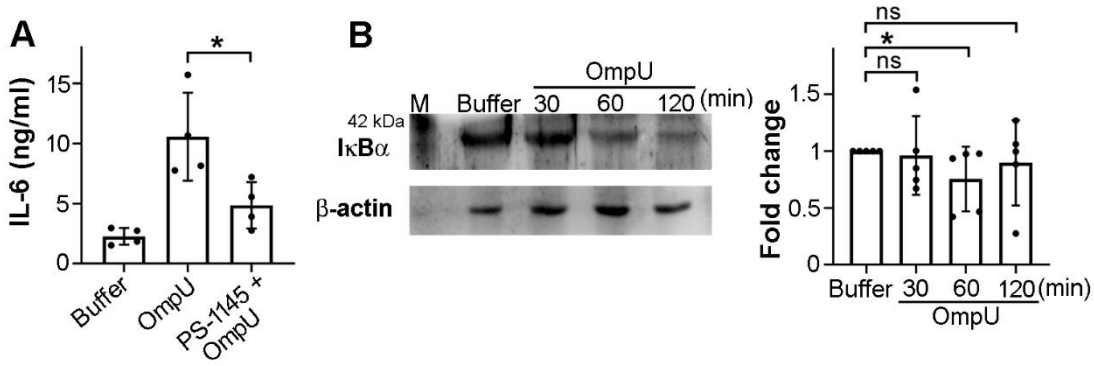


**Figure 5: IκB is degraded downstream of OmpU-mediated signalling in DCs**

*(A) OmpU-mediated cytokine production is inhibited in the presence of IKK inhibitor PS-1145 in DCs. BMDCs were pre-treated with 2.5 μM PS-1145 for 1 h, followed by OmpU (3 μg/ml) treatment for 24 h. Following incubation, culture supernatants were then checked for IL-6 production using ELISA. Bar graph represents mean ± SD from four independent experiments. *p< 0.05 versus OmpU-treated cells.*

*(B) Decrease in IκBα levels in OmpU-treated DCs. BMDCs were treated with OmpU (3 μg/ml) or buffer for the given time points, followed by whole-cell lysate preparation. The lysates were then analysed for IκBα levels by immunoblotting. β-actin was used as a loading control. The fold change was calculated with respect to buffer-treated cells. Bar graph represents mean ± SD from five independent experiments. Statistical analysis was done using student's two-sided t-test. *p< 0.05, ns denotes non-significant versus buffer-treated cells.*

### 3.7.2 OmpU activates MAP kinases p38, JNK and ERK in DCs to induce pro-inflammatory responses

As mentioned earlier, TLR signalling activates MAP kinases such as p38, JNK and ERK, which phosphorylate and activate their downstream targets, for instance, NFκB and AP-1 transcription factors and induce pro-inflammatory responses. Therefore, in the case of OmpU-induced DC activation, we probed whether MAPKs play a role in pro-inflammatory response generation. Previously my senior Dr. Sanica C. Sakharwade, investigated the role of p38 and JNK MAPKs in OmpU-mediated pro-inflammatory responses in DCs. She observed that in

presence of pharmacological inhibitors for p38 (VX745) and JNK (JNK-IN-8 and SP600125) there is a significant decrease in the cytokine responses by OmpU-treated DCs suggesting the involvement of p38 and JNK (Fig. 6A, B).

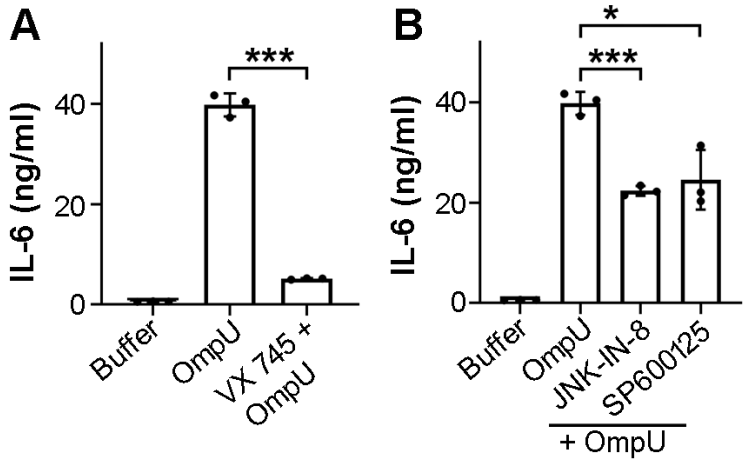


**Figure 6: MAPKs p38 and JNK are involved in OmpU-mediated cytokine production. (shown by Dr. Sanica C. Sakharwade)**

*(A, B) Decrease in OmpU-mediated cytokine production in the presence of p38 inhibitor VX745 (A) and JNK inhibitor (B) in DCs. BMDCs were pre-treated with 50 nM VX745 (A) and, 250 nM JNK-IN-8 and 20 µM SP600125 (B) for 1 h, followed by OmpU treatment (3 µg/ml) for 24 h. Following incubation, culture supernatants were checked for IL-6 production using ELISA. Bar graph represents mean ± SD from three independent experiments. Statistical analysis was done using student's two-sided t-test. *p< 0.05, ***p < 0.001 versus only OmpU-treated cells.*

Further to confirm the involvement of p38 and JNK, we have treated BMDCs with OmpU and prepared whole cell lysates at different time points and checked for the phosphorylation levels of p38 and JNK by western blotting. We observed an increase in phosphorylation levels in OmpU-treated samples compared to the buffer-treated cells. Also, we observed that phosphorylation levels of ERK were increased in response to OmpU in DCs. As phosphorylation status is indicative of their activation status, these data confirm the involvement of MAPKs in OmpU-mediated signalling in DCs (Fig. 7A, B & 8A).

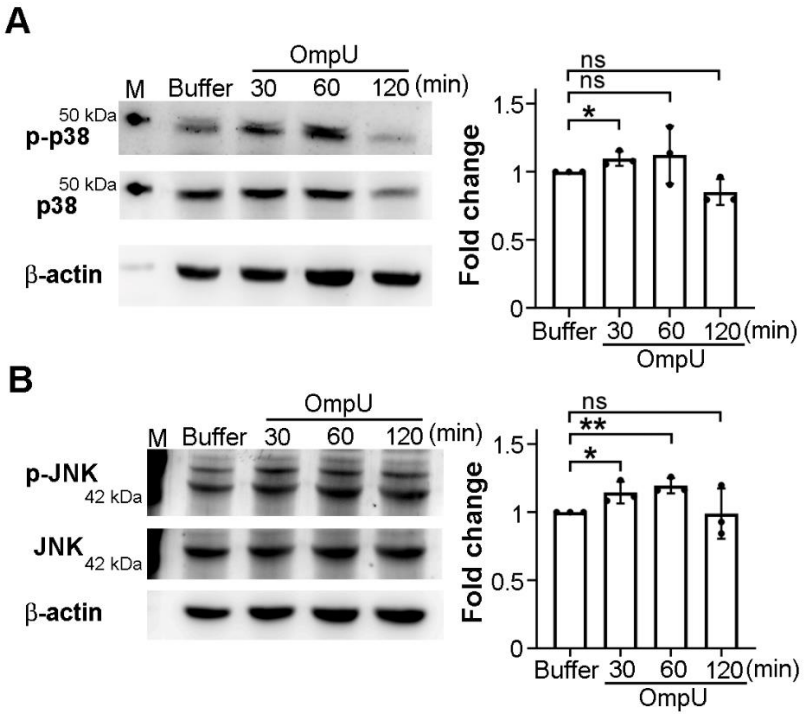


**Figure 7: MAP kinases p38 and JNK are involved in OmpU-mediated downstream signalling.**

*(A) Increase in MAPK phospho-p38 (p-p38) levels following OmpU treatment in DCs. BMDCs were treated with OmpU (3 μg/ml) or buffer for the given time points, followed by whole-cell lysate preparation. The lysates were then analysed for p-p38 and p38 levels by immunoblotting. β-actin was used as a loading control. The fold change was calculated with respect to buffer-treated cells. Bar graph represents mean ± SD from three independent experiments. *p< 0.05, ns denotes non-significant versus buffer-treated cells.*

*(B) Increase in MAPK phospho-JNK (p-JNK) levels following OmpU treatment in DCs. BMDCs were treated with OmpU (3 μg/ml) or buffer for the given time points, followed by whole-cell lysate preparation. The lysates were then analysed for p-JNK and JNK levels by immunoblotting. β-actin was used as a loading control. The fold change was calculated with respect to buffer-treated cells. Bar graph represents mean ± SD from three independent experiments. Statistical analysis was done using student's two-sided t-test. *p< 0.05, **p< 0.01, ns denotes non-significant versus buffer-treated cells.*

We further checked whether ERK is also involved in pro-inflammatory cytokine production in DCs and observed that using MEK inhibitor (PD184352), the IL-6 production was markedly reduced in OmpU-treated BMDCs (Fig. 8B). Thus, our results confirmed that MAPK ERK-mediated signalling also contributes to pro-inflammatory responses in OmpU-stimulated DCs.

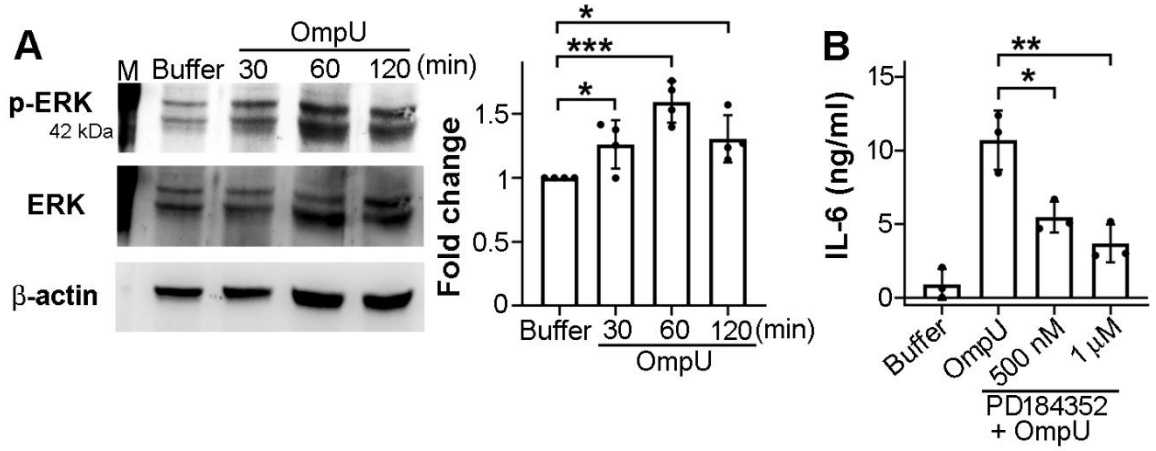


**Figure 8: MAPK ERK is involved in OmpU-mediated DC activation.**

*(A) Increase in MAPK phospho-ERK (p-ERK) levels after OmpU treatment in DCs. BMDCs were treated with OmpU (3 µg/ml) or buffer for the given time points, followed by whole-cell lysate preparation. The lysates were then analysed for p-ERK and ERK levels by immunoblotting. β-actin was used as a loading control. The fold change was calculated with respect to buffer-treated cells. Bar graph represents mean ± SD from four independent experiments. *p< 0.05, ***p < 0.001 versus buffer-treated cells.*

*(B) Decrease in OmpU-mediated cytokine production in the presence of MEK inhibitor PD184352 in DCs. BMDCs were pre-treated with 500 nM and 1 µM PD184352 for 1 h, followed by OmpU treatment (3 µg/ml) for 24 h. Following incubation, culture supernatants were checked for IL-6 production using ELISA. Bar graph represents mean ± SD from three independent experiments. Statistical analysis was done using student's two-sided t-test. *p< 0.05, **p< 0.01 versus only OmpU-treated cells.*

### 3.7.3 OmpU-mediated DC activation leads to the signalling via PI3K-AKT

As mentioned earlier, apart from MAPKs, TLRs can activate the phosphoinositide-3-kinases (PI3Ks), which initiate downstream cascade, culminating in the generation of pro-inflammatory responses. Hence, we wanted to check whether PI3K pathway is activated in response to OmpU in DCs. To elucidate this, we treated BMDCs with OmpU at different time points, prepared whole cell lysates and estimated the levels of phosphorylated PI3K using western blotting. We observed an increase in phosphorylated PI3K at 60 min and 120 min following OmpU treatment compared to buffer-treated cells (Fig. 9A). Further, we observed a significant decrease in IL-6 production in presence of a general PI3K inhibitor (LY294002) in OmpU-treated BMDCs (Fig. 9B).

As PI3K is categorised into three different types: class I PI3K (PI3Kα, β, γ, δ isoforms), class II PI3K (PI3KC2α, C2β, C2γ isoforms) and class III PI3K (Vps34), to discern the class of PI3K involved in OmpU signalling, we, GDC-0941, a class I/class II PI3K-specific inhibitor, and

SAR 405, a class III PI3K-specific inhibitor. We observed a significant decrease in IL-6 production in OmpU-activated DCs which were pre-treated with GDC-0941 but not with SAR 405, confirming that class I/class II PI3K is involved in OmpU-mediated DC activation (Fig. 9C, D).

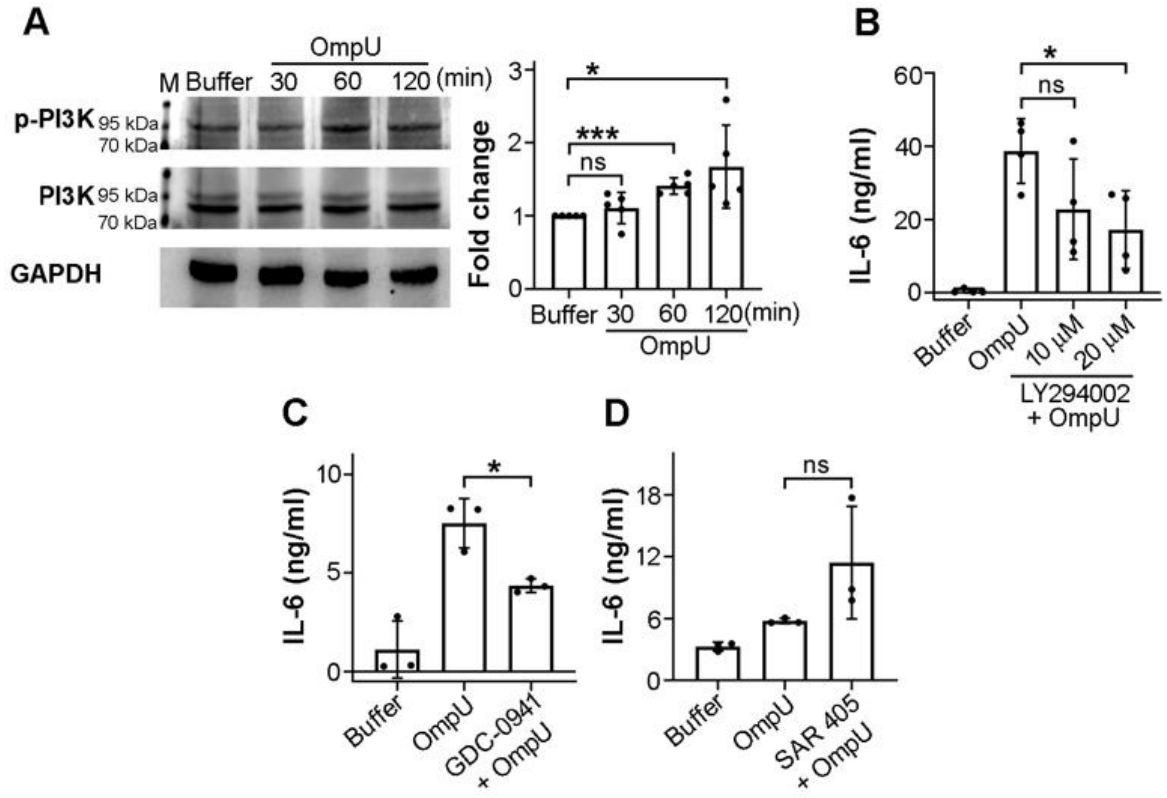


**Figure 9: PI3K is activated in OmpU-mediated signalling in DCs.**

*(A) Increase in phospho-PI3K (p-PI3K) levels following OmpU treatment in DCs. BMDCs were treated with OmpU (3 μg/ml) or buffer for the given time points, and then whole-cell lysates were prepared. The lysates were analysed for p-PI3K and PI3K by immunoblotting. GAPDH was used as a loading control. The fold change was calculated with respect to buffer-treated cells. Bar graph represents mean ± SD from five independent experiments. *p< 0.05, ***p < 0.001, ns denotes non-significant versus buffer-treated cells.*

*(B, C) OmpU-mediated cytokine production was decreased in the presence of a general PI3K inhibitor and PI3K class I inhibitor in OmpU-treated DCs. BMDCs were pre-treated with 10 μM and 20 μM PI3K inhibitor LY294002 (B) and 1 μM PI3K class I- specific inhibitor GDC-0941 (C) for 1 h, followed by OmpU (3 μg/ml) treatment for 24 h. Following incubation, the culture supernatants were checked for IL-6 production using ELISA. Bar graph represents mean ± SD from three to four independent experiments. *p< 0.05, ns indicates non-significant versus OmpU-treated cells.*

*(D) PI3K class III inhibitor SAR 405 showed no inhibition in OmpU-mediated cytokine production. BMDCs were pre-treated with 200 nM SAR 405 for 1 h, followed by OmpU (3 μg/ml) treatment for 24 h, and the culture supernatants were probed for IL-6 production using ELISA. Bar graph represents mean ± SD from three independent experiments. Statistical analysis was done using student's two-sided t-test. ns indicates non-significant versus OmpU-treated cells.*

AKT is a conventional downstream target of PI3K. As we observed PI3K is involved, we further explored whether AKT is involved in OmpU-mediated DC activation. We treated BMDCs with OmpU at different time points and probed for phosphorylation status of AKT in the whole cell lysate using western blotting. We observed that the level of phosphorylation of AKT was increased at 60 min and 120 min in OmpU-treated compared to the buffer-treated BMDCs suggesting the activation of AKT in OmpU-mediated signalling (Fig. 10A). To determine the role of AKT in pro-inflammatory responses in OmpU-activated DCs, we used an inhibitor, AKT VIII and observed that IL-6 production was reduced in OmpU-treated BMDCs in presence of AKT VIII (Fig. 10B). Thus, from our experiments we concluded that PI3K-AKT signalling is activated in OmpU-treated DCs and contributes to the pro-inflammatory responses.

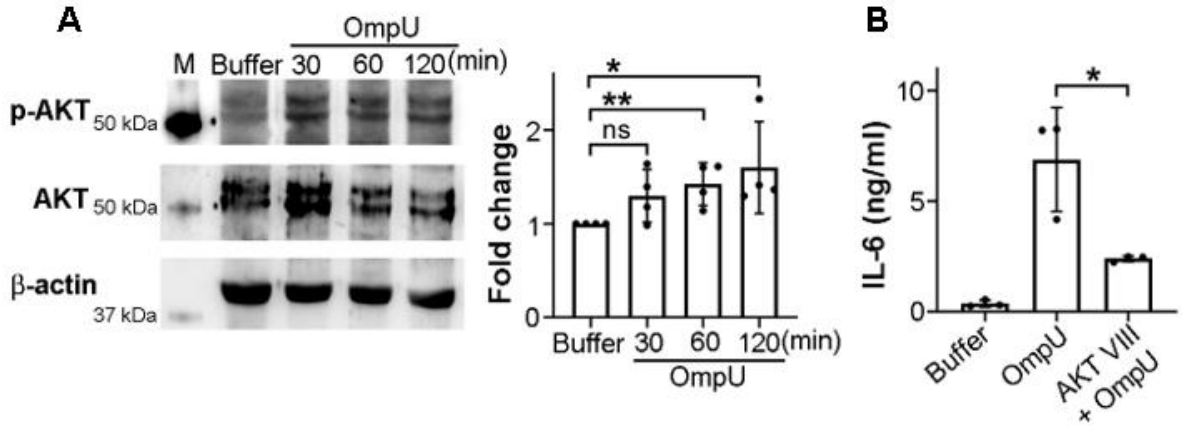


**Figure 10: AKT is involved in OmpU-mediated downstream signalling in DCs.**

*(A) The phospho-AKT (p-AKT) levels increased after OmpU treatment in DCs. BMDCs were treated with OmpU (3 μg/ml) or buffer for the given time points, followed by whole-cell lysate preparation, and the lysates were analysed for p-AKT and AKT levels by immunoblotting. β-actin was used as a loading control. The fold change was calculated compared to the buffer-treated cells. Bar graph represents mean ± SD from four independent experiments. *p< 0.05, **p< 0.01 and ns denotes non-significant versus buffer-treated cells.*

*(B) OmpU-mediated cytokine production was decreased in the presence of AKT inhibitor in DCs. BMDCs were pre-treated with 8 μM AKT VIII inhibitor for 1 h, followed by OmpU (3 μg/ml) treatment for 24 h. Following incubation, the culture supernatants were checked for IL-6 production using ELISA. Bar graph represents mean ± SD from three independent experiments. Statistical analysis was done using student's two-sided t-test. *p< 0.05 versus OmpU-treated cells.*

### 3.7.4 OmpU-mediated DC activation involves calcium signalling and PKC activation

As mentioned earlier, protein kinase C (PKCs) can be activated downstream of PI3Ks via calcium ($Ca^{2+}$) signalling and diacylglycerol (DAG) and lead to the phosphorylation of diverse inflammatory cellular proteins. Therefore, we have investigated whether $Ca^{2+}$ flux and PKC were involved in the OmpU-mediated activation of DCs.

Towards probing whether calcium flux is induced in OmpU-activated DCs, we have loaded the BMDCs with calcium-sensing dye, Fluo-4 AM and treated with OmpU or buffer or PMA + Ionomycin (positive control) prior to acquiring the cells in the flow cytometer. We observed that the fluorescence in OmpU-treated cells was enhanced compared to the buffer-treated cells in a time-dependent manner, implying a surge in intracellular calcium levels in response to OmpU (Fig. 11A). Moreover, we found that BAPTA-AM, an intracellular calcium chelator inhibited the calcium flux in response to OmpU (Fig. 11B).

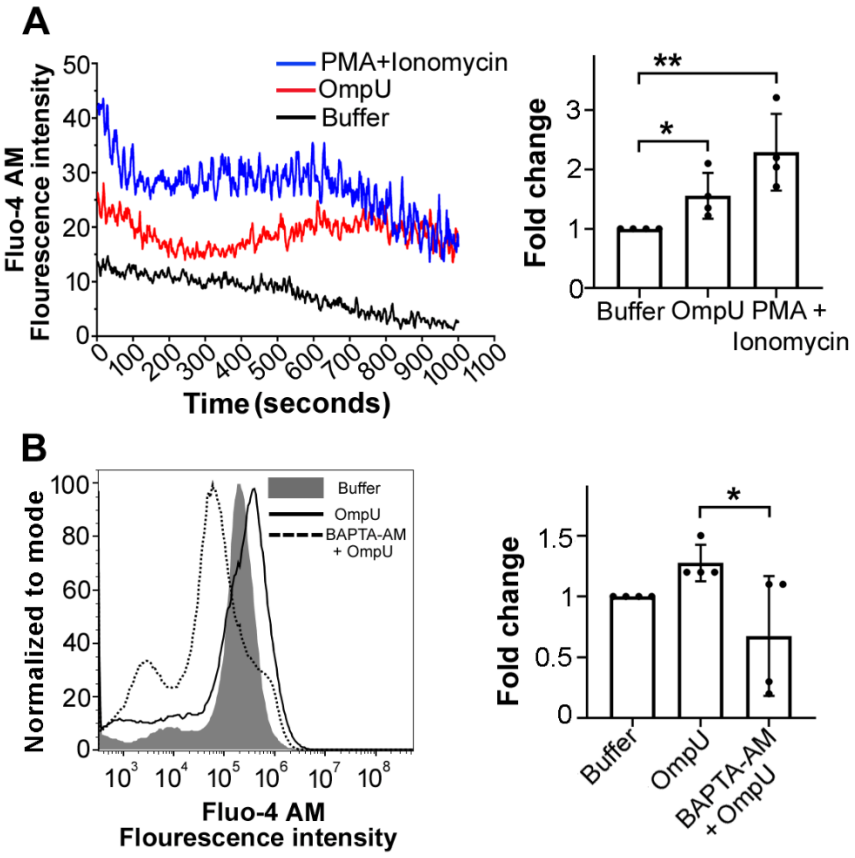


**Figure 11: OmpU induces calcium influx in DCs.**

*(A) Increase in the intracellular calcium levels in DCs following OmpU treatment. BMDCs were loaded with Fluo-4 (AM) dye mixture for 1 h, and then the cells were washed and harvested in HBSS with calcium and magnesium. OmpU (5 µg/ml) or buffer were added to the cells before acquiring the samples*

*in the FACSCalibur flow cytometer for time kinetics. PMA (1 μg/ml) and Ionomycin (1 μg/ml) treated cells were used as a positive control. The time kinetics plot is representative of four independent experiments. Fold change was calculated with respect to buffer-treated cells. Bar graph represents mean ± SD from four independent experiments. *p< 0.05, **p< 0.01 versus buffer-treated cells.*

*(B) OmpU-induced calcium flux in DCs was abrogated in the presence of BAPTA-AM. BMDCs were pre-treated with BAPTA-AM for 1 h and loaded with Fluo-4 (AM) dye mixture. The cells were harvested, and OmpU (5 μg/ml) was added before acquiring the cells in the flow cytometer for the time kinetics. Histogram plot is representative of four independent experiments. Fold change was calculated compared to buffer-treated cells. Bar graph represents mean ± SD from four independent experiments. Statistical analysis was done using student's two-sided t-test. *p< 0.05 versus OmpU-treated cells.*

To probe whether OmpU-mediated signalling is involved in PKC activation, we have treated BMDCs with OmpU at different points and probed for phosphorylation status of PKC in the whole cell lysate by western blotting. We examined that the levels of phosphorylated PKC were increased in OmpU-treated BMDCs compared to the buffer-treated cells suggesting the activation of PKC (Fig. 12A). Further, to determine the role of PKC in OmpU-mediated pro-inflammatory responses, we assessed the cytokine production in OmpU-treated BMDCs in the presence of general PKC inhibitor, BIM IV. We observed that IL-6 and IL-1β production was significantly reduced in OmpU-treated cells in presence of BIM IV (Fig. 12B, C). Further, as the conventional PKCs can be categorised into different isoforms such as PKCα, βI, βII and γ. Therefore, to discern the isoform of PKC involved, we used PKCα/γ isoform-specific inhibitor HBDDE and checked for the IL-6 production following OmpU treatment. We found that IL-6 production was inhibited in the presence of HBDDE, suggesting the involvement of PKCα/γ in OmpU-mediated DC activation (Fig. 12D).

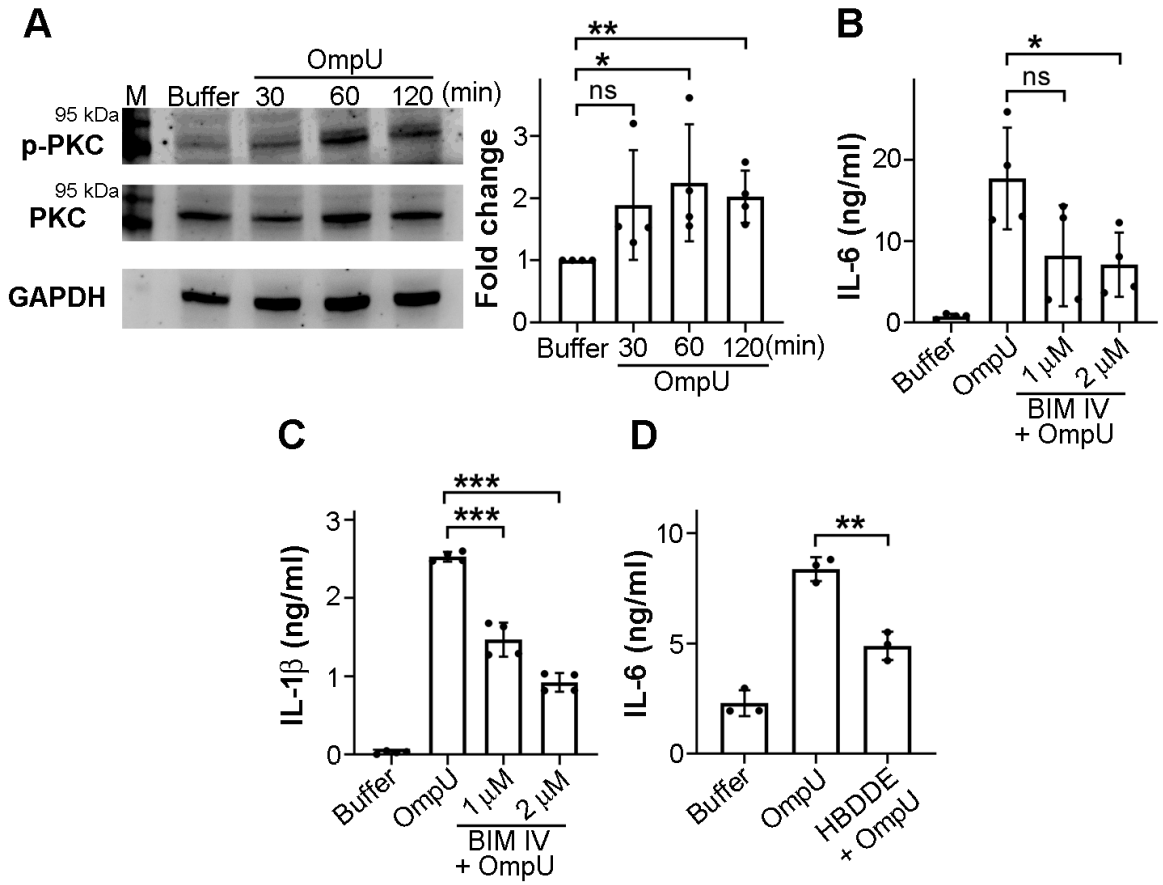


**Figure 12: PKC induced signalling is involved in OmpU-mediated responses.**

*(A) Increase in phospho-PKC (p-PKC) levels following OmpU treatment in DCs. BMDCs were treated with OmpU (3 µg/ml) or buffer for the given time points followed by whole-cell lysate preparation, and then the lysates were analysed for p-PKC and PKC levels by immunoblotting. GAPDH was used as a loading control. The fold change was calculated with respect to buffer-treated cells. Bar graph represents mean ± SD from four independent experiments. *p< 0.05, **p< 0.01 versus buffer-treated cells.*

*(B, C) OmpU-mediated cytokine production was decreased in OmpU-treated DCs in the presence of a general PKC inhibitor. BMDCs were pre-treated with 1 µM and 2 µM PKC inhibitor BIM IV for 1 h, followed by treatment with OmpU (3 µg/ml) for 24 h. After incubation, culture supernatants were analysed for (B) IL-6 and (C) IL-1β production using ELISA. Bar graph represents mean ± SD from three independent experiments. *p< 0.05, ***p < 0.001, ns indicates non-significant versus only OmpU-treated cells.*

*(D) OmpU-induced IL-6 production was decreased in the presence of PKCα/γ-isoform inhibitor HBDDE in DCs. BMDCs were pre-treated with 50 µM HBDDE for 1 h, followed by treatment with OmpU (3 µg/ml) for 24 h. Following incubation, culture supernatants were analysed for IL-6 using ELISA. Bar graph represents mean ± SD from three independent experiments. Statistical analysis was done using student's two-sided t-test. **p< 0.01 versus only OmpU-treated cells.*

### 3.7.5 OmpU-mediated activation of calcium signalling, PKC, MAPKs p38 and ERK, and NFκB was TLR2 dependent, while PI3K and MAPK JNK activation was TLR2 independent

As we observed that OmpU-mediated signalling activates various signalling molecules, we probed whether TLR2 induces the downstream signalling for activation of MAPKs, PI3K, PKC, calcium flux and NFκB. For this, we treated the BMDCs from wildtype and $TLR2^{-/-}$ transgenic mice with OmpU and probed for the signalling molecules. We observed that OmpU-induced calcium influx was abrogated in the BMDCs from $TLR2^{-/-}$ transgenic mice suggesting that calcium influx was TLR2 dependent (Fig. 13G). Further, we observed that the phosphorylation of MAPKs p38 and ERK, and PKC was decreased in OmpU-treated $TLR2^{-/-}$ BMDCs compared to the wildtype (Wt) BMDCs but the phosphorylation levels of PI3K and MAPK JNK were unaffected in the absence of TLR2 (Fig. 13A-E). Also, the IκBα levels were enhanced in the OmpU-treated $TLR2^{-/-}$ BMDCs compared to the Wt BMDCs (Fig. 13F). These results indicate that MAPKs p38 and ERK, PKC and NFκB activation depends on TLR2 while the activation of MAPK JNK and PI3K was TLR2 independent. Thus, some other receptor could be involved in the activation of JNK and PI3K.

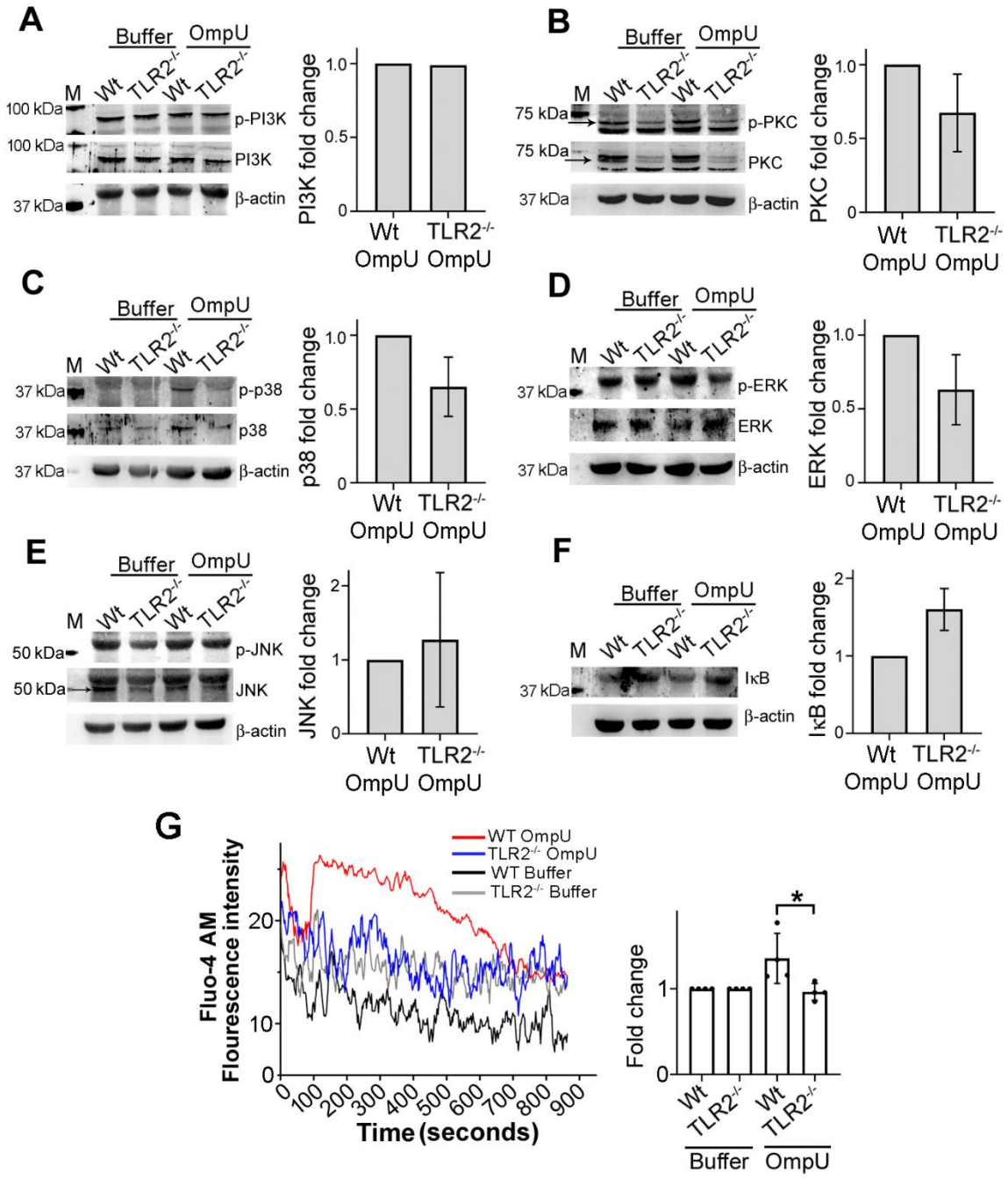


**Figure 13: OmpU induced activation of MAPKs p38 and ERK, PKC, IκB and calcium influx is TLR2 dependent while MAPK JNK and PI3K activation is TLR2 independent.**

*(A to F) BMDCs from wildtype (Wt) and TLR2$^{-/-}$ mice were treated with 3 μg/mL of OmpU or buffer for 30 min, followed by whole cell lysate preparation. The lysates were then analysed for (A) p-PI3K, PI3K, (B) p-PKC, PKC, (C) p-p38, p38 (D) p-ERK and ERK, (E) p-JNK and JNK, and (F) IkB by immunoblotting. β-Actin was used as a loading control. The blots shown are representative of two independent experiments. The bar graph indicates the fold change over wild-type OmpU-treated BMDCs and represents the mean ± SD from two independent experiments.*
*(G) BMDCs from wildtype (Wt) and TLR2$^{-/-}$ mice were loaded with Fluo-4 (AM) dye mixture for 1 h. Following washing using 1x PBS, the cells were harvested in HBSS with calcium and magnesium.*

*OmpU (5 μg/mL) or buffer was added to the cells, and the cells were acquired in the flow cytometer. The time kinetics plot is representative of four independent experiments. Fluo-4 (AM) fluorescence was measured per second for 800 s, and a histogram was obtained by plotting the mean fluorescence intensity (MFI) obtained for the total time. The bar graph represents the mean ± SD from four independent experiments. Statistical analysis was done using student's two-sided t-test. *p< 0.05 versus wild-type OmpU-treated cells.*

### 3.8 Conclusion

In this study, we questioned if *Vibrio cholerae* OmpU induces the activation and maturation of DCs and further explored the signalling involved in the production of various pro-inflammatory responses. Previous observations by Dr. Sanica C. Sakharwade from our lab suggested that OmpU can activate DCs probably by acting as a PAMP and induces the production of pro-inflammatory cytokines IL-6, TNFα and IL-1β. Further, I have observed that OmpU induces an increase in the expression of MHC II and co-stimulatory molecules, indicating DC maturation.

To discern the PRR in OmpU-mediated DC activation, we observed that MyD88 was involved in OmpU-mediated DC activation, suggesting the PRR must be a TLR. Further, we confirmed that OmpU signals via TLR2, which acts as a PRR leading to pro-inflammatory cytokine production *ex vivo* in BMDCs as well as *in vivo* in splenic DCs isolated from mice immunized with OmpU.

We delved into the downstream signalling induced by OmpU in DCs and observed that IKK is involved in OmpU-induced cytokine responses and, it further, leads to the activation of transcription factor NFκB. As the activation of transcription factor requires activation of various upstream signalling mediators, our investigation further revealed that MAPKs p38, JNK and ERK were activated in OmpU-treated DCs, indicating their role in OmpU-mediated pro-inflammatory signalling. Further, the inhibitor studies of MAPKs confirmed their role in OmpU-induced pro-inflammatory responses. We observed that OmpU elicited PI3K-AKT signalling to induce the pro-inflammatory responses in DCs. It further induced calcium influx in OmpU-treated DCs and led to activation of PKC, which contributed to the pro-inflammatory cytokine production. Furthermore, TLR2 was involved in the activation of MAPKs p38 and ERK, PKC and NFκB whereas the activation of MAPK JNK and PI3K was TLR2 independent.

**Aim 2:** To explore whether inflammasome complex is involved in OmpU-mediated DC activation.

**Specific aim 1:** Whether and which inflammasome complex is involved in OmpU-mediated DC activation?

**Specific aim 2:** How the inflammasome complex is activated in DCs in response to OmpU?

# Aim 2: To explore whether inflammasome complex is involved in OmpU-mediated DC activation.

## 4.1 Production of IL-1β involves signalling via inflammasome

Inflammasome serve as major cytoplasmic signalling complex in innate immune cells, such as macrophages, DCs, neutrophils and many more. It is a multiprotein assembly formed by oligomerization of receptor proteins/sensors, adaptor protein known as apoptosis-associated speck-like protein containing CARD domain (ASC) and pro-caspase-1 and triggered by diverse stimuli such as PAMPs, DAMPs and cellular stress [131]. This complex is prompted by different NOD-like receptor (NLRs) family proteins which act as sensors and recruit ASC to the complex. Consequently, ASC self-oligomerizes by pyrin domain interactions (PYD) and recruits pro-caspase-1 via the CARD domain interactions. This triggers the self-cleavage of pro-caspase-1 into active caspase-1 which further acts on pro-IL-1β/IL-18 leading to the secretion of mature IL-1β/IL-18 from the cells (as shown in the illustration 8) [132]. Further, caspase-1 also activates intra-cellular host protein gasdermin D which upon activation form pores on the cell membrane and can mediate, a form of lytic cell death, termed pyroptosis in the cells [133].

## 4.2 Mechanism of NLRP3 inflammasome activation

On the basis of variations in the receptor structures and ligand recognition, inflammasome complexes can be of different types such as NLRP1, NLRP3, NLRP6, NLRP7, NLRC4 and AIM2 among others [134]. NLRP3 and NLRC4 inflammasomes are generally activated during bacterial pathogenesis [135, 136]. Generally, NLRP3 inflammasome recognises varied signals ranging from bacterial, fungal and viral agonists to ion flux imbalances [137]. Numerous Gram-negative bacteria such as *Salmonella enterica*, *Vibrio cholerae* and *Vibrio vulnificus* activate NLRP3 inflammasome in macrophages [138, 139]. Further, bacterial ligands such as flagellin, toxins (MARTX, haemolysin and many more) and LPS are known inducers of NLRP3 inflammasome [139, 140]. Potassium efflux from the cell, chloride efflux, calcium mobilization, changes in mitochondrial membrane potential (MMP), mitochondrial ROS (mitoROS) and lysosomal destabilization and rupture can trigger the NLRP3 inflammasome activation as shown in illustration 8 [137, 141-143].

Besides microbe-derived signals, various sterile and particulate ligands such as alum crystals, cholesterol crystals and amyloid fibrils also trigger NLRP3 inflammasome which aggravate diseases such as atherosclerosis, Alzheimer's disease and gout [144-146]. Thus, although NLRP3 inflammasome is critical in generating host immune responses, it can also exacerbate the pathogenesis of various inflammatory disorders.

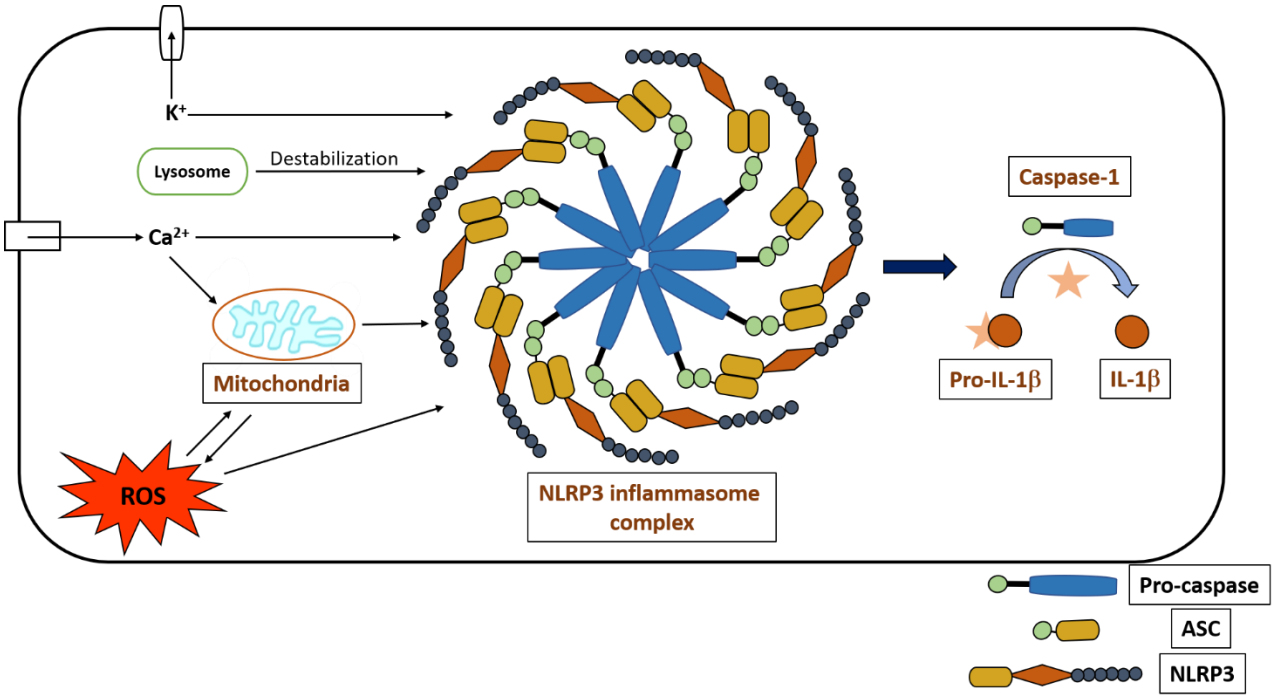


**Illustration 8: Mechanisms of NLRP3 activation.**

*The NLRP3 inflammasome is activated by various stimuli such as ion imbalances and reactive oxygen species (ROS) triggered in response to diverse pathogen-associated molecular patterns (PAMPs) and damage-associated molecular patterns (DAMPs). The activation and assembly of NLRP3 leads to cleavage of pro-caspase-1 into active caspase-1 and the active caspase-1 acts on pro-IL-1β secreting mature IL-1β from the cells.*

### 4.3 Specific aim 1: Whether and which inflammasome complex is involved in OmpU-mediated DC activation?

Previously in our laboratory, we have observed that OmpU induces the production of IL-1β in DCs. As discussed in the above sections, IL-1β release from the cells require activation of inflammasome, therefore, we wanted to probe whether in case of OmpU-mediated DC activation any inflammasome complex is involved.

### 4.3.1 OmpU induces the activation of caspase-1 in DCs

The secretion of IL-1β from cell requires two signals; one signal involves activation of TLRs which leads to the transcriptional upregulation of inflammasome components and pro-IL-1β while the other signal perceived by the inflammasome leads to the cleavage of pro-caspase-1 into active caspase-1 [147]. The activation of caspase-1 results in the release of IL-1β from the cells. Therefore, to investigate the involvement of inflammasome in response to OmpU, we studied whether caspase-1 is involved in IL-1β production in DCs. For this, we pre-treated the cells with caspase-1 specific inhibitor Ac-YVAD-fmk, and checked for IL-1β production in the culture supernatant following OmpU treatment for 24 h [148]. We found that the IL-1β levels were significantly reduced in presence of Ac-YVAD-fmk indicating the role of caspase-1 in OmpU-mediated IL-1β production (Fig. 13).

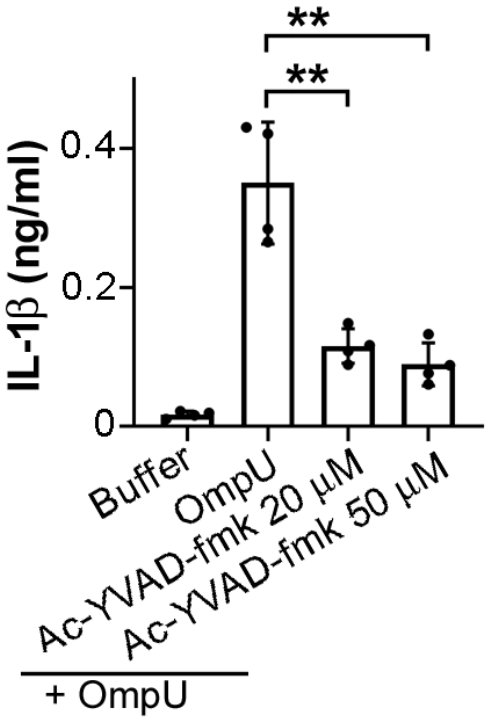


**Figure 14: IL-1β production is inhibited in presence of caspase-1 inhibitor.**

*BMDCs were pre-treated with specific caspase-1 inhibitor Ac-YVAD-fmk for 1 h, followed by OmpU (3 μg/ml) treatment for 24 h. IL-1β levels were measured by ELISA in the culture supernatants. Results are expressed as mean ± SD and represent the average of four independent experiments. Statistical analysis was done using student's two-sided t-test. **p< 0.01 versus OmpU-treated DCs.*

Further, to confirm the involvement of caspase-1, we checked the levels of active caspase-1 and pro-caspase 1 in OmpU-treated DCs. We have observed that in OmpU-treated DCs the

active caspase-1 levels were upregulated compared to the buffer-treated cells suggesting that inflammasome complex is probably activated in response to OmpU in DCs (Fig. 14).

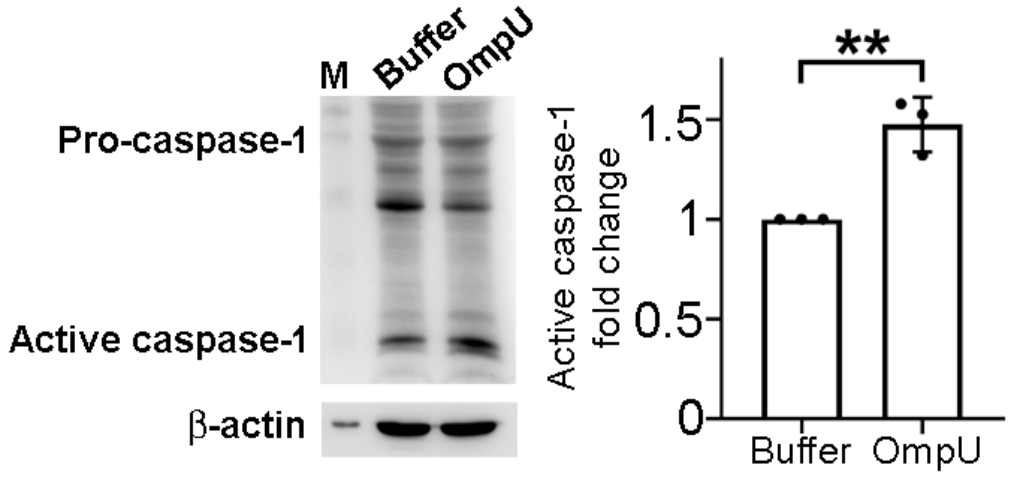


**Figure 15: OmpU induces caspase-1 activation in DCs.**

*BMDCs were treated with OmpU (3 μg/ml) for 2 h. Whole-cell lysates were prepared and analysed for pro-caspase-1 and active caspase-1 by immunoblotting. β-actin was used as a loading control. Blot shown is representative of three independent experiments. Fold change for active caspase-1 was calculated over the buffer-treated cells. Bar graph represents mean ± SD and includes the average of three independent experiments. Statistical analysis was done using student's two-sided t-test. **p< 0.01 versus OmpU-treated DCs.*

### 4.3.2 OmpU induces NLRP3 inflammasome activation in DCs

As we have observed caspase-1 activation in DCs, we further probed for the inflammasome complex involved in OmpU-mediated IL-1β production. Out of the several inflammasome complexes reported, NLRP3 is the most studied inflammasome in case of bacterial ligands and can be activated via various stimuli. Therefore, we investigated whether NLRP3 is involved in OmpU-mediated IL-1β production. By immunoblotting, we found that the expression of NLRP3 is increased at protein level in OmpU-treated cells compared to the buffer-treated cells (Fig. 15).

In literature it is being reported that NLRP3 is recruited to mitochondria for activation and interacts with various mitochondrial membrane proteins such as mitochondrial antiviral-signal protein (MAVS), mitofusin 2 and cardiolipin [149-152]. Therefore, we probed whether NLRP3 is recruited to mitochondria in response to OmpU in DCs. We treated BMDCs with buffer or

OmpU for 30 min and using confocal microscopy, we have observed that NLRP3 colocalized with the mitochondrial marker TIM23 indicating that NLRP3 might be the inflammasome complex involved in OmpU-mediated IL-1β production in DCs (Fig. 16A).

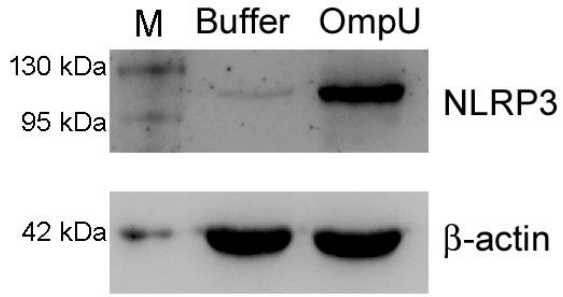


**Figure 16: NLRP3 is upregulated in OmpU-treated DCs.**

*Increase in expression of NLRP3 protein in OmpU-treated DCs as compared to buffer-treated cells. BMDCs were treated with OmpU (3 μg/ml) or buffer for 3 h. Whole-cell lysates were prepared and analysed for NLRP3 by immunoblotting. Blots are representative of three independent experiments.*

To confirm the role of NLRP3 inflammasome, we cultured BMDCs from NLRP3$^{-/-}$ mice and treated them with buffer or OmpU for 24 h. After incubation, the culture supernatant was collected and assessed for IL-1β production by ELISA. We detected that the OmpU-treated BMDCs from NLRP3$^{-/-}$ mice showed significantly low IL-1β levels compared to the OmpU-treated BMDCs from wildtype (Wt) mice (Fig. 16B). Thus, our results confirmed that NLRP3 is the inflammasome complex responsible for OmpU-induced IL-1β production in DCs.

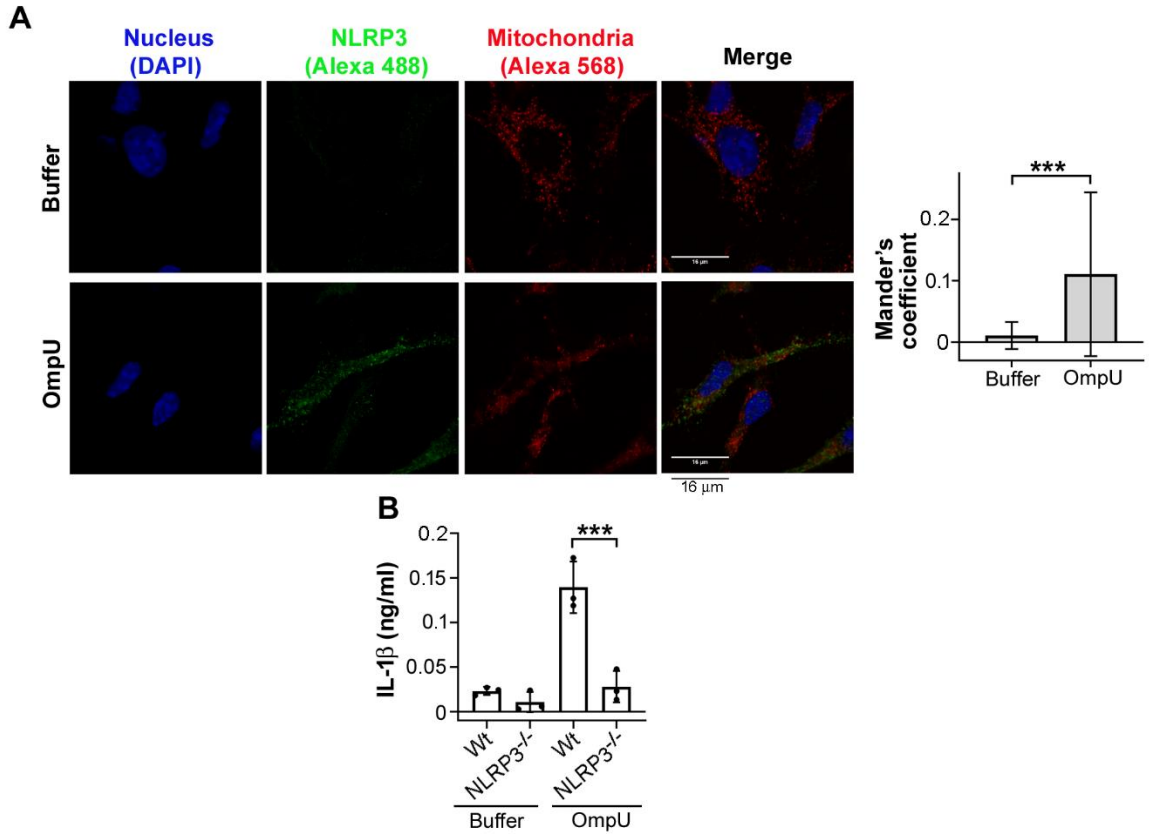


**Figure 17: NLRP3 inflammasome is involved in OmpU-mediated IL-1β production in DCs.**

*(A) Colocalization of NLRP3 with mitochondrial marker TIM23 in OmpU-treated DCs. BMDCs were treated with OmpU (3 µg/ml) or buffer for 30 min. Following incubation, cells were fixed using paraformaldehyde (PFA) and incubated with anti-NLRP3 and anti-TIM23 primary antibodies. Further, cells were then stained with Alexa-488 (for NLRP3), Alexa-568 (for TIM23) secondary antibodies and DAPI for the nucleus. Co-localisation was quantified using Mander's coefficient, taking 10 or more fields per experiment. Scale bar represents 16 µm. The bar graph represents mean ± SD from three independent experiments. ***p < 0.001 versus OmpU treatment.*

*(B) Decrease in OmpU-mediated IL-1β production in BMDCs from NLRP3$^{-/-}$ mice compared to BMDCs from Wt (wildtype) mice. BMDCs from Wt and NLRP3$^{-/-}$ mice were treated with OmpU (3 µg/ml) or buffer for 24 h. Following treatment, levels of IL-1β were measured by ELISA in culture supernatants. Results are expressed as mean ± SD and represent the average of three independent experiments. Statistical analysis was done using student's two-sided t-test. ***p < 0.001 versus OmpU-treated Wt BMDCs.*

## 4.4 Specific aim 2: How the inflammasome complex is activated in DCs in response to OmpU?

As we observed that NLRP3 inflammasome was involved in OmpU-mediated IL-1β production in DCs, we next investigated the mechanism involved in triggering the activation of NLRP3 inflammasome.

### 4.4.1 OmpU-mediated NLRP3 inflammasome activation in DCs is independent of potassium efflux from the cells

Several studies suggested that NLRP3 inflammasome can be triggered by myriad of signals in the cell which led to assembling of all the inflammasome components and culminate in the release of IL-1β from the cells. Potassium efflux from the cells has been described as a unifying mechanism for NLRP3 inflammasome induction in case of an array of PAMPs [143]. Therefore, we probed whether $K^+$ efflux from the cells induces the NLRP3 inflammasome in response to OmpU. We cultured BMDCs in presence of high extracellular $K^+$ concentration in the media which inhibits $K^+$ efflux from the cells and then treated the cells with OmpU for 24 h or with positive control LPS+ATP. After incubation, the culture supernatant was collected and IL-1β levels were assessed by ELISA. We observed that there was no decrease in the IL-1β levels compared to the OmpU-treated BMDCs while the positive control, LPS+ATP-treated cells, showed inhibition in IL-1β production in presence of high extracellular $K^+$ concentration (Fig. 17). Our results indicated that OmpU-mediated IL-1β production in DCs does not depend on $K^+$ efflux from the cells.

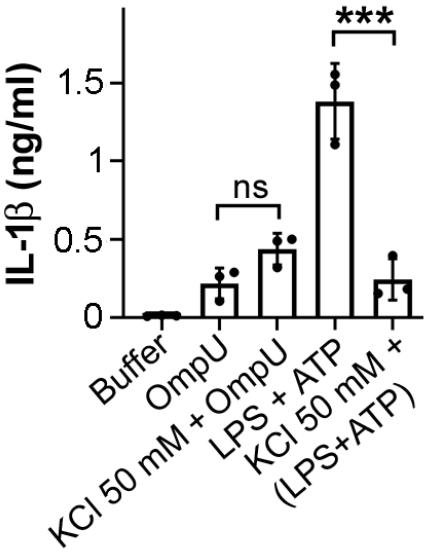


**Figure 18: OmpU-mediated IL-1β production is independent of K+ efflux.**

*BMDCs were pre-treated with 50 mM KCl for 30 min followed by OmpU (3 μg/ml) treatment for 24 h. For positive control, BMDCs were treated with LPS (50 ng/ml) for 3 h followed by 5 mM ATP for 30 min. Following respective incubations, IL-1β levels were measured by ELISA in culture supernatants. Results are expressed as mean ± SD and represent the average of three independent experiments. Statistical analysis was done using student's two-sided t-test. ns denotes non-significant versus OmpU-treated BMDCs, ***p < 0.001 versus LPS + ATP-treated BMDCs.*

### 4.4.2 Calcium flux induces the OmpU-mediated NLRP3 inflammasome activation in DCs

Calcium influx from extracellular milieu or increase in intracellular calcium caused by efflux from other organelles is a known inducer of NLRP3 inflammasome in immune cells [153]. As we have already observed that OmpU induces calcium influx in BMDCs and the calcium chelator BAPTA-AM, inhibits the OmpU-induced calcium influx, we further investigated the role of this calcium influx in OmpU-mediated NLRP3 activation. For this, we pre-treated BMDCs with BAPTA-AM followed by OmpU or buffer treatment for 24 h and assessed the culture supernatant for IL-1β production by ELISA. Our experiment revealed that IL-1β production was diminished in OmpU-treated cells in presence of BAPTA-AM compared to the OmpU-treated BMDCs (Fig. 18). Thus, our results indicated that OmpU-mediated calcium flux is involved in IL-1β production in DCs.

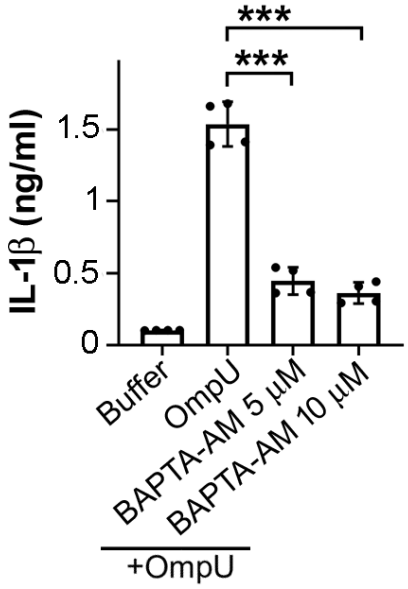


**Figure 19: NLRP3 inflammasome activation in DCs depends on calcium flux triggered in response to OmpU.**

*BMDCs were pre-treated with BAPTA-AM for 1 h followed by OmpU (3 μg/ml) treatment for 24 h. IL-1β levels were measured by ELISA in the culture supernatants. Bar graph represents mean ± SD from four independent experiments. Statistical analysis was done using student's two-sided t-test. ***p < 0.001 versus OmpU-treated cells.*

### 4.4.3 OmpU-mediated NLRP3 inflammasome activation in DCs depends on mitoROS generation

The role of mitochondria in NLRP3 activation has been widely studied. The mitochondrial ROS (mitoROS) ensuing due to calcium ($Ca^{2+}$) uptake by mitochondria and opening of mitochondrial permeability transition pore (MPTP) or electron transport chain (ETC) activity can signal NLRP3 activation [154, 155]. Therefore, to explore whether mitoROS has any role to play in OmpU-induced NLRP3 activation, we first checked whether mitoROS is produced in response to OmpU in DCs using MitoSOX dye. We have incubated the DCs with mitochondrial ROS scavenger, MitoTEMPO followed by loading the cells with MitoSOX dye. Then, the cells were treated with OmpU and the mitoROS production was assessed by fluorescence microscopy and flow cytometry. We observed that mitoROS was produced in OmpU-treated BMDCs and further, inhibited in the MitoTEMPO pre-treated cells (Fig. 19A, B). Further, when we probed for IL-1β production in OmpU activated BMDCs in presence of MitoTEMPO we observed that IL-1β levels were significantly reduced in MitoTEMPO pre-treated cells compared to only OmpU-treated cells indicating the involvement of mitoROS in OmpU-mediated NLRP3 activation (Fig. 19C).

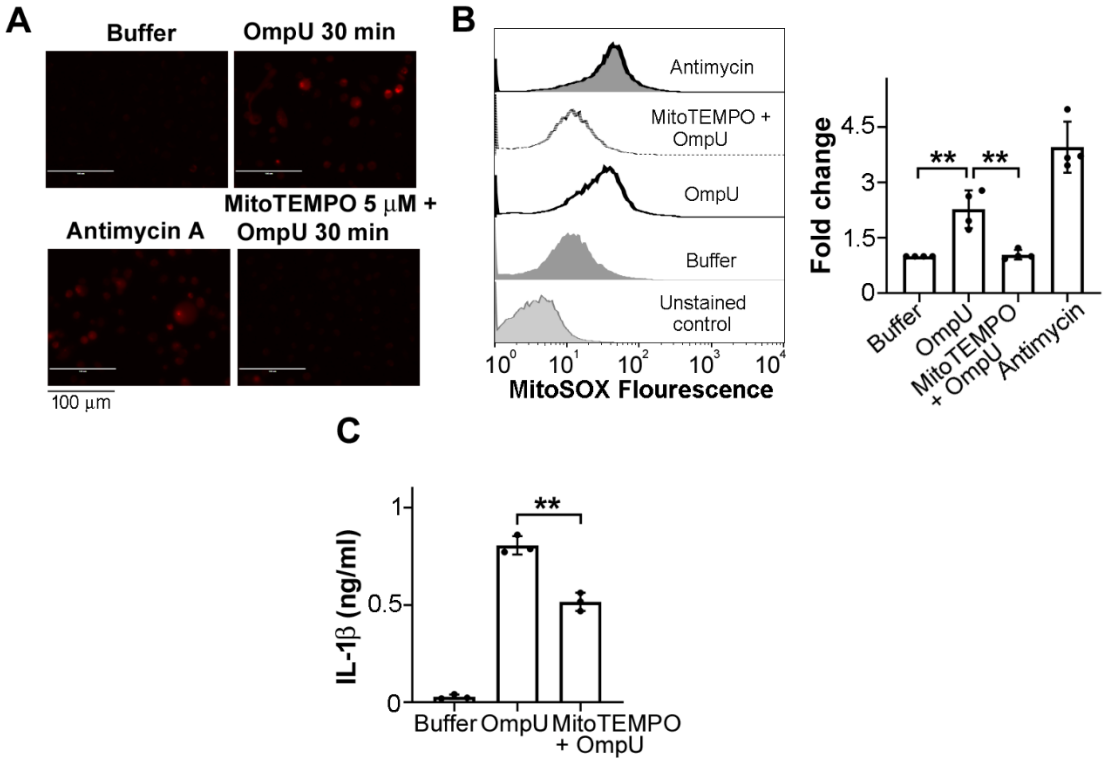


**Figure 20: OmpU induces mitoROS which signals NLRP3 inflammasome activation in DCs.**

*(A, B) OmpU treatment leads to mitoROS production in DCs. BMDCs were pre-treated with mitoROS scavenger, MitoTEMPO, for 2 h and following washing, the cells were loaded with MitoSOX red dye for 20 min. After washing twice, the cells were treated with OmpU (3 μg/ml) for 30 min. Buffer and Antimycin A were used as negative and positive controls, respectively. (A) Then the cells were observed under an EVOS fluorescence microscope with 40 x magnification. Images shown are representative of three independent experiments with 10-15 fields per experiment. Scale bar represents 100 μm. (B) The cells were harvested and acquired in FACSCalibur flow cytometer. Histogram plot is representative of four independent experiments. Fold change was calculated compared to buffer-treated cells. Bar graph represents mean ± SD from four independent experiments. **p< 0.01 versus buffer and OmpU-treated cells*

*(C) MitoROS production contributes to OmpU induced IL-1β production in DCs. BMDCs were pre-treated with MitoTEMPO for 1 h followed by OmpU (3 μg/ml) treatment for 24 h. Buffer-treated and only OmpU-treated cells served as controls. IL-1β levels were measured by ELISA in the culture supernatants. Bar graph represents mean ± SD from three independent experiments. Statistical analysis was done using student's two-sided t-test. **p< 0.01 versus OmpU-treated cells.*

### 4.4.4 OmpU translocation to mitochondria triggers mitoROS generation in DCs

We further wanted to probe the trigger for mitoROS production in DCs. Previously, Gupta et al, from our laboratory had shown that *V. cholerae* OmpU can translocate to the host cell mitochondria and induce caspase-independent programmed cell death via the loss of mitochondrial membrane potential and AIF release using THP-1 monocytes, HEK 293 epithelial cells and Caco-2 intestinal epithelial cells [80]. Further, Prasad et al, from our laboratory had shown that OmpU translocation to mitochondria leads to mitoROS generation in case of monocytes and macrophages [78]. Therefore, to elucidate how mitoROS is produced in DCs in response to OmpU, we first wanted to check whether OmpU translocate to the mitochondria in BMDCs. Towards that, we have treated BMDCs with OmpU or buffer and isolated the mitochondrial fraction from the cells. We observed that OmpU was present in the OmpU-treated mitochondrial fractions using western blotting (Fig. 20) and also, using confocal microscopy, we found that OmpU colocalized with the mitochondrial marker TOM20 (Fig. 21).

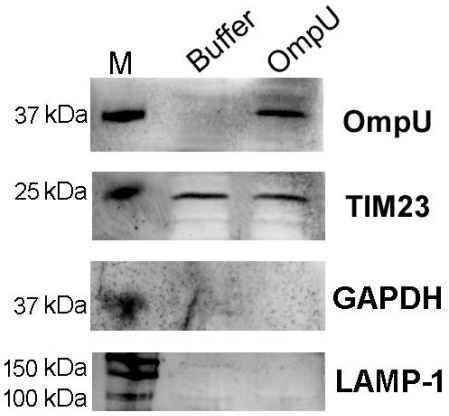


**Figure 21: OmpU translocate to mitochondria of DCs.**

*BMDCs were treated with OmpU (5 µg/ml) or buffer for 30 min. Following treatment, the mitochondria were isolated from the cells and analysed for the presence of OmpU by immunoblotting. TIM23 was used as the mitochondrial marker. GAPDH and LAMP-1 were used as cytoplasmic and lysosomal controls. Blot shown is representative of four independent experiments.*

Further, we observed that by using cytochalasin D (cyt. D), an actin polymerisation inhibitor OmpU translocation to the mitochondria in DCs can be inhibited (Fig. 22).

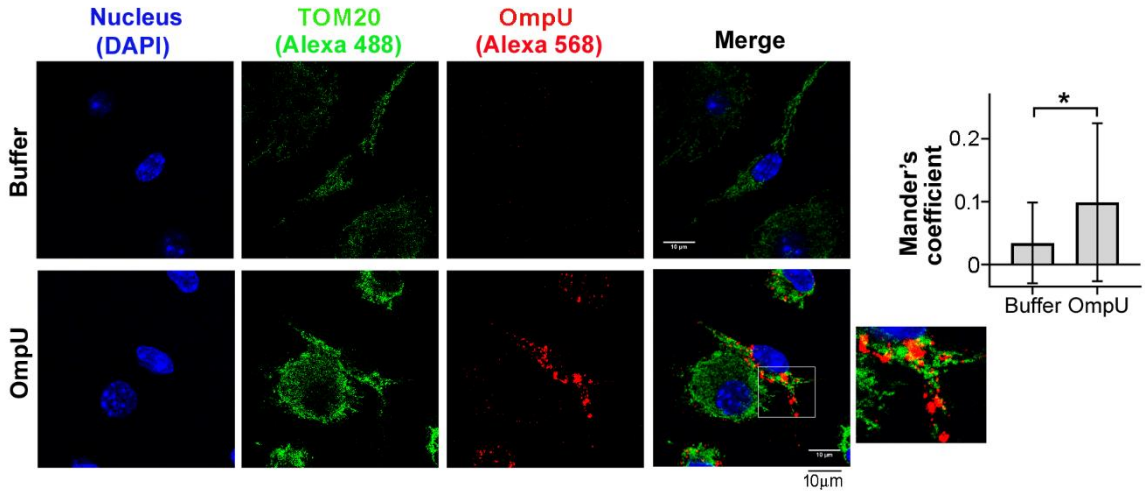


**Figure 22: OmpU colocalizes with mitochondrial marker TOM20.**

*BMDCs were treated with OmpU (5 µg/ml) or buffer for 30 min. After treatment the cells were fixed using paraformaldehyde (PFA) and incubated with anti-OmpU and anti-TOM20 primary antibodies. Further, cells were stained with Alexa-488- (for anti-TOM20), Alexa-568- (for anti-OmpU) conjugated secondary antibodies and DAPI for the nucleus. Images shown are representative of three independent experiments, and each experiment constitutes 10 or more fields. Scale bar represents 10 µm. Co-localization was quantified using Mander's coefficient. The bar graph represents mean ± SD from three independent experiments. Statistical analysis was done using student's two-sided t-test. *p< 0.05 versus buffer-treated cells.*

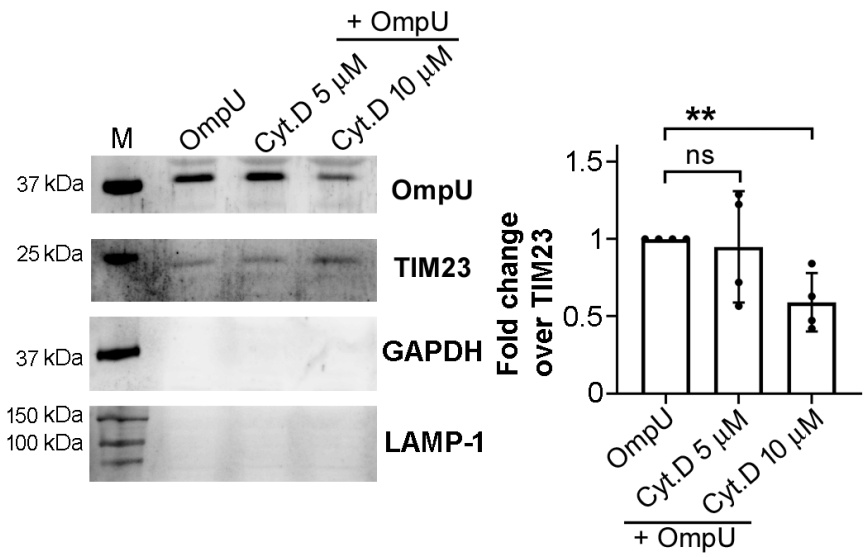


**Figure 23: Cytochalasin D inhibits the OmpU translocation to mitochondria of DCs.**

*BMDCs were pre-treated with cytochalasin D (cyt. D) for 30 min followed by OmpU (5 µg/ml) treatment for 30 min. Following treatment, the mitochondria were isolated from the cells and analysed for the presence of OmpU by immunoblotting. TIM23 was used as the mitochondrial marker. GAPDH and LAMP-1 were used as cytoplasmic and lysosomal controls. Blot shown is representative of four independent experiments. Bar graph represents mean ± SD from four independent experiments. Statistical analysis was done using student's two-sided t-test. ns- non-significant, **p< 0.01 versus OmpU-treated cells.*

To determine whether OmpU translocation to mitochondria is responsible for the mitoROS generation, we pre-treated BMDCs with cyt. D and checked mitoROS generation in OmpU-treated BMDCs using fluorescence microscopy (Fig. 23A) and flow cytometry (Fig. 23B). We observed that mitoROS was scavenged in OmpU-treated BMDCs in presence of cyt. D indicating that OmpU translocation to mitochondria was involved in mitoROS production in BMDCs.

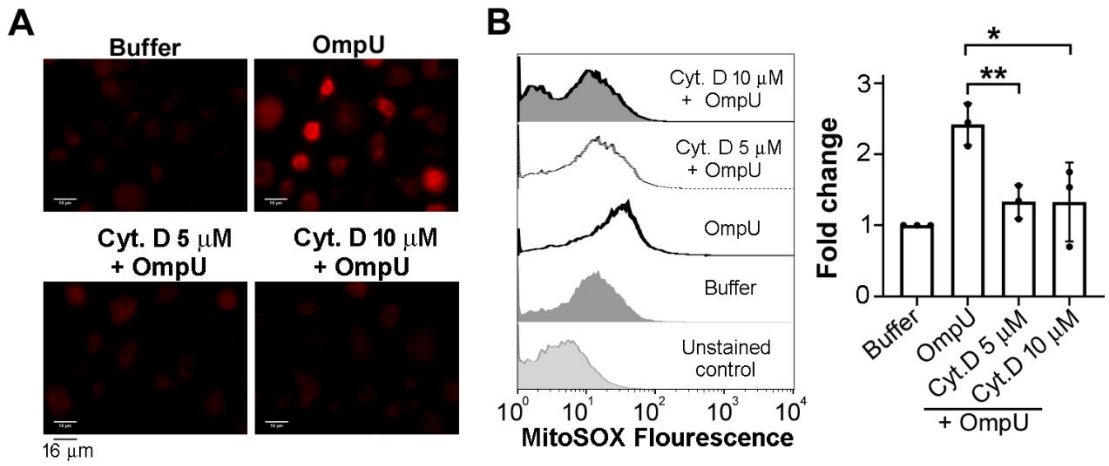


**Figure 24: OmpU-induced mitoROS depends on OmpU translocation to mitochondria of DCs.**

*(A, B) OmpU translocation to mitochondria contributes to mitoROS generation in DCs. BMDCs were pre-treated with cyt. D for 30 min followed by OmpU (3 μg/ml) treatment for 30 min. (A) Following incubation, cells were fixed and mounted onto glass slides to observe under Zeiss Axio Observer Z1 inverted microscope with 63 x oil immersion objective. Images shown are representative of 30-40 fields. Scale bar represents 16 μm.*

*(B) Cells were harvested and acquired in FACSCalibur flow cytometer. Histogram plot is representative of three independent experiments. Fold change was calculated compared to buffer-treated cells. Bar graph represents mean ± SD from three independent experiments. Statistical analysis was done using student's two-sided t-test. *p< 0.05, **p< 0.01 versus OmpU-treated cells.*

### 4.4.5 Calcium influx in DCs contributes to mitoROS generation

Calcium flux in the cells is known to influence mitochondrial membrane permeability and it can also induce mitoROS production. Therefore, we investigated whether calcium flux in BMDCs is involved in mitoROS production. Towards this, we probed mitoROS generation in OmpU-treated DCs in presence of calcium chelator BAPTA-AM and analysed the cells using fluorescence microscopy (Fig. 24A) and flow cytometry (Fig. 24B). We observed that mitoROS was inhibited in presence of BAPTA-AM in OmpU-treated DCs. Thus, our results suggest that OmpU-mediated calcium flux also plays a role in mitoROS generation in response to OmpU leading to NLRP3 inflammasome activation.

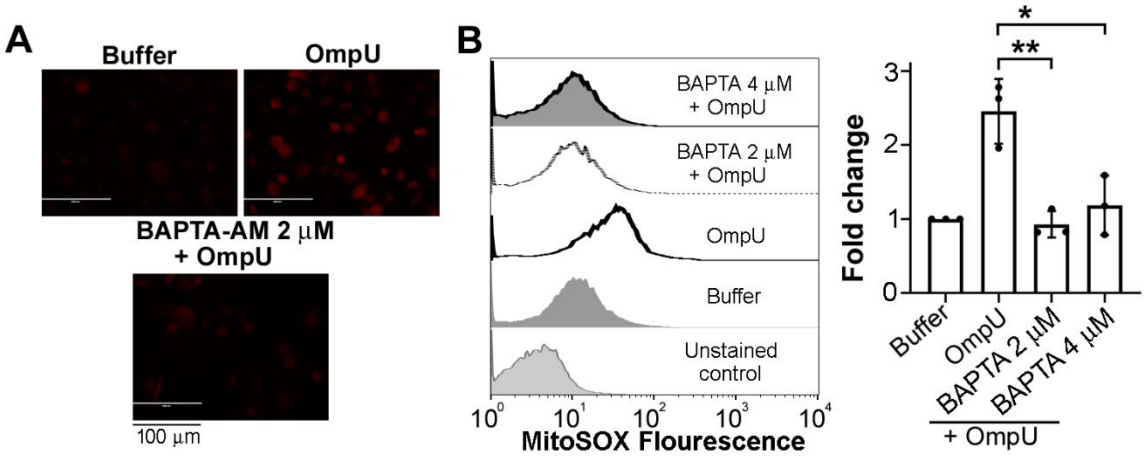


**Figure 25: OmpU-induced calcium flux is involved in mitoROS generation in DCs.**

*(A, B) OmpU-mediated calcium flux induces mitoROS generation in BMDCs. Cells were pre-treated with BAPTA-AM for 1 h followed by OmpU (3 μg/ml) treatment. (A) Following incubation, cells were stained using MitoSOX red dye and observed under an EVOS fluorescence microscope. Images shown are representative of 30-40 fields. Scale bar represents 100 μm.*

*(B) Following MitoSOX staining, the cells were acquired in FACSCalibur flow cytometer. Histogram plot is representative of three independent experiments. Fold change was calculated compared to buffer-treated cells. Bar graph represents mean ± SD from three independent experiments. Statistical analysis was done using student's two-sided t-test. *p< 0.05, **p< 0.01 versus OmpU-treated cells.*

## 4.5 Conclusion

In this study, we investigated about the inflammasome complex involved in IL-1β production in OmpU-activated DCs and further, delineated the signalling behind the IL-1β production. We observed that NLRP3 inflammasome was activated leading to caspase-1 activation which was responsible for the production of OmpU-induced IL-1β production in DCs.

We further investigated the signal triggering the NLRP3 activation in response to OmpU. We found that calcium influx induced in response to OmpU triggers the IL-1β production in DCs. Further, we observed that OmpU triggered mitoROS generation in DCs which also contributes to IL-1β production. Furthermore, we explored the signalling involved in mitoROS generation and found that OmpU translocation to the mitochondria of DCs along with the calcium influx prompted mitoROS generation in response to OmpU and contributes to the IL-1β production in DCs.

## Aim 3: To investigate whether there is any role of ROS in OmpU-mediated DC activation.

**Specific aim 1:** Whether OmpU-induces ROS generation in OmpU-activated DCs and whether ROS play any role in activation of DCs?

**Specific aim 2:** To understand the signalling mechanism underlying ROS generation.

# Aim 3: To investigate whether there is any role of ROS in OmpU-mediated DC activation.

## 5.1 ROS as a mediator of inflammation

Reactive oxygen species (ROS) act as a second messenger in pro-inflammatory signalling pathways and regulate the functioning of several signalling molecules involved in inflammation. ROS family majorly includes free radicals $O_2^-$ and $OH^-$; non-radicals such as $H_2O_2$ and singlet $^1O_2$ as shown in illustration 9 [156, 157]. ROS functions as a chemotactic factor at the site of inflammation for the early recruitment of leukocytes [158]. ROS can be produced during the downstream signalling of several inflammatory agonists leading to pro-inflammatory cytokine production and inflammasome activation [158]. It is well established that ROS can activate various transcription factors involved in inflammatory pathways including NFκB, AP-1, ATF [159]. In addition, ROS not only plays a role in leukocyte recruitment but also in their retention in the endothelium during inflammatory processes which helps in neutrophil survival [158, 160]. ROS were also found to be involved in signalling which promotes the formation of neutrophil extracellular traps (NETs) and thus, helping in the NETosis-mediated killing of microbes [161]. Further, elevated ROS levels can also mediate cell damage via oxidation of DNA, RNA, proteins and lipids leading to cell death through apoptosis or necrosis [162]. Therefore, ROS plays a role in myriad events involved in inflammation and inflammatory signalling cascades.

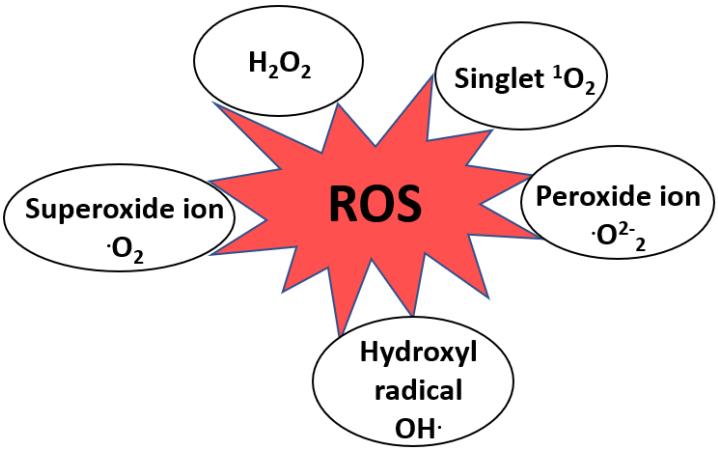


**Illustration 9: Different moieties present in ROS.**

*Reactive oxygen species (ROS) consists of different reactive moieties $O_2^-$, $OH^-$, $H_2O_2$ and singlet $^1O_2$.*

### 5.2 Sources of ROS

ROS can be produced from different complexes, enzymes or organelles in the cell. The prime sources of ROS include NADPH oxidase (NOX) complex, xanthine oxidase enzyme and organelles such as mitochondria and peroxisomes.

#### 5.2.1 NADPH oxidase-derived ROS

The major source of cytoplasmic ROS in the cells is produced by NADPH oxidase (NOX) complex. NOX family has seven isoforms (NOX1-5 and DUOX 1&2), out of which NOX2 is the isoform pre-dominantly found in phagocytes and other immune cells [163]. NOX2 complex is comprised of cytoplasmic sub-units p40, p47, p67 and Rac and plasma membrane-bound heterodimer sub-unit composed of gp91 and p22. Upon stimulation, p47 is phosphorylated which prompts the translocation of whole cytosolic complex to the membrane-bound sub-unit to form the active oxidase as highlighted in the illustration 10. The superoxide radical is generated by the transfer of electrons from NADPH in the cytosolic region to oxygen present either in lumen or in extracellular region [164]. NOX2 can be activated in a phenomenon called respiratory burst, which occurs when phagocytes ingest bacteria or fungi or other microbes [164]. In addition, several PRRs are also reported to mediate the activation of NOX2 complex and ROS generation in response to pathogenic ligands such as LPS, peptidoglycan, flagellin which can directly kill the microbes or act as mediator in a signalling pathway to orchestrate the inflammatory responses [165].

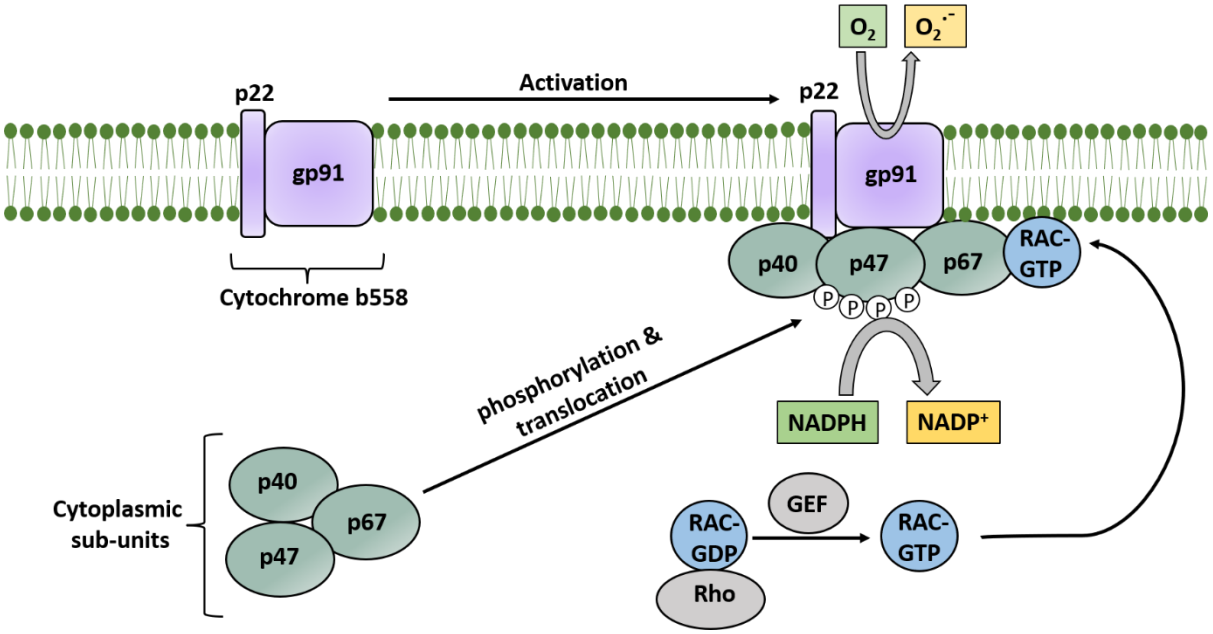


**Illustration 10: NOX2 assembly and activation.**

*NADPH oxidase (NOX2) is a multi-subunit assembly comprising the membrane-bound p22 and gp91 subunits and cytoplasmic p40, p67 and p47 sub-units. Upon receiving activation signal the cytoplasmic subunits together with RAC-GTP translocate to the membrane-bound subunits leading to activation of NOX2 complex and ROS generation.*

### 5.2.2 Mitochondrial ROS

Mitochondria are the central sites of aerobic respiration. This process is driven by transfer of electrons through several electron transport complexes (ETC) which lead to the production of ATP via the $F_0$-$F_1$ ATPase using the proton gradient across the mitochondrial membrane. Although, this process is tightly regulated, 1-2 % of the electrons leak out mainly from the complex I and III of the ETC to react with molecular oxygen and generate superoxide radicals which are the main contributors to mitochondrial ROS or mitoROS as shown in illustration 11. The superoxide radicals are converted to $H_2O_2$ by the mitochondrial dismutase which then escapes to the cytosol [166, 167]. MitoROS has been shown to play role in several inflammatory disorders and lead to the activation of transcription factors and pro-inflammatory cytokines [108].

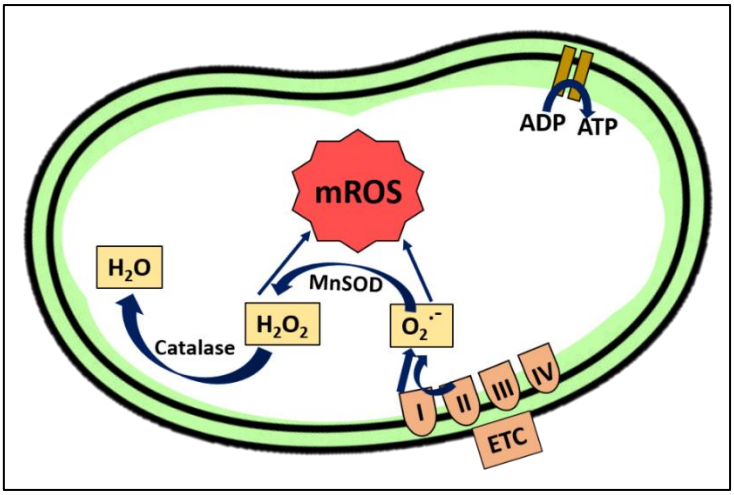


**Illustration 11: Sources of mitoROS production.**

*The mitochondrial ROS (mitoROS) is generated due to the electrons leaking from complex I and III of the electron transport chain (ETC). Superoxide forms the main reactive species in mitoROS which can be converted to hydrogen peroxide ($H_2O_2$) by mitochondrial superoxide dismutase (SOD).*

### 5.3 Role of ROS in DCs

DCs exhibit ROS production which aids in removal of pathogen as well as processing of the antigen [168, 169]. It was reported that ROS stimulation leads to the upregulation of MHC class II molecules and co-stimulatory markers CD40 and CD80 on the DCs [168]. Monocyte-derived DCs are shown to produce prolonged and millimolar concentrations of NOX-mediated ROS in the phagosome which helps in shaping the repertoire of antigen fragments for presentation to the helper T cells [170]. In addition, NOX-mediated ROS plays a critical role in processing of antigen in phagosome by regulating the pH and aiding in cross-presentation of antigens on DCs to cytotoxic T cells [169]. Thus, ROS can lead to the maturation of immature DCs and was also shown to enhance the migration pattern of the mature DCs [171]. Further, NOX2-derived ROS was reported to control the hyperinflammatory responses in DCs by regulating the IL-12 cytokine production and thus, can function as an anti-inflammatory mediator [172]. In addition to the NOX-mediated ROS, mitochondrial ROS too affects the functions of DCs. In case of plasmacytoid DCs (pDCs), mitochondrial ROS-dependent mechanism is involved in antigen processing which enables the pDCs to cross-present the antigen for activation of cytotoxic T cell responses [173].

### 5.4 PRR co-operation for ROS production

The role of TLRs for ROS production has been widely studied. TLR2 and TLR4 are shown to be involved in ROS production in macrophages in response to bacteria as well as bacterial ligands such as LPS [174]. TLR signalling can induce ROS generation in various ways including the induction of expression of NOX sub-units, prompting the assembly of NOX sub-units on the membrane or direct interaction of NOX and TLR in the membrane [175]. NOX1 upregulation has been reported in several colon cell lines in response to LPS and flagellin via the activation of TLR4 and TLR5 [165, 176]. Further, various TLR2 and TLR4 agonists induce the signalling for phosphorylation of p47 sub-unit and its recruitment to the plasma membrane for NOX2 activation [177]. In case of LPS-induced ROS production TLR4 has been shown to directly interact with NOX4 complex [178, 179].

Apart from TLRs, scavenger receptors have emerged as an important class of PRRs for recognition of several bacterial and endogenous ligands. CD36, a scavenger receptor, has been characterized to play a critical role in vascular oxidative stress [180]. CD36 is shown to co-operate with TLR2 in macrophages and mediate NOX activation leading to ROS production in response to atherogenic ligands such as oxLDL and lipoproteins [181]. Thus, interplay between different PRRs has emerged as an important aspect for ROS generation via NOX activation.

### 5.5 Specific aim 1: Whether OmpU-induces ROS generation in OmpU-activated DCs and whether ROS play any role in activation of DCs?

Immune cells detect PAMPs using the PRRs to induce an inflammatory signalling pathway which culminates in production of inflammatory cytokines. Often the PAMP-PRR interaction induces ROS generation. Previous studies from our laboratory established that OmpU can act as a PAMP. Further, our laboratory has shown that OmpU mediates MAPK JNK activation in macrophages via CD36-dependent NOX-mediated ROS generation [78]. As ROS is one of the major components for induction of pro-inflammatory responses and can induce DC activation, we wanted to investigate whether OmpU can induce ROS generation in DCs.

### 5.5.1 OmpU induces the production of cytoplasmic ROS in DCs

Towards checking whether OmpU induces ROS generation, we treated BMDCs with OmpU for different time points and using dichlorofluorescein diacetate (DCFDA) dye, we detected the intracellular ROS. We observed an increased level of ROS generation in response to OmpU at 8 h and 12 h post-treatment using flow cytometry (Fig. 25). There was decrease in ROS levels at 24 h and this can be due to the fact that higher ROS in the cells can also mediate cell damage as mentioned in the section 5.1. Therefore, as a part of signalling mechanism the antioxidant enzymes could act to reduce the ROS levels.

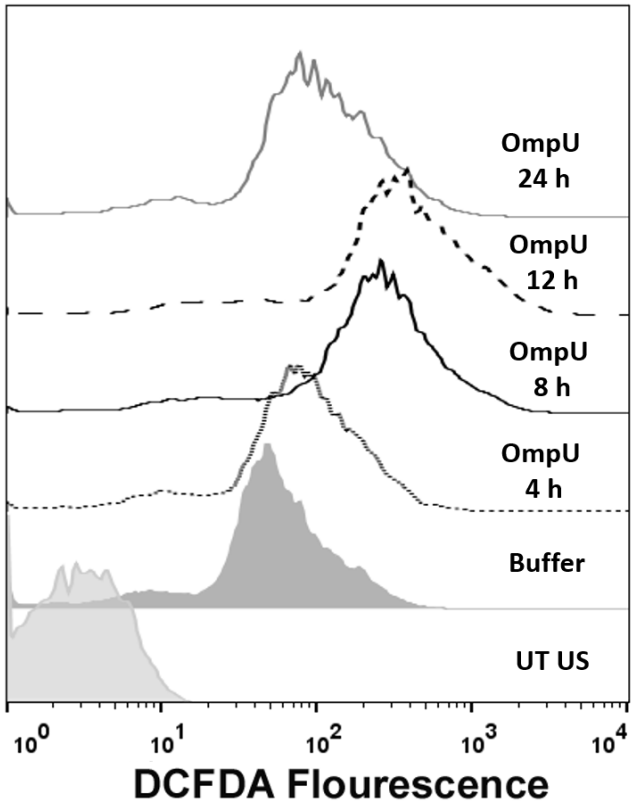


**Figure 26: ROS production in OmpU-treated BMDCs.**

*Significant ROS generation observed in BMDCs at 8 h and 12 h after OmpU treatment. BMDCs were treated with OmpU (3 μg/ml) for 4 h, 8 h, 12 h and 24 h followed by staining with DCFDA dye for 30 min. DCFDA fluorescence was assessed using FACSCalibur flow cytometer. The offset histogram is representative of three independent experiments.*

### 5.5.2 NOX2 complex is involved in ROS generation in OmpU-treated DCs

To check whether NOX2 is the source of OmpU-mediated ROS generation in DCs we have treated BMDCs with OmpU in presence of chemical inhibitor of NOX complex, diphenyleneiodonium chloride (DPI). We observed that ROS production was significantly inhibited in the presence of DPI indicating the involvement of NOX2 in ROS generation in BMDCs (Fig. 26).

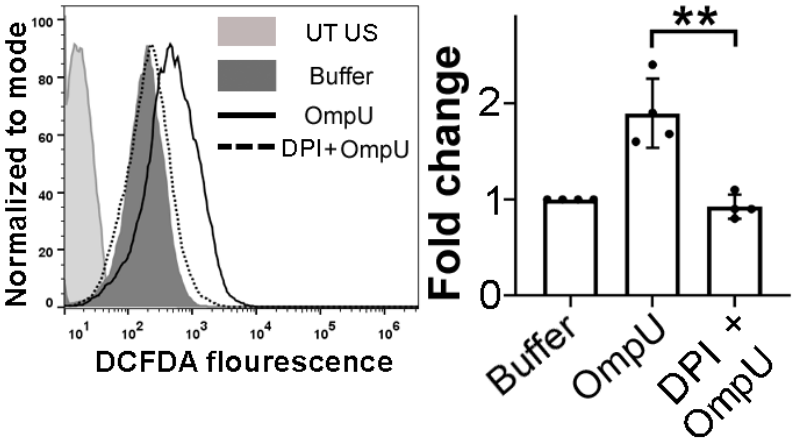


**Figure 27: ROS inhibition using NOX inhibitor (DPI).**

*BMDCs were pre-treated with DPI for 1 h followed by OmpU (3 μg/ml) treatment for 8 h. Cells were incubated with DCFDA and analysed using flow cytometer. The histogram is a representative of three independent experiments and results are expressed as mean ± SD in the bar graph. Statistical analysis was done using student's two-sided t-test. **p < 0.01 versus OmpU-treated BMDCs.*

As mentioned earlier NOX2 is a multi-sub-unit complex and the cytoplasmic subunits of NOX2 complex are translocated to the plasma membrane to form the active NOX2 complex upon receiving the activation signal. Therefore, to validate the role of NOX2 in OmpU-mediated ROS production we probed the translocation of p47 cytoplasmic sub-unit to the plasma membrane and colocalization with the marker $Na^+$-$K^+$ ATPase upon OmpU treatment. We observed that the p47 sub-unit colocalized with $Na^+$-$K^+$ ATPase on the plasma membrane confirming the activation of NOX2 in response to OmpU in DCs (Fig. 27).

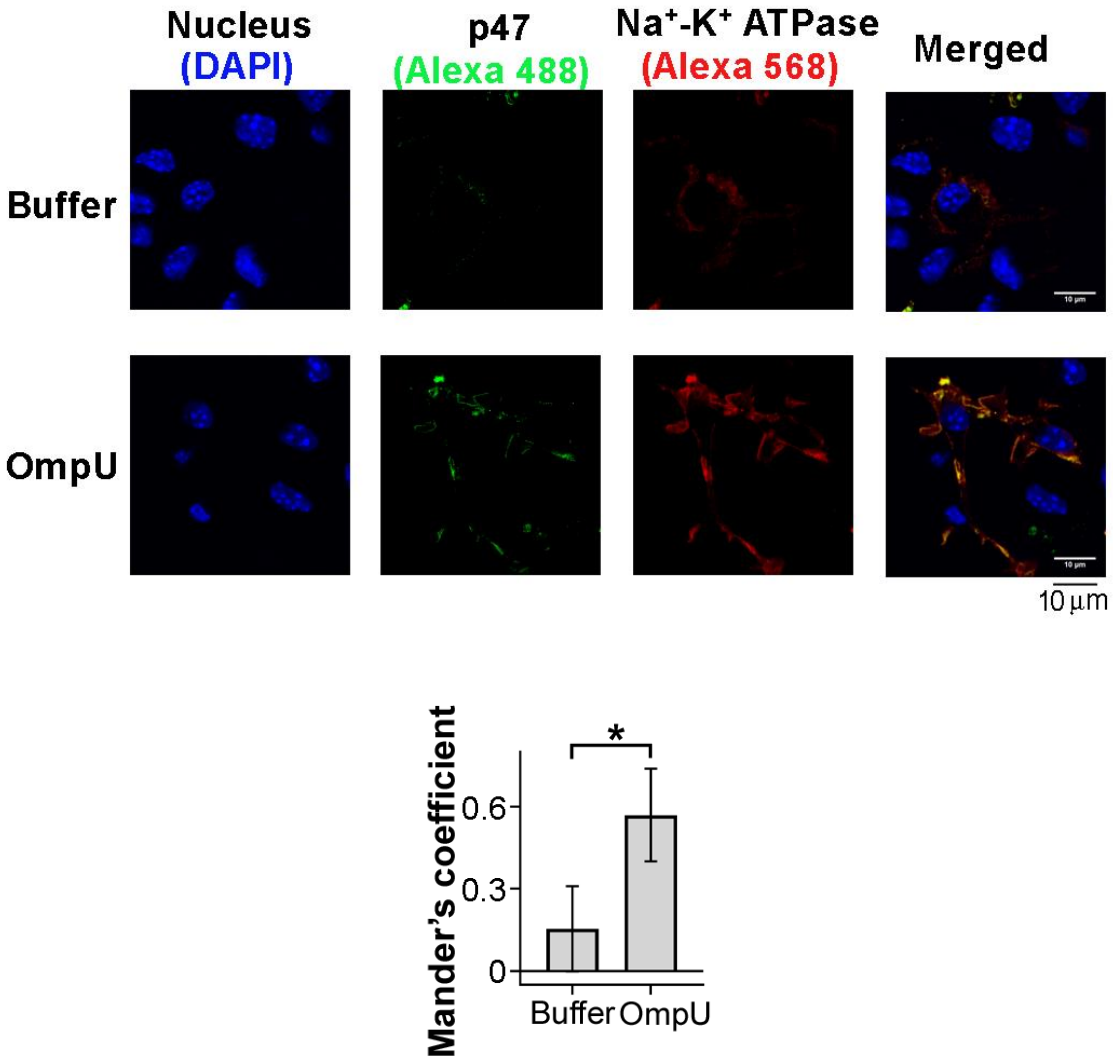


**Figure 28: Colocalization of p47 with plasma membrane in OmpU-treated DCs.**

*BMDCs were treated with OmpU (3 µg/ml) or buffer for 4 h. Following incubation, cells were fixed using paraformaldehyde (PFA) and incubated with anti-p47 and anti-$Na^+$-$K^+$ ATPase primary antibodies. Further, cells were then stained with Alexa-488 (for p47), Alexa-568 (for $Na^+$-$K^+$ ATPase) secondary antibodies and DAPI for the nucleus. The experiment was performed three times to obtain a total of 30 images for each treatment. The images shown are representative of three independent experiments and results are expressed as mean ± SD in the bar graph. Statistical analysis was done using student's two-sided t-test. *p< 0.05 versus OmpU-treated BMDCs.*

### 5.5.3 ROS generation contributes to induction of pro-inflammatory responses in DCs

As ROS is widely documented to act as an intermediate in various signalling cascades which result in pro-inflammatory responses and cytokine production, and we have observed that OmpU induces pro-inflammatory responses in DCs, we, further, investigated whether ROS

play any role in OmpU-mediated pro-inflammatory responses in DCs. Towards this we pre-treated the cells with total ROS scavenger, N-acetylcysteine (NAC) and observed that it led to inhibition of the OmpU-induced ROS generation (Fig. 28).

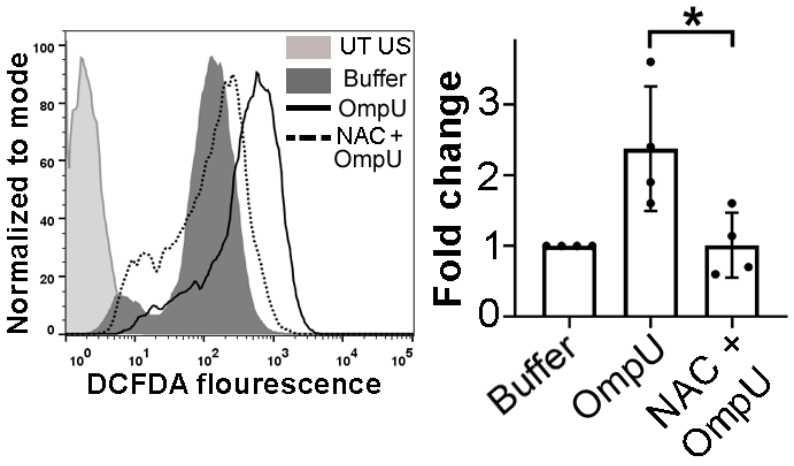


**Figure 29: OmpU-induced ROS is scavenged by NAC.**

*BMDCs were pre-treated with NAC for 2 h followed by OmpU (3 μg/ml) treatment for 8 h. Cells were incubated with DCFDA and analysed using flow cytometer. The histogram is a representative of three independent experiments. The results are expressed as mean ± SD in the bar graph. Statistical analysis was done using student's two-sided t-test. *p< 0.05 versus OmpU-treated BMDCs.*

Further, we pre-treated the BMDCs with NAC followed by OmpU treatment for 24 h. We observed a significant decrease in levels of pro-inflammatory cytokine production by OmpU-treated BMDCs in presence of NAC indicating that ROS is involved in OmpU-mediated pro-inflammatory responses. Similarly, we pre-treated the BMDCs with NOX inhibitor, DPI, followed by OmpU treatment and observed a significant decrease in ROS production in presence of DPI (Fig. 29).

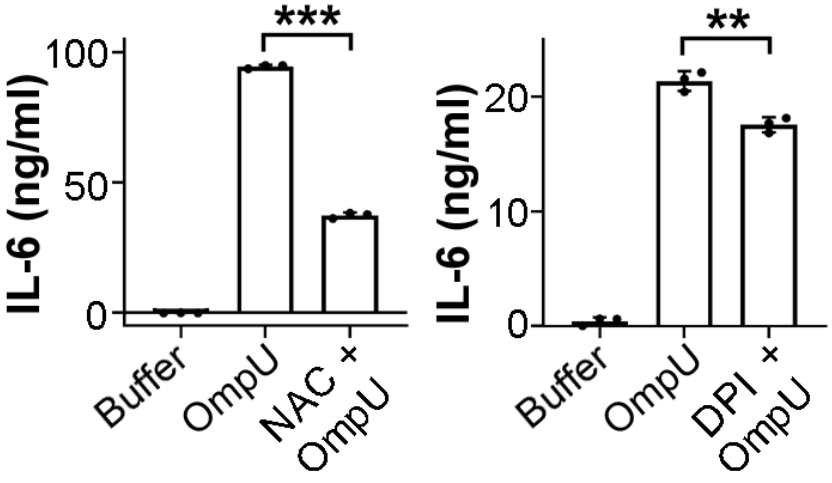


**Figure 30: Inhibition of pro-inflammatory responses using ROS scavengers.**

*Significant decrease in IL-6 production in presence of ROS scavengers, NAC and DPI in OmpU-treated DCs. BMDCs were pre-treated with NAC for 2 h and DPI for 1 h followed by OmpU (3 μg/ml) treatment for 24 h. The culture supernatant was collected and assessed for IL-6 production using ELISA. Results are expressed as mean ± SD and represent the average of three to six independent experiments. Statistical analysis was done using student's two-sided t-test. **p < 0.01, ***p < 0.001 versus OmpU-treated BMDCs.*

## 5.6 Specific aim 2: To understand the signalling mechanism underlying ROS generation.

As we have observed that NOX2 is involved in OmpU-induced ROS production in DCs, we next questioned which PRR could mediate the signalling for ROS generation and further, probed the mechanism underlying ROS production in OmpU-activated DCs.

### 5.6.1 TLR2 plays a role in OmpU-mediated ROS generation in DCs

Several studies have suggested that TLR2-mediated signalling can activate NOX complex which leads to the ROS generation [175, 179]. We have also observed that TLR2 is involved in OmpU-mediated cytokine production in DCs, therefore, we further explored the role of TLR2 in OmpU-induced ROS production. We cultured the BMDCs from $TLR2^{-/-}$ mice and treated them with OmpU for 8 h followed by ROS estimation using DCFDA dye. We found that ROS levels were diminished in the BMDCs from $TLR2^{-/-}$ mice as compared to the BMDCs from wildtype (Wt) mice (Fig. 30).

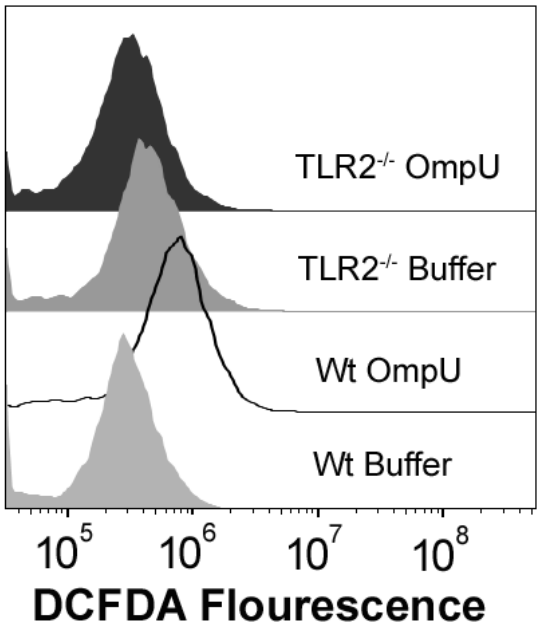


**Figure 31: TLR2 is involved in ROS production in DCs.**

*Considerable reduction in ROS generation in OmpU-treated BMDCs in the absence of TLR2. BMDCs from Wt (wildtype) and TLR2$^{-/-}$ mice were treated with OmpU (3 μg/ml) or buffer for 8 h followed by staining with DCFDA. Cells were harvested and further analysed using flow cytometry. The histogram is a representative of three independent experiments.*

Furthermore, following staining of the BMDCs from wildtype (Wt) and TLR2$^{-/-}$ mice for NOX2 cytosolic sub-unit p47 and plasma membrane marker $Na^+$-$K^+$ ATPase, we observed significantly reduced colocalization of p47 with $Na^+$-$K^+$ ATPase in TLR2$^{-/-}$ mice confirming the role of TLR2 in the activation of NOX2 in response to OmpU in DCs (Fig 31).

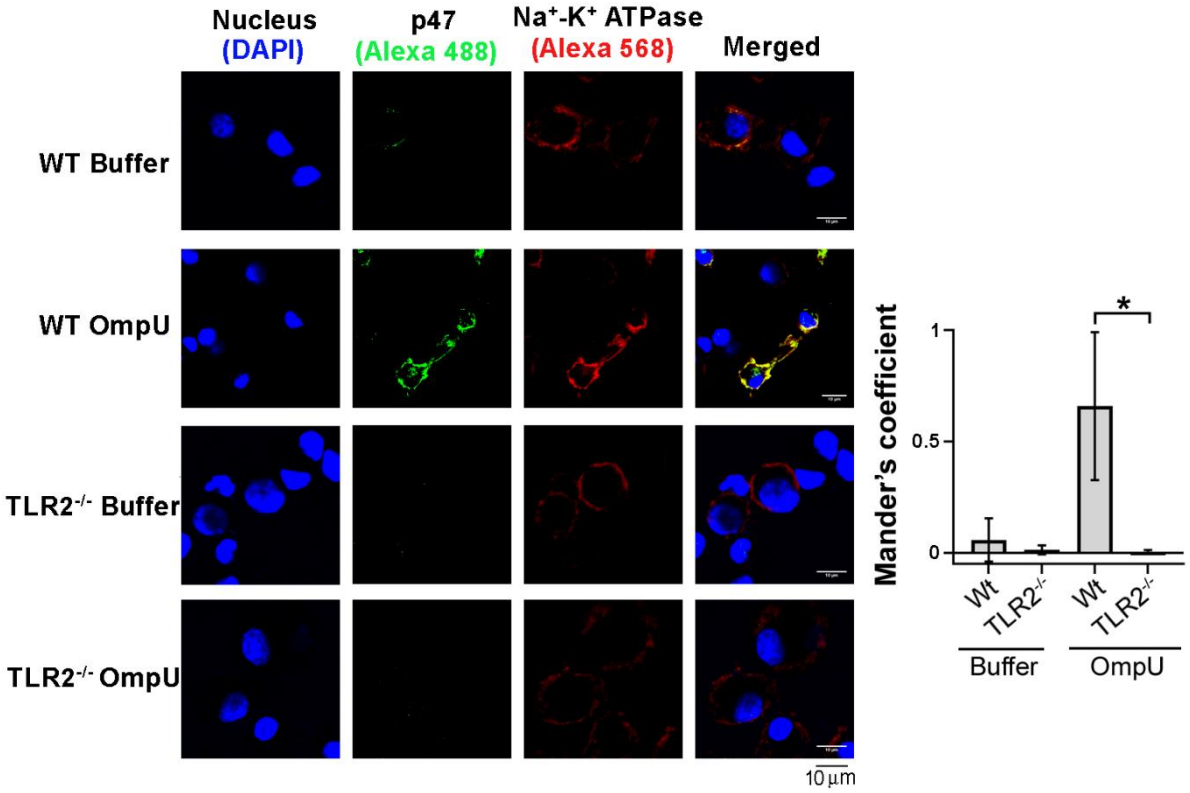


**Figure 32: Inhibition of translocation of p47 sub-unit to plasma membrane in OmpU-treated TLR2$^{-/-}$ BMDCs.**

*Colocalization p47 sub-unit with the plasma membrane marker $Na^+$-$K^+$ ATPase was inhibited in OmpU-treated DCs in absence of TLR2. BMDCs from wildtype (Wt) and TLR2$^{-/-}$ mice were treated with OmpU (3 µg/ml) or buffer for 4 h. Following incubation, cells were fixed using paraformaldehyde (PFA) and incubated with anti-p47 and anti-$Na^+$-$K^+$ ATPase primary antibodies. Further, cells were then stained with Alexa-488 (for p47), Alexa-568 (for $Na^+$-$K^+$ ATPase) secondary antibodies and DAPI for the nucleus. The experiment was performed three times to obtain a total of 30 images for each treatment. The images shown are representative of three independent experiments and results are expressed as mean ± SD in the bar graph. Statistical analysis was done using student's two-sided t-test. *p< 0.05 versus Wt OmpU-treated BMDCs.*

### 5.6.2 OmpU interacts with CD36

As CD36 has been shown to be involved in OmpU-induced NOX-mediated ROS production in macrophages [78]. Therefore, we also wanted to explore the role of CD36 in OmpU-induced ROS generation in DCs and for this, we first checked whether OmpU interacts with CD36 in DCs. We have treated the cells with OmpU and prepared whole-cell lysate. Using the whole-cell lysates, we performed immunoprecipitation employing the anti-CD36 antibody and

observed that it resulted in the co-immunoprecipitation of OmpU along with CD36 (Fig. 32). Thus, our data suggested that OmpU interacts with CD36.

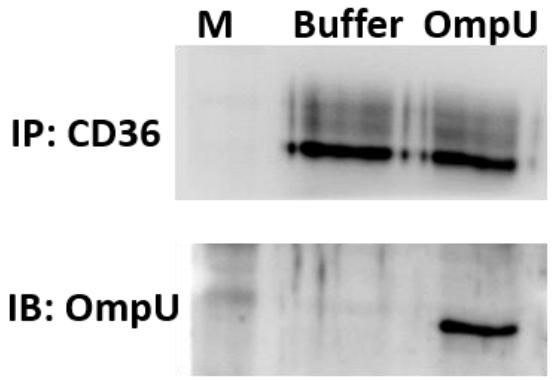


**Figure 33: OmpU interacts with CD36 in OmpU-treated DCs.**

*Co-immunoprecipitation of OmpU with the immunoprecipitation of OmpU-treated BMDCs cell lysate using anti-CD36 antibody. BMDCs were treated with OmpU (5 μg/ml) or buffer for 30 min followed by whole cell lysate preparation. The whole cell lysate was immunoprecipitated using anti-CD36 antibody and finally pulled down using IgG-tagged agarose beads. The complex was eluted by SDS loading dye and probed for CD36 as well as OmpU by immunoblotting. The blot shown is a representative of three independent experiments.*

### 5.6.3 CD36 is required for OmpU-mediated ROS generation in DCs

We, further, checked the role of CD36 in OmpU-mediated ROS generation in DCs. Towards it, we have treated the BMDCs from wildtype (Wt) and $CD36^{-/-}$ mice with OmpU for 8 h and assessed the ROS levels using DCFDA dye. We observed that the ROS generation were remarkably reduced in the absence of CD36 (Fig. 33).

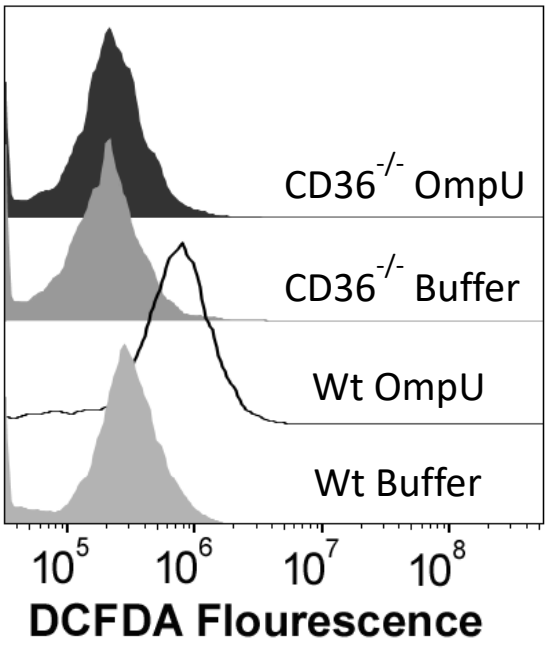


**Figure 34: CD36 is involved in ROS generation in DCs.**

*Considerable reduction in ROS generation in OmpU-treated CD36$^{-/-}$ BMDCs. BMDCs from Wt (wildtype) and CD36$^{-/-}$ mice were treated with OmpU (3 μg/ml) or buffer for 8 h followed by staining with DCFDA dye. Cells were harvested and further analysed using flow cytometry. The histogram is a representative of three independent experiments.*

Further, the BMDCs from wildtype (Wt) and CD36$^{-/-}$ mice were stained for p47 and plasma membrane marker $Na^+$-$K^+$ ATPase and it was observed that the colocalization of p47 sub-unit with $Na^+$-$K^+$ ATPase on the plasma membrane was abrogated in the BMDCs from CD36$^{-/-}$ mice highlighting the critical role of CD36 in OmpU-mediated NOX2 activation in DCs (Fig. 34).

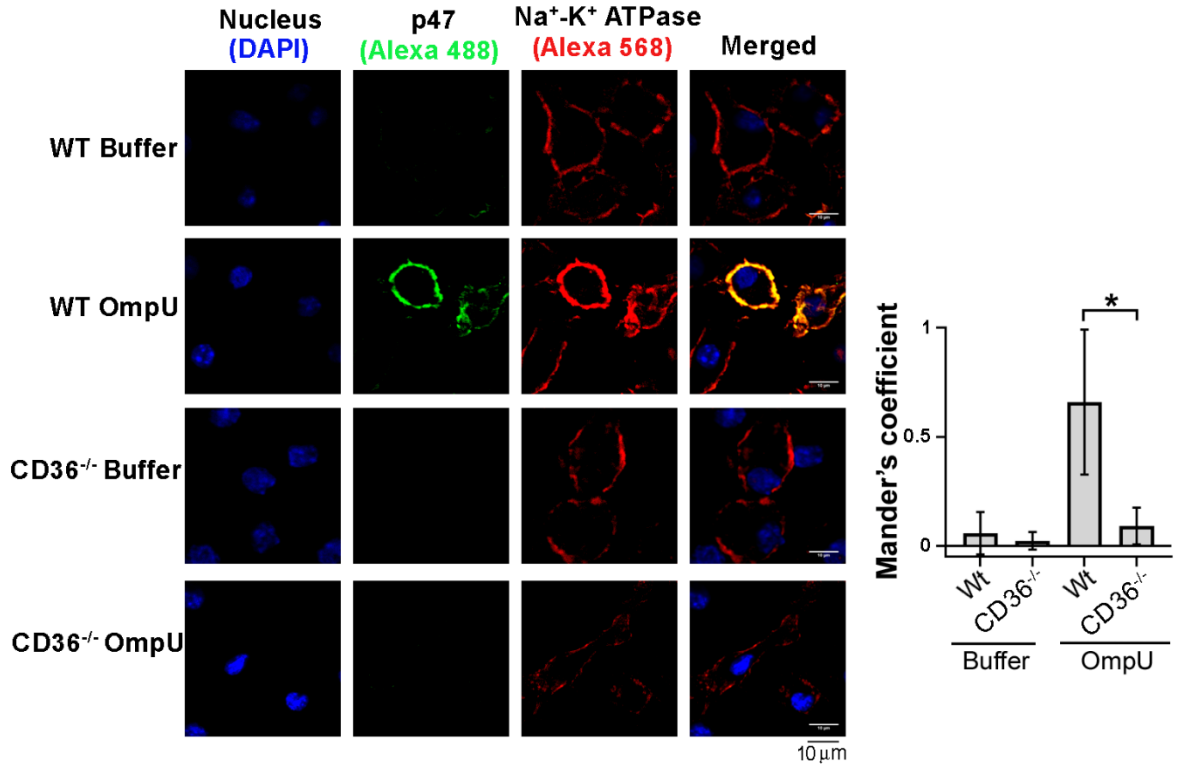


**Figure 35: Inhibition of translocation of p47 sub-unit to plasma membrane in CD36$^{-/-}$ BMDCs.**

*Colocalization p47 sub-unit with the plasma membrane marker Na$^{+}$-K$^{+}$ ATPase was inhibited in OmpU-treated DCs in absence of CD36. BMDCs from wildtype (Wt) and CD36$^{-/-}$ mice were treated with OmpU (3 µg/ml) or buffer for 4 h. Following incubation, cells were fixed using paraformaldehyde (PFA) and incubated with anti-p47 and anti-Na$^{+}$-K$^{+}$ ATPase primary antibodies. Further, cells were then stained with Alexa-488 (for p47), Alexa-568 (for Na$^{+}$-K$^{+}$ ATPase) secondary antibodies and DAPI for the nucleus. The experiment was performed three times to obtain a total of 30 images for each treatment. The images shown are representative of three independent experiments and results are expressed as mean ± SD in the bar graph. Statistical analysis was done using student's two-sided t-test. *p< 0.05 versus Wt OmpU-treated BMDCs.*

### 5.6.4 OmpU-mediated ROS production is independent of src kinase

The translocation and phosphorylation of cytosolic sub-units of NOX2 complex requires activation via various kinases. Previously, our lab showed that CD36-dependent src kinase activation is crucial in OmpU-induced NOX2 activation in macrophages [78]. As we observed CD36 plays a role in ROS production in DCs, we explored if src kinases were involved in OmpU-induced ROS generation in BMDCs. We pre-treated the cells with src kinase inhibitor (PP2) followed by OmpU treatment for 8 h. Then the cells were incubated with DCFDA dye for 30 min and followed by washing with 1x PBS, the cells were analysed using flow cytometer.

We observed that there was no effect on the ROS levels by OmpU-treated BMDCs in presence of src kinase inhibitor indicating that signalling via src kinase is probably not involved in ROS generation in DCs (Fig. 35).

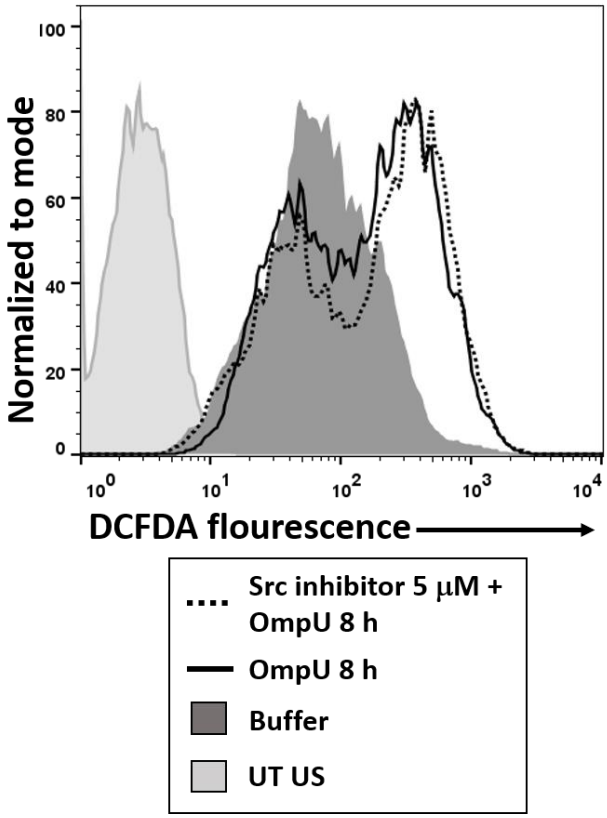


**Figure 36: Src kinase is not involved in OmpU-mediated ROS generation in DCs.**

*Src kinase inhibition did not affect OmpU-mediated ROS generation in DCs. BMDCs were pre-treated with src kinase inhibitor (PP2) for 1 h followed by OmpU (3 μg/ml) for 8 h and then stained with DCFDA dye. The cells were analysed for ROS production using flow cytometry. Histogram shown is a representative of three independent experiments.*

### 5.6.5 OmpU-mediated ROS production depends on MAPK JNK while MAPKs p38 and ERK are not involved

Several MAPKs have been shown to instigate the activation of cytoplasmic sub-units of NOX2 complex [182, 183]. In the current study, we have seen that MAPKs were activated in response to OmpU in DCs. Therefore, we explored whether the MAPKs were involved in OmpU-mediated ROS production in DCs. We pre-treated BMDCs with ERK inhibitor (PD138452) followed by OmpU treatment and analysed the DCFDA labelled cells in flow cytometer. There

was no decrease observed in the ROS levels in presence of ERK inhibitor indicating that ERK does not play any role in ROS generation in DCs (Fig. 36).

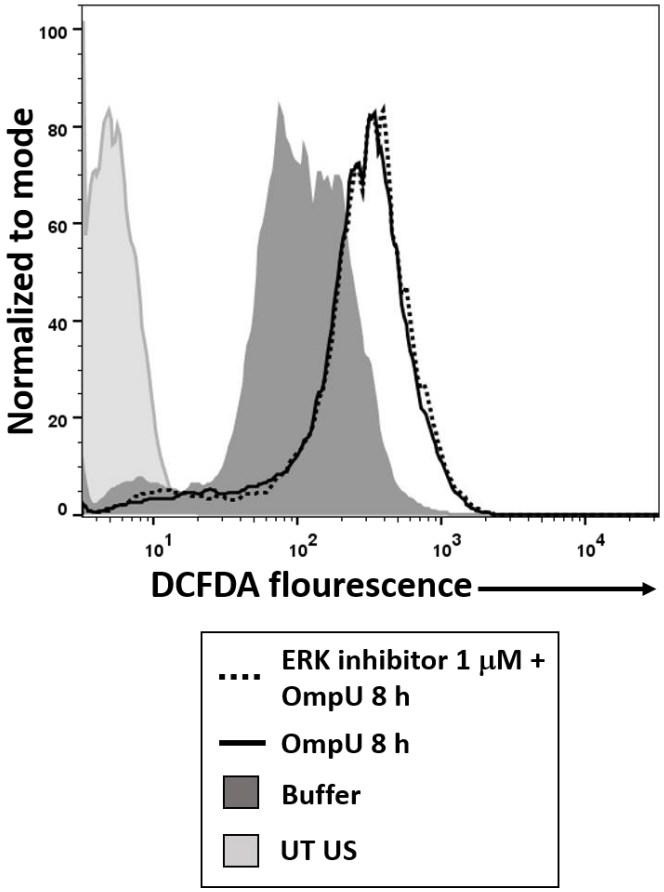


**Figure 37: MAPK ERK is not involved in ROS generation in DCs.**

*MAPK ERK inhibition did not affect OmpU-mediated ROS generation in DCs. BMDCs were pre-treated with ERK inhibitor (PD184352) for 1 h followed by OmpU (3 μg/ml) for 8 h and then stained with DCFDA dye. The cells were analysed for ROS production using flow cytometry. Histogram shown is a representative of three independent experiments.*

Further, we probed the role of MAPKs p38 and JNK in OmpU-induced ROS production using p38 inhibitor (SB202190) and JNK inhibitor (SP600125). We observed that ROS production was inhibited in BMDCs pre-treated with JNK inhibitor but not in p38 inhibitor pre-treated cells (Fig. 37A, B). This suggests that MAPK JNK plays a role in ROS generation in OmpU-treated DCs.

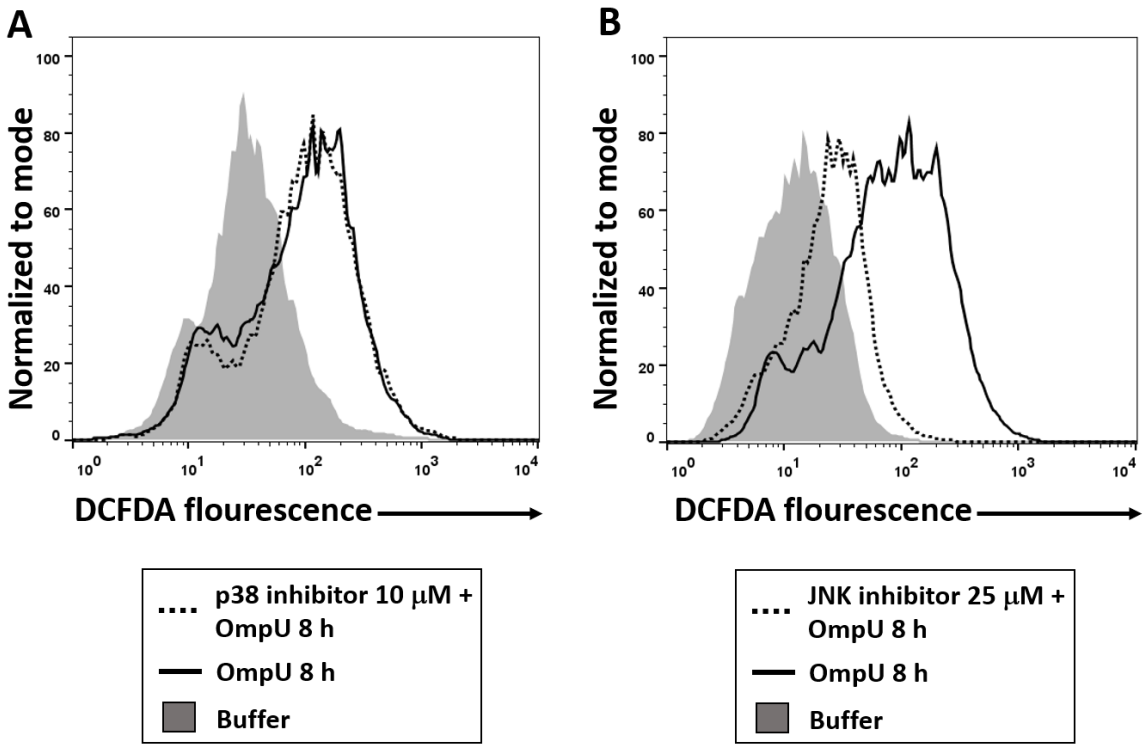


**Figure 38: OmpU-mediated ROS generation is dependent on MAPK JNK but independent of MAPK p38.**

*(A) MAPK p38 inhibition did not affect OmpU-mediated ROS generation in DCs. BMDCs were pre-treated with p38 inhibitor (SB202190) for 1 h followed by OmpU (3 μg/ml) for 8 h and then stained with DCFDA dye. The cells were analysed for ROS production using flow cytometry. Histogram shown is a representative of three independent experiments.*

*(B) MAPK JNK was involved in OmpU-induced ROS generation in BMDCs. Cells were pre-treated with JNK inhibitor (SP600125) for 1 h followed by OmpU (3 μg/ml) treatment for 8 h. Cells were stained with DCFDA dye and were analysed in flow cytometer. Histogram shown is a representative of three independent experiments.*

## 5.7 Conclusion

We explored the role of *V. cholerae* OmpU in ROS production in DCs and observed that OmpU induces significant ROS generation in DCs at 8 h and 12 h. OmpU-induced ROS production in DCs is scavenged in presence of NOX inhibitor (DPI) indicating it is NOX2 dependent. Further, we confirmed NOX2 activation by demonstrating the colocalization of p47 sub-unit with the plasma membrane $Na^+$-$K^+$ ATPase. In the present study, we also concluded that OmpU-mediated ROS contributes to the pro-inflammatory cytokine production in DCs. In addition, we observed that both TLR2 and CD36 are involved in OmpU-mediated ROS

generation in DCs and MAPK JNK is probably involved in downstream signalling for ROS generation in DCs.

# IV. Discussion

## Discussion

The generation of innate immune responses plays a pivotal role in restricting the pathogenic infection and further decides the fate of adaptive immune responses. The innate immune cells, such as macrophages, neutrophils and DCs can phagocytose and kill the antigen. Further, they can recognise the PAMPs through PRRs and activate appropriate signalling pathways eliciting pro-inflammatory responses. In addition to its innate role, DCs play a very crucial function in initiating adaptive responses by acting as professional antigen-presenting cells. Immature DCs express numerous cell surface receptors which aid in capturing the antigen leading to antigen processing and further, maturation of the DCs. The mature DCs are efficient in presenting the antigen to the naïve T-cells inducing either T-cell activation or immune tolerance [110]. PAMPs dictate the maturation of DCs and the type of adaptive immune responses it will generate, however, immune micro-environment is also important for T cell bias [184].

DCs possess a number of cell surface as well as endogenous receptors such as PRRs, scavenger receptors, complement receptors and Fc receptors (FcRs) which help in carrying out the aforementioned functions. Among the PRRs, surface TLRs recognise different PAMPS present on the surface of pathogen, such as LPS; endogenous TLRs majorly recognise nucleic acids; NLRs detect the cytosolic PAMPs or PAMP-mediated cell-derived signals, such as, loss of membrane integrity and ion flux imbalances and can form inflammasomes [96, 184]. In addition to pro-inflammatory responses, activation of NLRs can regulate DC migration, maturation and further, antigen presentation to T-cells [185]. Also, DCs express various CLRs, such as, DC-SIGN, DEC-205, Dectin 1&2 and CD206 which are lectin or mannosylated ligand binding receptors. They help in pro-inflammatory responses, antigen uptake, DC maturation, migration and interaction of DCs with the T-cells [186, 187]. The FcRs mainly FcγRs present on the DCs bind to IgG motifs or immune complexes and induce DC activation via the expression of co-stimulatory molecules [98]. In addition, several scavenger receptors such as, SR-A, CD36, SR-B1 and SREC-1 play a role in pathogen clearance and DC activation [188]. Activation of scavenger receptors, e.g., SR-A induces DC maturation and further, results in T-cell stimulation [189]. Scavenger receptors are also known to act as co-receptors with TLRs to activate DCs [190, 191].

As mentioned, the recognition of PAMPs or DAMPs by the PRRs on the DCs help in the generation of pro-inflammatory responses and further, decide the fate of adaptive immune responses. Numerous Gram-negative bacteria or bacterial components are recognized as

PAMPs by the receptors present on DCs. The Gram-negative bacterial outer membrane is comprised of several antigenic moieties such as, LPS, lipoproteins, porins and other outer membrane proteins. Porins are β-barrel channel proteins which allow the passive transport of hydrophilic molecules through them [47]. In addition to their channel property and playing a role in bacterial antibiotic resistance, several studies from pathogenic Gram-negative bacteria such as *Neisseria meningitidis* and *Shigella flexneri* have reported that porins are recognised by TLR2, which mediates the pro-inflammatory responses [192, 193]. Previously in our lab, we have observed that OmpU, an outer membrane porin from *Vibrio cholerae* activates innate immune cells such as, monocytes and macrophages to induce pro-inflammatory responses [77]. *V. cholerae* is a gastrointestinal Gram-negative bacterium which colonizes the small intestine in humans and causes the diarrhoeal disease, cholera. *V. cholerae* secretes several toxins and possesses a variety of outer membrane proteins which help in bacterial pathogenesis. The expression of OmpU on *V. cholerae* is increased drastically in presence of bile in the gut and in our lab, we have elaborately studied the role of OmpU as a PAMP in monocytes and macrophages [41, 77, 78]. Further, we have observed that murine DCs recognise *V. cholerae* OmpU, producing pro-inflammatory cytokines IL-6, TNFα and IL-1β (Fig. 1). We have also observed that OmpU-treated DCs showed increased expression of co-stimulatory markers CD80 and CD86, and MHC-II molecules suggesting activation and maturation of DCs (Fig. 2).

In the present study, we have investigated which PRRs are involved in OmpU-mediated pro-inflammatory responses in DCs and what are the downstream signalling molecules. Similar to as our lab has reported earlier in case of macrophages and monocytes, in the present study we observed that *V. cholerae* OmpU induces its signal in DCs via TLR2 and MyD88 (Fig. 3A-C, 4A-F).

The induction of PRRs via PAMPs activate various signalling mediators such as, kinases and transcription factors which partake in the inflammatory responses. Generally, the pro-inflammatory responses involve activation of transcription factors NF-κB and AP-1. NF-κB remains in the cytoplasm in inactivated condition bound to its inhibitor IκB. IκB kinase (IKK) phosphorylates IκB and followed by phosphorylation it gets ubiquitinated and degraded. To check whether OmpU can induce activation of NF-κB transcription factor in OmpU-induced cytokine responses, we used IKK inhibitor PS-1145 and observed a decrease in IL-6 levels in OmpU-stimulated BMDCs (Fig. 5A). We also observed that IκBα levels were reduced in

response to OmpU stimulation in DCs indicating activation of NF-κB transcription factor (Fig. 5B).

Activation of AP-1 transcription factor needs the activation of MAP kinases. The activation of MAPKs in response to different TLR ligands is known to be important for phenotypic (upregulation of DC markers) as well as functional maturation (secretion of specific cytokines) of DCs [194, 195]. We observed that OmpU-mediated DC activation results in upregulation of phosphorylation levels of MAPKs p38, JNK and ERK (Fig. 7A, B & 8A). Further, in presence of MAPK inhibitors, we observed reduced levels of OmpU-induced IL-6 production indicating the role involvement of MAPKs in OmpU-mediated pro-inflammatory cytokine responses (Fig. 6A, B & 8B).

In addition to MAPKs, TLR signalling has been shown to activate myriad kinases such as, PI3Ks, PKCs [119, 120]. Towards probing whether OmpU activates PI3K in DCs, we detected increased levels of phosphorylated-PI3K (p-PI3K) in OmpU-treated BMDCs (Fig. 9A). Further, we observed a significant reduction in pro-inflammatory responses in the presence of PI3K inhibitor, LY294002, in OmpU-activated DCs (Fig. 9B). PI3Ks have been classified into three different classes: Class I, II and III. They are comprised of different PI3K isoforms. There are four class I isoforms (PI3Kα, β, γ and δ), three class II isoforms (PI3KC2α, β and γ) and one class III isoform (Vps34). It has been shown that different PI3K isoforms show selective expression in different cell types [196]. By using PI3K class I/II inhibitor, GDC-0941 and class III inhibitor, SAR 405 we have determined that PI3K class I/II isoforms are involved in OmpU-mediated pro-inflammatory responses in DCs (Fig. 9C, D). Further, as it is known that PI3K signalling can lead to activation of AKT, we probed whether OmpU activates AKT in DCs. We observed an increased levels of phosphorylated-AKT (p-AKT) and a significant decrease in pro-inflammatory responses following using of AKT inhibitor suggesting involvement of AKT in OmpU-activated DCs (Fig. 10A, B).

Further, we checked whether OmpU induces calcium signalling. We observed an increased calcium influx in DCs upon exposure to OmpU (Fig. 11A). PI3K signalling along with calcium flux can induce the activation of various kinases such as PKCs [128]. We observed that in case of OmpU-activated DCs, the phosphorylation of PKC was considerably increased and further in presence of PKC inhibitor BIM IV, there is a significant decrease in OmpU-mediated pro-inflammatory cytokine production (Fig. 12A-C). PKC has various isoforms: PKC α, βI, βII and γ. Different PKC isoforms play different roles in DC function and activation, such as, PKC

βII mediates DC differentiation and PKC α contributes in MyD88-dependent cytokine responses in response to TLR ligands in DCs [197, 198]. Our investigation using PKCα/γ inhibitor HBDDE and established that PKCα/γ isoforms are involved in OmpU-induced pro-inflammatory cytokine responses (Fig. 12D). In addition, we observed that activation of MAPKs p38 and ERK, IκB, PKC and calcium influx was TLR2 dependent while PI3K and MAPK JNK activation were TLR2 independent (Fig. 13A-G).

Further, in OmpU-activated DCs we have observed IL-1β production, which requires involvement of inflammasome, a cytosolic multi-protein complex, in the cells. Activation of inflammasome leads to cleavage of pro-caspase-1 into active caspase-1. We have shown that OmpU activates the NLRP3 inflammasome complex in DCs leading to the cleavage of pro-caspase-1 to active caspase-1 and release of IL-1β from the cells (Fig. 13, 14, 15, 16B).

In literature, it has been shown that inflammasome activation assist in regulating the innate immune responses of DCs as well as shaping the outcome of the T-cell responses. The activation of inflammasome and IL-1β release in DCs play an important role in T-cell priming by aiding in release of cytokines such as, IL-12. The recognition of PAMP by NLRs warrants the mature DCs for activation of naïve T-cells. Thus, the inflammasome activation in DCs drive the immune responses generated by DCs and also regulates the T-cell polarization and activation [199, 200]. Inflammasome activation requires two signals, one signal is provided by activation of TLR signalling pathway which helps in the transcriptional upregulation of the key components of the inflammasome complex and generation of pro-IL-1β and the second signal involves triggering the NLR leading to assembly and activation of inflammasome [201]. As, we observed that TLR2 signalling is activated in OmpU-treated DCs, it can mediate the signal for the production of components of NLRP3 inflammasome. The assembly and activation of NLRP3 inflammasome can be triggered through various signals ranging from disruption of ion balance in the cell, changes in mitochondrial membrane potential (MMP) to ligand internalization by scavenger receptors.

Over the last decade, mitochondria have evolved as an indispensable platform for pro-inflammatory signalling events. They have been recognized as ‘supramolecular organizing centres’ (SMOCs) for NLRP3 assembly and activation [202]. The interaction of various mitochondrial proteins such as MAVS (mitochondrial antiviral-signalling protein), mitofusin 2 and cardiolipin with different components of NLRP3 machinery, further leads to its activation highlighting the role played by mitochondria for NLRP3 inflammasome assembly and

activation [149-151]. In the present study, we observed that mitochondria interact with NLRP3 inflammasome in the OmpU-stimulated BMDCs (Fig. 16A). Further, mitochondria-derived signals and molecules such as, mitochondrial DNA (mtDNA), mitochondrial ROS (mitoROS) and imbalance in MMP induced in response to mitochondrial damage can serve as activation signal for NLRP3 activation [152, 154]. We established that OmpU induces mitoROS generation in DCs which is involved in NLRP3 activation (19A, B, C). Next, we probed what could be the trigger behind the mitoROS generation in OmpU-activated DCs. Several bacteria have evolved the mechanism to target their virulence factors to mitochondria of the host cells culminating in mitochondrial damage or evasion of host cellular machinery [63, 203, 204]. Previously, in our lab, Gupta et al, have demonstrated that *V. cholerae* OmpU translocate to the host cell mitochondria inducing caspase-independent programmed cell death pathway via AIF (apoptosis-inducing factor) release in monocytes and epithelial cells [80]. Further, Prasad et al, from our laboratory have shown that OmpU translocation to the mitochondria is involved in mitoROS generation in macrophages [78]. Therefore, in our case, we probed whether OmpU translocates to the mitochondria of DCs and observed that OmpU was present in the mitochondrial fractions isolated from OmpU-treated DCs (Fig. 20, 21). Further, we observed that the translocation of OmpU to mitochondria of DCs was inhibited in presence of cytochalasin D (Fig. 22). Using cytochalasin D, we established that OmpU translocation to mitochondria is important to induce mitoROS generation in DCs (Fig. 23A, B).

Further, calcium mobilization through various $Ca^{2+}$ channels such as TRPM2 and TRPV2 have been reported to trigger NLRP3 inflammasome assembly and activation. Increased calcium flux in response to various PAMPs and PAMP-derived signals can lead to mitochondrial damage, loss of MMP and mitoROS generation [153, 205]. We have observed that in addition to mitoROS the OmpU-mediated calcium influx also plays a role in IL-1β generation in DCs (Fig. 18). Using BAPATA-AM inhibitor we showed that OmpU-mediated calcium influx is involved in mitoROS generation in DCs (Fig. 24A, B). These results suggested that both OmpU translocation to mitochondria of DCs and OmpU-mediated calcium influx are crucial for mitoROS generation leading to NLRP3 activation in DCs.

In this study, we have shown that OmpU activates DCs via TLR2 which can also provide the first signal for the activation of NLRP3 inflammasome. Moreover, OmpU translocation to the mitochondria of DCs and upregulated calcium influx induces mitoROS generation which provides the second signal for NLRP3 activation and triggers inflammasome assembly. Such a mechanism for NLRP3 activation and providing dual signals for triggering the inflammasome

has not been reported for any of the related bacterial porins. Based on these observations, the signalling mechanism proposed is summarised in the illustration 12.

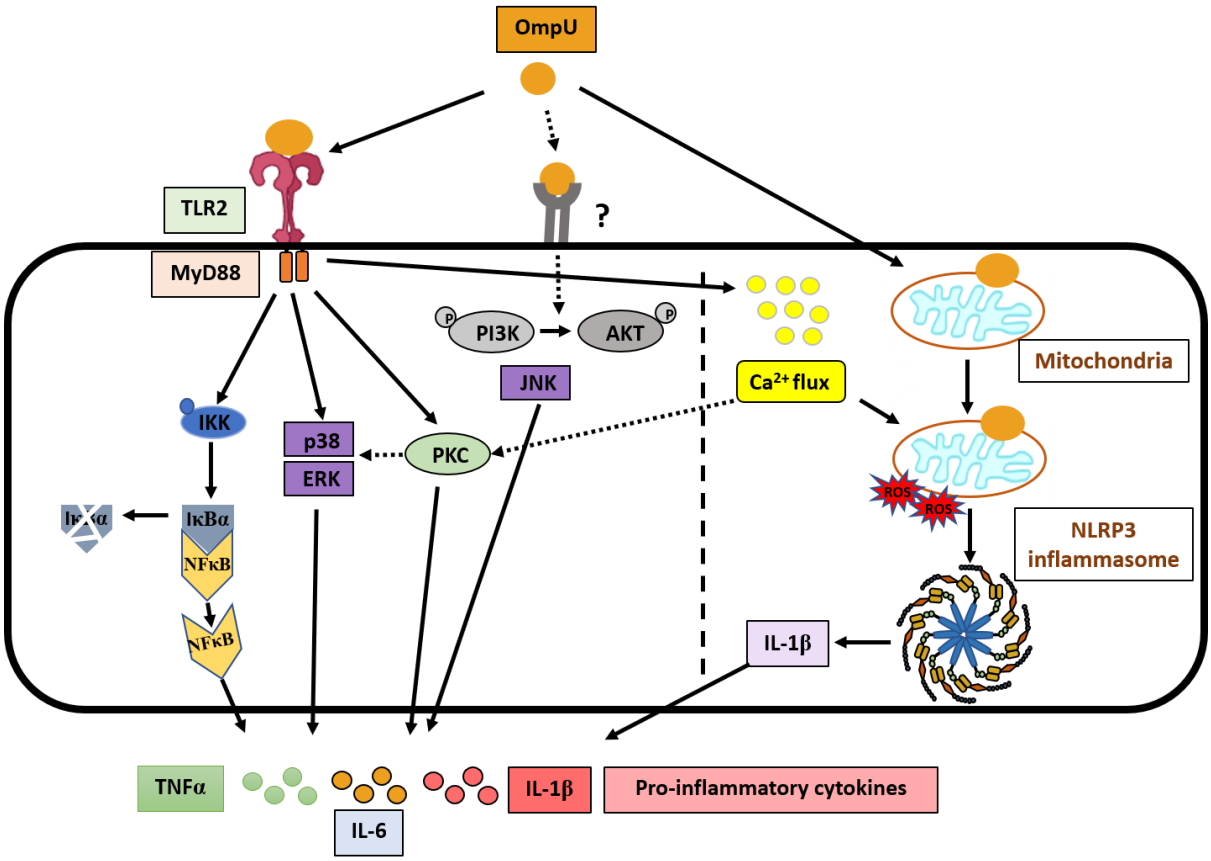


**Illustration 12: OmpU-induced signalling for production of pro-inflammatory cytokines in DCs.**

*OmpU is recognized by TLR2 in DCs leading to downstream signalling via MyD88, IKK, MAPKs p38 and ERK, and PKC while activation of PI3K-AKT and MAPK JNK are probably downstream to some other receptor. This signalling triggers the release of pro-inflammatory cytokines. Additionally, OmpU induces calcium influx and also translocates to mitochondria in DCs, both of which, trigger the mitoROS generation. OmpU-induced mitoROS, further, leads to activation of NLRP3 inflammasome and IL-1β release in DCs.*

Further, we observed that in addition to mitochondrial ROS, OmpU induces cytoplasmic ROS generation in DCs (Fig. 25). We observed a decrease in pro-inflammatory responses in OmpU-stimulated BMDCs upon scavenging of total ROS using ROS scavengers (NAC & DPI) (Fig. 28 & 29). In addition to generation of inflammatory cytokine responses, the role of reactive oxygen species (ROS) has been implicated in the pathogenesis of several bacterial infections. ROS not only help in eliminating the pathogen but are also emerging as second messengers in

the PAMP-mediated signalling cascades [156, 179]. Previously, Prasad et al, from our lab have demonstrated that OmpU induces NOX2-mediated ROS generation in macrophages [78]. To probe the source of cytoplasmic ROS in BMDCs, we used DPI, a NOX complex inhibitor and observed that OmpU-induced ROS was inhibited in presence of DPI (Fig. 26). Further, to confirm the involvement of NOX2 in OmpU-induced ROS generation, we probed for the translocation of cytoplasmic NOX2 sub-unit p47 to the plasma membrane. We observed that p47 colocalized with the plasma membrane marker, $Na^+$-$K^+$ ATPase confirming the role of NOX2 in response to OmpU (Fig. 27).

Different PRRs including TLR2, TLR4 and Dectin-1 have been known to recognise PAMPs for activation of NOX2 complex in DCs [206, 207]. As we have observed that TLR2 mediates the pro-inflammatory cytokine responses in OmpU-stimulated DCs, we explored the role of TLR2 in OmpU-induced ROS production and found that the ROS generation and NOX activation depends on TLR2 (Fig. 30 & 31).

The role of scavenger receptors has been explored as a co-receptor for TLRs. It has been shown that scavenger receptor CD36 mediates the inflammatory responses in co-operation with TLR2/1 in LPS-induced endothelial cells [208]. However, Prasad et al, from our laboratory have shown that in response to OmpU in case of macrophages, CD36 itself is capable of inducing ROS generation. Therefore, we checked whether OmpU interacts with CD36 in DCs and observed that OmpU co-immunoprecipitated with CD36 (Fig. 32). Consequently, we explored the role of CD36 in OmpU-induced ROS production and found that along with TLR2, CD36 is involved in ROS generation (Fig. 33). Moreover, we observed that the colocalization of p47 with $Na^+$-$K^+$ ATPase was inhibited in response to OmpU in BMDCs from both $TLR2^{-/-}$ and $CD36^{-/-}$ mice (Fig. 31 & 34). Thus, we concluded that both TLR2 and CD36 are indispensable for ROS generation and NOX activation in DCs stimulated with OmpU.

Further, we questioned how the OmpU-induced signalling mediates the activation of NOX2 complex. Prasad et al, from our laboratory have shown that CD36-mediated signalling activates src kinases in response to OmpU to induce NOX2-mediated ROS generation in macrophages [78]. However, in DCs, we observed that src kinase does not play any role in OmpU-induced ROS generation (Fig. 35). Several studies have suggested that MAPKs including p38, JNK and ERK can phosphorylate the cytoplasmic sub-units of NOX2 complex leading to its activation [182, 183, 207]. Towards, probing whether any of the MAPKs are involved in OmpU-mediated ROS generation in DCs, we observed that JNK but not p38 or ERK can activate the NOX2-

mediated ROS generation in OmpU-activated DCs (Fig. 36 & 37A, B). Therefore, from these results we determined that OmpU-induced ROS generation in DCs involves the activation of NOX2 complex via JNK. The other MAPKs such as ERK and p38 as well as src kinases are not involved in the OmpU-induced ROS production. These results are summarised in the illustration 13 as shown:

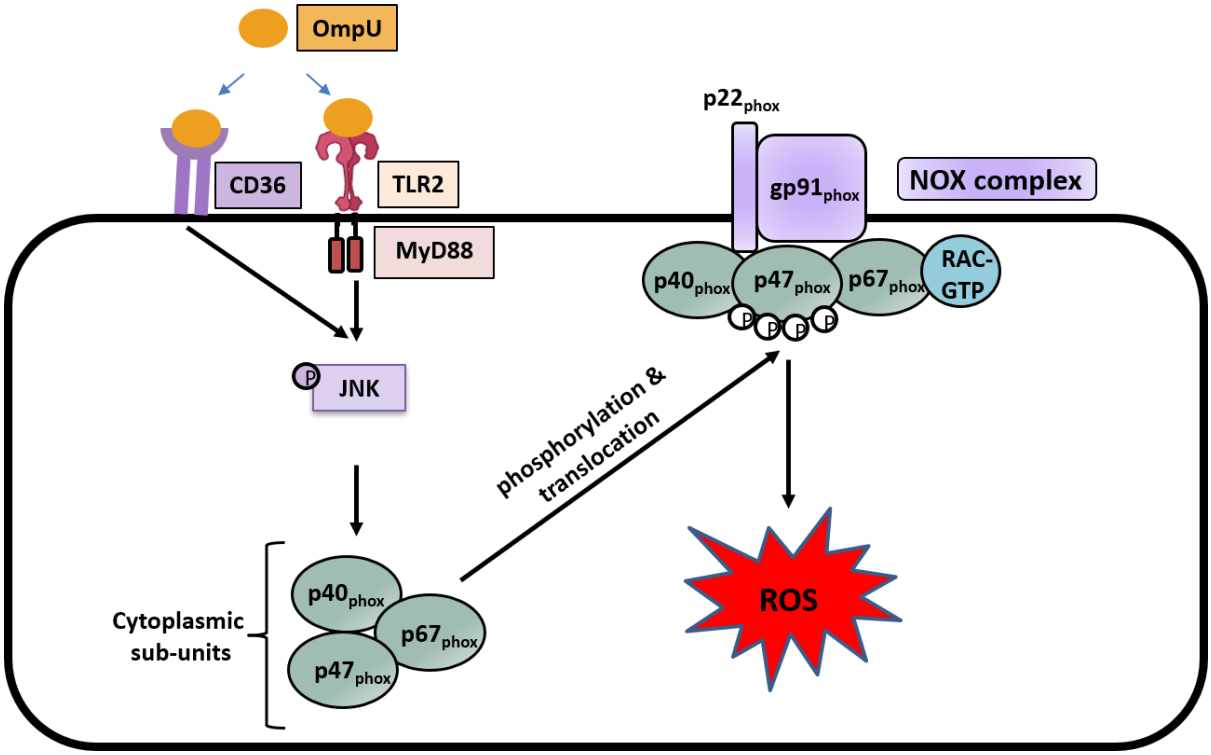


**Illustration 13: Activation of NOX2 complex for ROS generation in OmpU-stimulated DCs.**

*OmpU interacts with both TLR2 and CD36 leading to activation of MAPK JNK which signals the activation of NOX2 complex by translocation and colocalization of cytoplasmic NOX2 subunits to the plasma membrane.*

# V. References

# References


1. Finkelstein, R.A., *Cholera, Vibrio cholerae O1 and O139, and Other Pathogenic Vibrios*, in *Medical Microbiology*, th and S. Baron, Editors. 1996: Galveston (TX).
2. Snow, J., *On the Mode of Communication of Cholera.* Edinb Med J, 1856. **1**(7): p. 668-670.
3. Carboni, G.P., *The enigma of Pacini's Vibrio cholerae discovery.* J Med Microbiol, 2021. **70**(11).
4. Hall, R.H., *A De in the life of cholera.* Indian J Med Res, 2011. **133**: p. 146-52.
5. Almagro-Moreno, S. and R.K. Taylor, *Cholera: Environmental Reservoirs and Impact on Disease Transmission.* Microbiol Spectr, 2013. **1**(2).
6. Weir, E. and S. Haider, *Cholera outbreaks continue.* CMAJ, 2004. **170**(7): p. 1092-3.
7. Clemens, J.D., et al., *Cholera.* Lancet, 2017. **390**(10101): p. 1539-1549.
8. D'Mello-Guyett, L., et al., *Prevention and control of cholera with household and community water, sanitation and hygiene (WASH) interventions: A scoping review of current international guidelines.* PLoS One, 2020. **15**(1): p. e0226549.
9. Nelson, E.J., et al., *Cholera transmission: the host, pathogen and bacteriophage dynamic.* Nat Rev Microbiol, 2009. **7**(10): p. 693-702.
10. Almagro-Moreno, S., K. Pruss, and R.K. Taylor, *Intestinal Colonization Dynamics of Vibrio cholerae.* PLoS Pathog, 2015. **11**(5): p. e1004787.
11. Hay, A.J. and J. Zhu, *Host intestinal signal-promoted biofilm dispersal induces Vibrio cholerae colonization.* Infect Immun, 2015. **83**(1): p. 317-23.
12. Kim, S., A. Covington, and E.G. Pamer, *The intestinal microbiota: Antibiotics, colonization resistance, and enteric pathogens.* Immunol Rev, 2017. **279**(1): p. 90-105.
13. Millet, Y.A., et al., *Insights into Vibrio cholerae intestinal colonization from monitoring fluorescently labeled bacteria.* PLoS Pathog, 2014. **10**(10): p. e1004405.
14. Erfanimanesh, S., et al., *Capsaicin inhibitory effects on Vibrio cholerae toxin genes expression.* Avicenna J Phytomed, 2019. **9**(3): p. 187-194.
15. Mitchell, K.C., et al., *Quantifying Vibrio cholerae Enterotoxicity in a Zebrafish Infection Model.* Appl Environ Microbiol, 2017. **83**(16).
16. Bishop, A.L., B. Patimalla, and A. Camilli, *Vibrio cholerae-induced inflammation in the neonatal mouse cholera model.* Infect Immun, 2014. **82**(6): p. 2434-47.
17. Lekshmi, N., et al., *Changing facades of Vibrio cholerae: An enigma in the epidemiology of cholera.* Indian J Med Res, 2018. **147**(2): p. 133-141.
18. Ramamurthy, T., et al., *Virulence Regulation and Innate Host Response in the Pathogenicity of Vibrio cholerae.* Front Cell Infect Microbiol, 2020. **10**: p. 572096.
19. Boyd, E.F. and M.K. Waldor, *Evolutionary and functional analyses of variants of the toxin-coregulated pilus protein TcpA from toxigenic Vibrio cholerae non-O1/non-O139 serogroup isolates.* Microbiology (Reading), 2002. **148**(Pt 6): p. 1655-1666.
20. Sanchez, J. and J. Holmgren, *Cholera toxin structure, gene regulation and pathophysiological and immunological aspects.* Cell Mol Life Sci, 2008. **65**(9): p. 1347-60.
21. Perez-Reytor, D., et al., *Accessory Toxins of Vibrio Pathogens and Their Role in Epithelial Disruption During Infection.* Front Microbiol, 2018. **9**: p. 2248.
22. Rivera, I.G., et al., *Detection of cholera (ctx) and zonula occludens (zot) toxin genes in Vibrio cholerae O1, O139 and non-O1 strains.* World J Microbiol Biotechnol, 1995. **11**(5): p. 572-7.
23. Trucksis, M., et al., *Accessory cholera enterotoxin (Ace), the third toxin of a Vibrio cholerae virulence cassette.* Proc Natl Acad Sci U S A, 1993. **90**(11): p. 5267-71.
24. Satchell, K.J.F., *Multifunctional-autoprocessing repeats-in-toxin (MARTX) Toxins of Vibrios.* Microbiol Spectr, 2015. **3**(3).
25. Rai, A.K. and K. Chattopadhyay, *Vibrio cholerae cytolysin: structure-function mechanism of an atypical beta-barrel pore-forming toxin.* Adv Exp Med Biol, 2015. **842**: p. 109-25.

26. Kathuria, R. and K. Chattopadhyay, *Vibrio cholerae cytolysin: Multiple facets of the membrane interaction mechanism of a beta-barrel pore-forming toxin.* IUBMB Life, 2018. **70**(4): p. 260-266.
27. Richard A. Alm, G.B., Renato Morona, Paul A. Manning, *Detection of an OmpA-like protein in Vibrio cholerae.* FEMS Microbiol Lett, 1986. **37**(1): p. 99-104.
28. Sthitmatee, N., et al., *Protection of chickens from fowl cholera by vaccination with recombinant adhesive protein of Pasteurella multocida.* Vaccine, 2008. **26**(19): p. 2398-407.
29. Deb, A., D. Bhattacharyya, and J. Das, *A 25-kDa beta-lactam-induced outer membrane protein of Vibrio cholerae. Purification and characterization.* J Biol Chem, 1995. **270**(7): p. 2914-20.
30. Inoue, T., S. Matsuzaki, and S. Tanaka, *A 26-kDa outer membrane protein, OmpK, common to Vibrio species is the receptor for a broad-host-range vibriophage, KVP40.* FEMS Microbiol Lett, 1995. **125**(1): p. 101-5.
31. Fu, X., et al., *The Outer Membrane Protein OmpW Enhanced V. cholerae Growth in Hypersaline Conditions by Transporting Carnitine.* Front Microbiol, 2017. **8**: p. 2703.
32. Nandi, B., et al., *Structural features, properties and regulation of the outer-membrane protein W (OmpW) of Vibrio cholerae.* Microbiology (Reading), 2005. **151**(Pt 9): p. 2975-2986.
33. Xu, D., et al., *Outer membrane protein OmpW is the receptor for typing phage VP5 in the Vibrio cholerae O1 El Tor biotype.* J Virol, 2014. **88**(12): p. 7109-11.
34. Chakrabarti, S.R., et al., *Porins of Vibrio cholerae: purification and characterization of OmpU.* J Bacteriol, 1996. **178**(2): p. 524-30.
35. Lang, H. and T.K. Korhonen, *The OmpS maltoporin of Vibrio cholerae as carrier of foreign epitopes.* Behring Inst Mitt, 1997(98): p. 400-9.
36. Stevenson, G., et al., *Purification of the 25-kDa Vibrio cholerae major outer-membrane protein and the molecular cloning of its gene: ompV.* Eur J Biochem, 1985. **148**(2): p. 385-90.
37. Ottemann, K.M., V.J. DiRita, and J.J. Mekalanos, *ToxR proteins with substitutions in residues conserved with OmpR fail to activate transcription from the cholera toxin promoter.* J Bacteriol, 1992. **174**(21): p. 6807-14.
38. Tow, L.A. and V.E. Coyne, *Cloning and characterisation of a novel ompB operon from Vibrio cholerae 569B.* Biochim Biophys Acta, 1999. **1444**(2): p. 269-75.
39. Heidelberg, J.F., et al., *DNA sequence of both chromosomes of the cholera pathogen Vibrio cholerae.* Nature, 2000. **406**(6795): p. 477-83.
40. Simonet, V.C., et al., *The Vibrio cholerae porins OmpU and OmpT have distinct channel properties.* J Biol Chem, 2003. **278**(19): p. 17539-45.
41. Wibbenmeyer, J.A., et al., *Vibrio cholerae OmpU and OmpT porins are differentially affected by bile.* Infect Immun, 2002. **70**(1): p. 121-6.
42. Fan, F., et al., *The outer-membrane protein TolC of Vibrio cholerae serves as a second cell-surface receptor for the VP3 phage.* J Biol Chem, 2018. **293**(11): p. 4000-4013.
43. Bina, J.E. and J.J. Mekalanos, *Vibrio cholerae tolC is required for bile resistance and colonization.* Infect Immun, 2001. **69**(7): p. 4681-5.
44. Butterton, J.R., S.A. Boyko, and S.B. Calderwood, *Use of the Vibrio cholerae irgA gene as a locus for insertion and expression of heterologous antigens in cholera vaccine strains.* Vaccine, 1993. **11**(13): p. 1327-35.
45. Goulart, C.L., et al., *Molecular analysis of VCA1008: a putative phosphoporin of Vibrio cholerae.* FEMS Microbiol Lett, 2009. **298**(2): p. 241-8.
46. Goulart, C.L., et al., *VCA1008: An Anion-Selective Porin of Vibrio Cholerae.* Biochim Biophys Acta, 2015. **1848**(2): p. 680-7.
47. Nikaido, H., *Porins and specific channels of bacterial outer membranes.* Mol Microbiol, 1992. **6**(4): p. 435-42.

48. Achouak, W., T. Heulin, and J.M. Pages, *Multiple facets of bacterial porins.* FEMS Microbiol Lett, 2001. **199**(1): p. 1-7.
49. Domenech-Sanchez, A., et al., *Role of Klebsiella pneumoniae OmpK35 porin in antimicrobial resistance.* Antimicrob Agents Chemother, 2003. **47**(10): p. 3332-5.
50. Gill, M.J., et al., *Gonococcal resistance to beta-lactams and tetracycline involves mutation in loop 3 of the porin encoded at the penB locus.* Antimicrob Agents Chemother, 1998. **42**(11): p. 2799-803.
51. Bartsch, A., et al., *An antibiotic-resistance conferring mutation in a neisserial porin: Structure, ion flux, and ampicillin binding.* Biochim Biophys Acta Biomembr, 2021. **1863**(6): p. 183601.
52. Choi, U. and C.R. Lee, *Distinct Roles of Outer Membrane Porins in Antibiotic Resistance and Membrane Integrity in Escherichia coli.* Front Microbiol, 2019. **10**: p. 953.
53. Nikaido, H., *Structure and mechanism of RND-type multidrug efflux pumps.* Adv Enzymol Relat Areas Mol Biol, 2011. **77**: p. 1-60.
54. Nikaido, H. and Y. Takatsuka, *Mechanisms of RND multidrug efflux pumps.* Biochim Biophys Acta, 2009. **1794**(5): p. 769-81.
55. Jeannin, P., et al., *Outer membrane protein A (OmpA): a new pathogen-associated molecular pattern that interacts with antigen presenting cells-impact on vaccine strategies.* Vaccine, 2002. **20 Suppl 4**: p. A23-7.
56. Wu, H.H., et al., *OmpA is the critical component for Escherichia coli invasion-induced astrocyte activation.* J Neuropathol Exp Neurol, 2009. **68**(6): p. 677-90.
57. Serino, L., et al., *Identification of a new OmpA-like protein in Neisseria gonorrhoeae involved in the binding to human epithelial cells and in vivo colonization.* Mol Microbiol, 2007. **64**(5): p. 1391-403.
58. Platt, A., et al., *In vivo and in vitro characterization of the immune stimulating activity of the Neisserial porin PorB.* PLoS One, 2013. **8**(12): p. e82171.
59. Cervantes-Barragan, L., et al., *TLR2 and TLR4 signaling shapes specific antibody responses to Salmonella typhi antigens.* Eur J Immunol, 2009. **39**(1): p. 126-35.
60. Singleton, T.E., P. Massari, and L.M. Wetzler, *Neisserial porin-induced dendritic cell activation is MyD88 and TLR2 dependent.* J Immunol, 2005. **174**(6): p. 3545-50.
61. Perez-Toledo, M., et al., *Salmonella Typhi Porins OmpC and OmpF Are Potent Adjuvants for T-Dependent and T-Independent Antigens.* Front Immunol, 2017. **8**: p. 230.
62. Biswas, A., et al., *Porin of Shigella dysenteriae activates mouse peritoneal macrophage through Toll-like receptors 2 and 6 to induce polarized type I response.* Mol Immunol, 2007. **44**(5): p. 812-20.
63. Deo, P., et al., *Outer membrane vesicles from Neisseria gonorrhoeae target PorB to mitochondria and induce apoptosis.* PLoS Pathog, 2018. **14**(3): p. e1006945.
64. Tiku, V., et al., *Outer membrane vesicles containing OmpA induce mitochondrial fragmentation to promote pathogenesis of Acinetobacter baumannii.* Sci Rep, 2021. **11**(1): p. 618.
65. Nie, D., et al., *Outer membrane protein A (OmpA) as a potential therapeutic target for Acinetobacter baumannii infection.* J Biomed Sci, 2020. **27**(1): p. 26.
66. Duperthuy, M., et al., *The major outer membrane protein OmpU of Vibrio splendidus contributes to host antimicrobial peptide resistance and is required for virulence in the oyster Crassostrea gigas.* Environ Microbiol, 2010. **12**(4): p. 951-63.
67. Lv, T., et al., *Outer membrane protein OmpU is related to iron balance in Vibrio alginolyticus.* Microbiol Res, 2020. **230**: p. 126350.
68. Liu, X., et al., *Outer membrane protein U (OmpU) mediates adhesion of Vibrio mimicus to host cells via two novel N-terminal motifs.* PLoS One, 2015. **10**(3): p. e0119026.
69. Cai, S.H., et al., *Immune response in Lutjanus erythropterus induced by the major outer membrane protein (OmpU) of Vibrio alginolyticus.* Dis Aquat Organ, 2010. **90**(1): p. 63-8.

70. Wang, Q., et al., *Identification and evaluation of an outer membrane protein OmpU from a pathogenic Vibrio harveyi isolate as vaccine candidate in turbot (Scophthalmus maximus).* Lett Appl Microbiol, 2011. **53**(1): p. 22-9.
71. Fu, Y., et al., *Immunogenicity study of OmpU subunit vaccine against Vibrio mimicus in yellow catfish, Pelteobagrus fulvidraco.* Fish Shellfish Immunol, 2021. **108**: p. 80-85.
72. Goo, S.Y., et al., *Identification of OmpU of Vibrio vulnificus as a fibronectin-binding protein and its role in bacterial pathogenesis.* Infect Immun, 2006. **74**(10): p. 5586-94.
73. Jung, C.R., M.J. Park, and M.S. Heo, *Immunization with major outer membrane protein of Vibrio vulnificus elicits protective antibodies in a murine model.* J Microbiol, 2005. **43**(5): p. 437-42.
74. Gulati, A., R. Kumar, and A. Mukhopadhaya, *Differential Recognition of Vibrio parahaemolyticus OmpU by Toll-Like Receptors in Monocytes and Macrophages for the Induction of Proinflammatory Responses.* Infect Immun, 2019. **87**(5).
75. Provenzano, D. and K.E. Klose, *Altered expression of the ToxR-regulated porins OmpU and OmpT diminishes Vibrio cholerae bile resistance, virulence factor expression, and intestinal colonization.* Proc Natl Acad Sci U S A, 2000. **97**(18): p. 10220-4.
76. Mathur, J. and M.K. Waldor, *The Vibrio cholerae ToxR-regulated porin OmpU confers resistance to antimicrobial peptides.* Infect Immun, 2004. **72**(6): p. 3577-83.
77. Sakharwade, S.C., P.K. Sharma, and A. Mukhopadhaya, *Vibrio cholerae porin OmpU induces pro-inflammatory responses, but down-regulates LPS-mediated effects in RAW 264.7, THP-1 and human PBMCs.* PLoS One, 2013. **8**(9): p. e76583.
78. Prasad, G., V. Dhar, and A. Mukhopadhaya, *Vibrio cholerae OmpU Mediates CD36-Dependent Reactive Oxygen Species Generation Triggering an Additional Pathway of MAPK Activation in Macrophages.* J Immunol, 2019. **202**(8): p. 2431-2450.
79. Yu, J., et al., *Selection and characterization of a Vibrio parahaemolyticus OmpU antibody by phage display.* Microb Pathog, 2020. **143**: p. 104136.
80. Gupta, S., G.V. Prasad, and A. Mukhopadhaya, *Vibrio cholerae Porin OmpU Induces Caspase-independent Programmed Cell Death upon Translocation to the Host Cell Mitochondria.* J Biol Chem, 2015. **290**(52): p. 31051-68.
81. Paauw, A., et al., *OmpU as a biomarker for rapid discrimination between toxigenic and epidemic Vibrio cholerae O1/O139 and non-epidemic Vibrio cholerae in a modified MALDI-TOF MS assay.* BMC Microbiol, 2014. **14**: p. 158.
82. Li, H., W. Zhang, and C. Dong, *Crystal structure of the outer membrane protein OmpU from Vibrio cholerae at 2.2 A resolution.* Acta Crystallogr D Struct Biol, 2018. **74**(Pt 1): p. 21-29.
83. Pathania, M., et al., *Unusual Constriction Zones in the Major Porins OmpU and OmpT from Vibrio cholerae.* Structure, 2018. **26**(5): p. 708-721 e4.
84. Khan, J., P.K. Sharma, and A. Mukhopadhaya, *Vibrio cholerae porin OmpU mediates M1-polarization of macrophages/monocytes via TLR1/TLR2 activation.* Immunobiology, 2015. **220**(11): p. 1199-209.
85. Sakharwade, S.C. and A. Mukhopadhaya, *Vibrio cholerae porin OmpU induces LPS tolerance by attenuating TLR-mediated signaling.* Mol Immunol, 2015. **68**(2 Pt A): p. 312-24.
86. Iwasaki, A. and R. Medzhitov, *Control of adaptive immunity by the innate immune system.* Nat Immunol, 2015. **16**(4): p. 343-53.
87. Wilson, C.C. and R.T. Schooley, *Host Responses to Infection.* 2017: p. 26-39.e2.
88. Chandrasoma P, T.C., *The Acute Inflammatory Response.* Concise Pathology, 3e. McGraw Hill., 1998.
89. Mogensen, T.H., *Pathogen recognition and inflammatory signaling in innate immune defenses.* Clin Microbiol Rev, 2009. **22**(2): p. 240-73, Table of Contents.
90. Chen, L., et al., *Inflammatory responses and inflammation-associated diseases in organs.* Oncotarget, 2018. **9**(6): p. 7204-7218.

91. Chertov, O., et al., *Leukocyte granule proteins mobilize innate host defenses and adaptive immune responses.* Immunol Rev, 2000. **177**: p. 68-78.
92. Muller, W.A., *Getting leukocytes to the site of inflammation.* Vet Pathol, 2013. **50**(1): p. 7-22.
93. Nourshargh, S. and R. Alon, *Leukocyte migration into inflamed tissues.* Immunity, 2014. **41**(5): p. 694-707.
94. Li, D. and M. Wu, *Pattern recognition receptors in health and diseases.* Signal Transduct Target Ther, 2021. **6**(1): p. 291.
95. Waisman, A., et al., *Dendritic cells as gatekeepers of tolerance.* Semin Immunopathol, 2017. **39**(2): p. 153-163.
96. Dalod, M., et al., *Dendritic cell maturation: functional specialization through signaling specificity and transcriptional programming.* EMBO J, 2014. **33**(10): p. 1104-16.
97. Steinman, R.M. and H. Hemmi, *Dendritic cells: translating innate to adaptive immunity.* Curr Top Microbiol Immunol, 2006. **311**: p. 17-58.
98. Guilliams, M., et al., *The function of Fcgamma receptors in dendritic cells and macrophages.* Nat Rev Immunol, 2014. **14**(2): p. 94-108.
99. Mahnke, K., et al., *The dendritic cell receptor for endocytosis, DEC-205, can recycle and enhance antigen presentation via major histocompatibility complex class II-positive lysosomal compartments.* J Cell Biol, 2000. **151**(3): p. 673-84.
100. Clark, G.J., et al., *The role of dendritic cells in the innate immune system.* Microbes Infect, 2000. **2**(3): p. 257-72.
101. Buckwalter, M.R. and M.L. Albert, *Orchestration of the immune response by dendritic cells.* Curr Biol, 2009. **19**(9): p. R355-61.
102. Reynes, M., et al., *Human follicular dendritic cells express CR1, CR2, and CR3 complement receptor antigens.* J Immunol, 1985. **135**(4): p. 2687-94.
103. Khan, J., et al., *Refolding and functional assembly of the Vibrio cholerae porin OmpU recombinantly expressed in the cytoplasm of Escherichia coli.* Protein Expr Purif, 2012. **85**(2): p. 204-10.
104. Vines, A., G.J. McBean, and A. Blanco-Fernandez, *A flow-cytometric method for continuous measurement of intracellular Ca(2+) concentration.* Cytometry A, 2010. **77**(11): p. 1091-7.
105. Kauffman, M.E., et al., *MitoSOX-Based Flow Cytometry for Detecting Mitochondrial ROS.* React Oxyg Species (Apex), 2016. **2**(5): p. 361-370.
106. Eruslanov, E. and S. Kusmartsev, *Identification of ROS using oxidized DCFDA and flow-cytometry.* Methods Mol Biol, 2010. **594**: p. 57-72.
107. Xie, Q., et al., *Lipopolysaccharide/adenosine triphosphate induces IL1beta and IL-18 secretion through the NLRP3 inflammasome in RAW264.7 murine macrophage cells.* Int J Mol Med, 2014. **34**(1): p. 341-9.
108. Li, X., et al., *Targeting mitochondrial reactive oxygen species as novel therapy for inflammatory diseases and cancers.* J Hematol Oncol, 2013. **6**: p. 19.
109. Ainscough, J.S., et al., *Interleukin-1beta Processing Is Dependent on a Calcium-mediated Interaction with Calmodulin.* J Biol Chem, 2015. **290**(52): p. 31151-61.
110. Cabeza-Cabrerizo, M., et al., *Dendritic Cells Revisited.* Annu Rev Immunol, 2021. **39**: p. 131-166.
111. Sichien, D., et al., *Development of conventional dendritic cells: from common bone marrow progenitors to multiple subsets in peripheral tissues.* Mucosal Immunol, 2017. **10**(4): p. 831-844.
112. Sallusto, F. and A. Lanzavecchia, *The instructive role of dendritic cells on T-cell responses.* Arthritis Res, 2002. **4 Suppl 3**: p. S127-32.
113. van Vliet, S.J., et al., *Innate signaling and regulation of Dendritic cell immunity.* Curr Opin Immunol, 2007. **19**(4): p. 435-40.
114. Pulendran, B., *Variegation of the immune response with dendritic cells and pathogen recognition receptors.* J Immunol, 2005. **174**(5): p. 2457-65.

115. O'Neill, L.A., *The role of MyD88-like adapters in Toll-like receptor signal transduction.* Biochem Soc Trans, 2003. **31**(Pt 3): p. 643-7.
116. Kawasaki, T. and T. Kawai, *Toll-like receptor signaling pathways.* Front Immunol, 2014. **5**: p. 461.
117. Yu, L., L. Wang, and S. Chen, *Endogenous toll-like receptor ligands and their biological significance.* J Cell Mol Med, 2010. **14**(11): p. 2592-603.
118. Gao, D. and W. Li, *Structures and recognition modes of toll-like receptors.* Proteins, 2017. **85**(1): p. 3-9.
119. Laird, M.H., et al., *TLR4/MyD88/PI3K interactions regulate TLR4 signaling.* J Leukoc Biol, 2009. **85**(6): p. 966-77.
120. Banerjee, A. and S. Gerondakis, *Coordinating TLR-activated signaling pathways in cells of the immune system.* Immunol Cell Biol, 2007. **85**(6): p. 420-4.
121. Lambrecht, B.N., K. Neyt, and C.H. GeurtsvanKessel, *Pulmonary defence mechanisms and inflammatory pathways in bronchiectasis.* 2011: p. 11-21.
122. Pennock, N.D., et al., *T cell responses: naive to memory and everything in between.* Adv Physiol Educ, 2013. **37**(4): p. 273-83.
123. Kyriakis, J.M. and J. Avruch, *Mammalian MAPK signal transduction pathways activated by stress and inflammation: a 10-year update.* Physiol Rev, 2012. **92**(2): p. 689-737.
124. Hawkins, P.T. and L.R. Stephens, *PI3K signalling in inflammation.* Biochim Biophys Acta, 2015. **1851**(6): p. 882-97.
125. Dan, H.C., et al., *Akt-dependent regulation of NF-{kappa}B is controlled by mTOR and Raptor in association with IKK.* Genes Dev, 2008. **22**(11): p. 1490-500.
126. Arcaro, A., et al., *Critical role for lipid raft-associated Src kinases in activation of PI3K-Akt signalling.* Cell Signal, 2007. **19**(5): p. 1081-92.
127. Brown, J., et al., *TLR-signaling networks: an integration of adaptor molecules, kinases, and cross-talk.* J Dent Res, 2011. **90**(4): p. 417-27.
128. Rameh, L.E., et al., *Phosphoinositide 3-kinase regulates phospholipase Cgamma-mediated calcium signaling.* J Biol Chem, 1998. **273**(37): p. 23750-7.
129. Loegering, D.J. and M.R. Lennartz, *Protein kinase C and toll-like receptor signaling.* Enzyme Res, 2011. **2011**: p. 537821.
130. Karin, M., *The beginning of the end: IkappaB kinase (IKK) and NF-kappaB activation.* J Biol Chem, 1999. **274**(39): p. 27339-42.
131. Skeldon, A. and M. Saleh, *The inflammasomes: molecular effectors of host resistance against bacterial, viral, parasitic, and fungal infections.* Front Microbiol, 2011. **2**: p. 15.
132. Martinon, F., K. Burns, and J. Tschopp, *The inflammasome: a molecular platform triggering activation of inflammatory caspases and processing of proIL-beta.* Mol Cell, 2002. **10**(2): p. 417-26.
133. Vande Walle, L. and M. Lamkanfi, *Snapshot of a Deadly Embrace: The Caspase-1-GSDMD Interface.* Immunity, 2020. **53**(1): p. 6-8.
134. Zheng, D., T. Liwinski, and E. Elinav, *Inflammasome activation and regulation: toward a better understanding of complex mechanisms.* Cell Discov, 2020. **6**: p. 36.
135. Kim, J.J. and E.K. Jo, *NLRP3 inflammasome and host protection against bacterial infection.* J Korean Med Sci, 2013. **28**(10): p. 1415-23.
136. Sundaram, B. and T.D. Kanneganti, *Advances in Understanding Activation and Function of the NLRC4 Inflammasome.* Int J Mol Sci, 2021. **22**(3).
137. Kelley, N., et al., *The NLRP3 Inflammasome: An Overview of Mechanisms of Activation and Regulation.* Int J Mol Sci, 2019. **20**(13).
138. Gram, A.M., et al., *Salmonella Flagellin Activates NAIP/NLRC4 and Canonical NLRP3 Inflammasomes in Human Macrophages.* J Immunol, 2021. **206**(3): p. 631-640.

139. Toma, C., et al., *Pathogenic Vibrio activate NLRP3 inflammasome via cytotoxins and TLR/nucleotide-binding oligomerization domain-mediated NF-kappa B signaling.* J Immunol, 2010. **184**(9): p. 5287-97.
140. He, Y., H. Hara, and G. Nunez, *Mechanism and Regulation of NLRP3 Inflammasome Activation.* Trends Biochem Sci, 2016. **41**(12): p. 1012-1021.
141. Kinnunen, K., et al., *Lysosomal destabilization activates the NLRP3 inflammasome in human umbilical vein endothelial cells (HUVECs).* J Cell Commun Signal, 2017. **11**(3): p. 275-279.
142. Gong, T., et al., *Orchestration of NLRP3 Inflammasome Activation by Ion Fluxes.* Trends Immunol, 2018. **39**(5): p. 393-406.
143. Munoz-Planillo, R., et al., *K(+) efflux is the common trigger of NLRP3 inflammasome activation by bacterial toxins and particulate matter.* Immunity, 2013. **38**(6): p. 1142-53.
144. Kool, M., et al., *Cutting edge: alum adjuvant stimulates inflammatory dendritic cells through activation of the NALP3 inflammasome.* J Immunol, 2008. **181**(6): p. 3755-9.
145. Duewell, P., et al., *NLRP3 inflammasomes are required for atherogenesis and activated by cholesterol crystals.* Nature, 2010. **464**(7293): p. 1357-61.
146. Liu, Y., et al., *Beta-amyloid activates NLRP3 inflammasome via TLR4 in mouse microglia.* Neurosci Lett, 2020. **736**: p. 135279.
147. McKee, C.M. and R.C. Coll, *NLRP3 inflammasome priming: A riddle wrapped in a mystery inside an enigma.* J Leukoc Biol, 2020. **108**(3): p. 937-952.
148. Garcia-Calvo, M., et al., *Inhibition of human caspases by peptide-based and macromolecular inhibitors.* J Biol Chem, 1998. **273**(49): p. 32608-13.
149. Park, S., et al., *The mitochondrial antiviral protein MAVS associates with NLRP3 and regulates its inflammasome activity.* J Immunol, 2013. **191**(8): p. 4358-66.
150. Ichinohe, T., et al., *Mitochondrial protein mitofusin 2 is required for NLRP3 inflammasome activation after RNA virus infection.* Proc Natl Acad Sci U S A, 2013. **110**(44): p. 17963-8.
151. Iyer, S.S., et al., *Mitochondrial cardiolipin is required for Nlrp3 inflammasome activation.* Immunity, 2013. **39**(2): p. 311-323.
152. Zhou, R., et al., *A role for mitochondria in NLRP3 inflammasome activation.* Nature, 2011. **469**(7329): p. 221-5.
153. Murakami, T., et al., *Critical role for calcium mobilization in activation of the NLRP3 inflammasome.* Proc Natl Acad Sci U S A, 2012. **109**(28): p. 11282-7.
154. Heid, M.E., et al., *Mitochondrial reactive oxygen species induces NLRP3-dependent lysosomal damage and inflammasome activation.* J Immunol, 2013. **191**(10): p. 5230-8.
155. Zhong, Z., et al., *TRPM2 links oxidative stress to NLRP3 inflammasome activation.* Nat Commun, 2013. **4**: p. 1611.
156. Checa, J. and J.M. Aran, *Reactive Oxygen Species: Drivers of Physiological and Pathological Processes.* J Inflamm Res, 2020. **13**: p. 1057-1073.
157. Sies, H. and D.P. Jones, *Reactive oxygen species (ROS) as pleiotropic physiological signalling agents.* Nat Rev Mol Cell Biol, 2020. **21**(7): p. 363-383.
158. Mittal, M., et al., *Reactive oxygen species in inflammation and tissue injury.* Antioxid Redox Signal, 2014. **20**(7): p. 1126-67.
159. Turpaev, K.T., *Reactive oxygen species and regulation of gene expression.* Biochemistry (Mosc), 2002. **67**(3): p. 281-92.
160. Nguyen, G.T., E.R. Green, and J. Mecsas, *Neutrophils to the ROScue: Mechanisms of NADPH Oxidase Activation and Bacterial Resistance.* Front Cell Infect Microbiol, 2017. **7**: p. 373.
161. Kotsafti, A., et al., *Reactive Oxygen Species and Antitumor Immunity-From Surveillance to Evasion.* Cancers (Basel), 2020. **12**(7).
162. Schieber, M. and N.S. Chandel, *ROS function in redox signaling and oxidative stress.* Curr Biol, 2014. **24**(10): p. R453-62.
163. Al Ghouleh, I., et al., *Oxidases and peroxidases in cardiovascular and lung disease: new concepts in reactive oxygen species signaling.* Free Radic Biol Med, 2011. **51**(7): p. 1271-88.

164. Panday, A., et al., *NADPH oxidases: an overview from structure to innate immunity-associated pathologies.* Cell Mol Immunol, 2015. **12**(1): p. 5-23.
165. Li, P. and M. Chang, *Roles of PRR-Mediated Signaling Pathways in the Regulation of Oxidative Stress and Inflammatory Diseases.* Int J Mol Sci, 2021. **22**(14).
166. Zorov, D.B., M. Juhaszova, and S.J. Sollott, *Mitochondrial reactive oxygen species (ROS) and ROS-induced ROS release.* Physiol Rev, 2014. **94**(3): p. 909-50.
167. Murphy, M.P., *How mitochondria produce reactive oxygen species.* Biochem J, 2009. **417**(1): p. 1-13.
168. Rutault, K., et al., *Reactive oxygen species activate human peripheral blood dendritic cells.* Free Radic Biol Med, 1999. **26**(1-2): p. 232-8.
169. Savina, A., et al., *NOX2 controls phagosomal pH to regulate antigen processing during crosspresentation by dendritic cells.* Cell, 2006. **126**(1): p. 205-18.
170. Paardekooper, L.M., et al., *Human Monocyte-Derived Dendritic Cells Produce Millimolar Concentrations of ROS in Phagosomes Per Second.* Front Immunol, 2019. **10**: p. 1216.
171. Cheong, T.C., et al., *Functional manipulation of dendritic cells by photoswitchable generation of intracellular reactive oxygen species.* ACS Chem Biol, 2015. **10**(3): p. 757-65.
172. Jendrysik, M.A., et al., *NADPH oxidase-2 derived ROS dictates murine DC cytokine-mediated cell fate decisions during CD4 T helper-cell commitment.* PLoS One, 2011. **6**(12): p. e28198.
173. Oberkampf, M., et al., *Mitochondrial reactive oxygen species regulate the induction of CD8(+) T cells by plasmacytoid dendritic cells.* Nat Commun, 2018. **9**(1): p. 2241.
174. Marcato, L.G., et al., *The role of Toll-like receptors 2 and 4 on reactive oxygen species and nitric oxide production by macrophage cells stimulated with root canal pathogens.* Oral Microbiol Immunol, 2008. **23**(5): p. 353-9.
175. Li, Y., et al., *Roles of Toll-Like Receptors in Nitroxidative Stress in Mammals.* Cells, 2019. **8**(6).
176. Liu, X., et al., *NADPH oxidase 1-dependent ROS is crucial for TLR4 signaling to promote tumor metastasis of non-small cell lung cancer.* Tumour Biol, 2015. **36**(3): p. 1493-502.
177. Pacquelet, S., et al., *Cross-talk between IRAK-4 and the NADPH oxidase.* Biochem J, 2007. **403**(3): p. 451-61.
178. Park, H.S., et al., *Cutting edge: direct interaction of TLR4 with NAD(P)H oxidase 4 isozyme is essential for lipopolysaccharide-induced production of reactive oxygen species and activation of NF-kappa B.* J Immunol, 2004. **173**(6): p. 3589-93.
179. Lugrin, J., et al., *The role of oxidative stress during inflammatory processes.* Biol Chem, 2014. **395**(2): p. 203-30.
180. Yang, M. and R.L. Silverstein, *CD36 signaling in vascular redox stress.* Free Radic Biol Med, 2019. **136**: p. 159-171.
181. Seimon, T.A., et al., *Atherogenic lipids and lipoproteins trigger CD36-TLR2-dependent apoptosis in macrophages undergoing endoplasmic reticulum stress.* Cell Metab, 2010. **12**(5): p. 467-82.
182. Khan, M.A., et al., *JNK Activation Turns on LPS- and Gram-Negative Bacteria-Induced NADPH Oxidase-Dependent Suicidal NETosis.* Sci Rep, 2017. **7**(1): p. 3409.
183. Schenten, V., et al., *Sphingosine kinases regulate NOX2 activity via p38 MAPK-dependent translocation of S100A8/A9.* J Leukoc Biol, 2011. **89**(4): p. 587-96.
184. Hemmi, H. and S. Akira, *TLR signalling and the function of dendritic cells.* Chem Immunol Allergy, 2005. **86**: p. 120-135.
185. Krishnaswamy, J.K., T. Chu, and S.C. Eisenbarth, *Beyond pattern recognition: NOD-like receptors in dendritic cells.* Trends Immunol, 2013. **34**(5): p. 224-33.
186. Figdor, C.G., Y. van Kooyk, and G.J. Adema, *C-type lectin receptors on dendritic cells and Langerhans cells.* Nat Rev Immunol, 2002. **2**(2): p. 77-84.
187. Geijtenbeek, T.B., et al., *Identification of DC-SIGN, a novel dendritic cell-specific ICAM-3 receptor that supports primary immune responses.* Cell, 2000. **100**(5): p. 575-85.

188. Wang, D., et al., *Role of scavenger receptors in dendritic cell function.* Hum Immunol, 2015. **76**(6): p. 442-6.
189. Jin, J.O., et al., *Ligand of scavenger receptor class A indirectly induces maturation of human blood dendritic cells via production of tumor necrosis factor-alpha.* Blood, 2009. **113**(23): p. 5839-47.
190. Canton, J., D. Neculai, and S. Grinstein, *Scavenger receptors in homeostasis and immunity.* Nat Rev Immunol, 2013. **13**(9): p. 621-34.
191. Beauvillain, C., et al., *The scavenger receptors SRA-1 and SREC-I cooperate with TLR2 in the recognition of the hepatitis C virus non-structural protein 3 by dendritic cells.* J Hepatol, 2010. **52**(5): p. 644-51.
192. Massari, P., et al., *Cutting edge: Immune stimulation by neisserial porins is toll-like receptor 2 and MyD88 dependent.* J Immunol, 2002. **168**(4): p. 1533-7.
193. Elena, G., et al., *Proinflammatory signal transduction pathway induced by Shigella flexneri porins in caco-2 cells.* Braz J Microbiol, 2009. **40**(3): p. 701-13.
194. Yu, Q., et al., *The role of the p38 mitogen-activated protein kinase, extracellular signal-regulated kinase, and phosphoinositide-3-OH kinase signal transduction pathways in CD40 ligand-induced dendritic cell activation and expansion of virus-specific CD8+ T cell memory responses.* J Immunol, 2004. **172**(10): p. 6047-56.
195. Guindi, C., et al., *Role of the p38 MAPK/C/EBPbeta Pathway in the Regulation of Phenotype and IL-10 and IL-12 Production by Tolerogenic Bone Marrow-Derived Dendritic Cells.* Cells, 2018. **7**(12).
196. Aksoy, E., L. Saveanu, and B. Manoury, *The Isoform Selective Roles of PI3Ks in Dendritic Cell Biology and Function.* Front Immunol, 2018. **9**: p. 2574.
197. Cejas, P.J., et al., *Protein kinase C betaII plays an essential role in dendritic cell differentiation and autoregulates its own expression.* J Biol Chem, 2005. **280**(31): p. 28412-23.
198. Langlet, C., et al., *PKC-alpha controls MYD88-dependent TLR/IL-1R signaling and cytokine production in mouse and human dendritic cells.* Eur J Immunol, 2010. **40**(2): p. 505-15.
199. Hatscher, L., et al., *Inflammasomes in dendritic cells: Friend or foe?* Immunol Lett, 2021. **234**: p. 16-32.
200. Hatscher, L., et al., *Select hyperactivating NLRP3 ligands enhance the TH1- and TH17-inducing potential of human type 2 conventional dendritic cells.* Sci Signal, 2021. **14**(680).
201. Ferreira, I., et al., *Inflammasome in Dendritic Cells Immunobiology: Implications to Diseases and Therapeutic Strategies.* Curr Drug Targets, 2017. **18**(9): p. 1003-1018.
202. Elliott, E.I., et al., *Cutting Edge: Mitochondrial Assembly of the NLRP3 Inflammasome Complex Is Initiated at Priming.* J Immunol, 2018. **200**(9): p. 3047-3052.
203. Massari, P., Y. Ho, and L.M. Wetzler, *Neisseria meningitidis porin PorB interacts with mitochondria and protects cells from apoptosis.* Proc Natl Acad Sci U S A, 2000. **97**(16): p. 9070-5.
204. Kaur, D., et al., *Pore formation-independent cell death induced by a beta-barrel pore-forming toxin.* FASEB J, 2022. **36**(10): p. e22557.
205. Hafner-Bratkovic, I. and P. Pelegrin, *Ion homeostasis and ion channels in NLRP3 inflammasome activation and regulation.* Curr Opin Immunol, 2018. **52**: p. 8-17.
206. Bode, K., et al., *Dectin-1 Binding to Annexins on Apoptotic Cells Induces Peripheral Immune Tolerance via NADPH Oxidase-2.* Cell Rep, 2019. **29**(13): p. 4435-4446 e9.
207. Singh, A., et al., *Correction to: The IRAK-ERK-p67phox-Nox-2 axis mediates TLR4, 2-induced ROS production for IL-1beta transcription and processing in monocytes.* Cell Mol Immunol, 2019. **16**(12): p. 946.
208. Triantafilou, M., et al., *Lipopolysaccharides from atherosclerosis-associated bacteria antagonize TLR4, induce formation of TLR2/1/CD36 complexes in lipid rafts and trigger TLR2-induced inflammatory responses in human vascular endothelial cells.* Cell Microbiol, 2007. **9**(8): p. 2030-9.

# VI. Synopsis

# Synopsis

## Study of modulation of immune function of dendritic cells by *Vibrio cholerae* outer membrane protein OmpU

**Vinica Dhar (PH14046)**

The innate immune cells such as macrophages, monocytes, neutrophils, etc. recognise pathogens through their innate receptors and activate signalling cascades to secrete pro-inflammatory mediators. The pro-inflammatory mediators, such as cytokines, chemokines, reactive oxygen species etc. function to eliminate the pathogen and/or further induce the activation of other immune cells. Antigen recognition through the innate receptors also activates pro-inflammatory pathways in dendritic cells (DCs) and enables them to mature and present the antigen to T-cells priming the adaptive immune responses. Thus, DCs serve as a crucial link between the innate and adaptive immune system [1].

The immune cells recognise various patterns on the pathogen called as pathogen-associated molecular patterns (PAMPs) by employing specific conserved receptors on them termed as pattern recognition receptors (PRRs). DCs possess numerous PRRs such as TLRs, NLRs, Dectin 1 & 2, DC-SIGN etc., which aid in the recognition of PAMPs and mediate the activation of signalling pathways leading to the production of pro-inflammatory mediators [2]. TLR signalling has been widely studied for the induction of signalling cascades leading to the expression and activation of transcription factors such as NFκB and AP-1 involved in inflammatory pathways.

Several bacteria or bacterial PAMPs activate the immune cells and induce inflammatory pathways. *Vibrio cholerae* is a Gram-negative human pathogen which infects the small intestine and causes the diarrhoeal disease cholera. *Vibrio cholerae* harbours several virulence factors, including toxins, adhesins, pili and outer membrane proteins, which aid in the pathogenesis of bacteria. OmpU is one of the major porins present in the outer membrane of *Vibrio cholerae.* The expression of OmpU is regulated by the ToxR regulon, which also controls the expression of other virulence factors of *Vibrio cholerae* [3]. OmpU imparts resistance against bile salts and certain antimicrobial peptides, and its expression is highly increased in the presence of bile secretions [4, 5].

In our lab, we have established that OmpU activates the innate immune cells, such as monocytes and macrophages, employing TLR1/2, leading to the production of pro-

inflammatory cytokines such as IL-6 and TNFα [6, 7]. Further, we have shown that OmpU triggers NOX-mediated ROS production in macrophages via activation of scavenger receptor CD36 [8]. In the current study, we explored whether and how DCs are activated in response to OmpU.

Towards that, we aimed to understand the following:

**AIM 1:** To probe whether and how OmpU induces the activation of DCs.

**AIM 2:** To explore whether inflammasome complex is involved in OmpU-mediated DC activation.

**AIM 3:** To investigate whether there is any role of ROS in OmpU-mediated DC activation.

**AIM 1: To probe whether and how OmpU induces the activation of DCs.**

We observed that OmpU stimulates DCs leading to the production of pro-inflammatory cytokines IL-6, TNFα and IL-1β and also induces the upregulation of maturation markers CD80 and CD86, and MHC II. Furthermore, we have investigated which PRR is involved in OmpU-mediated DC activation and the downstream signalling induced in response to OmpU. Towards this, we observed the following:

***OmpU induces DC activation via TLR2 and MyD88***

To explore whether MyD88 plays any role in DC activation, we used BMDCs from MyD88$^{-/-}$ background. We observed that the pro-inflammatory cytokine production was abrogated in BMDCs from MyD88$^{-/-}$ transgenic mice indicating the involvement of TLR in OmpU-mediated signalling as MyD88 works downstream to TLR signalling. Further, using neutralising antibodies, we observed that among the surface TLRs, TLR2 is probably involved in OmpU-induced cytokine production in DCs. We validated the involvement of TLR2 in OmpU-mediated DC activation using BMDCs from TLR2$^{-/-}$ transgenic mice. Moreover, we have also confirmed the role of TLR2 in DC activation *in vivo* by administering OmpU in wildtype and TLR2$^{-/-}$ transgenic mice. Therefore, our data shows that similar to monocytes and macrophages, OmpU also induces DC activation via TLR2.

Further, we wanted to check the downstream signalling pathway of OmpU-mediated DC activation.

***OmpU-mediated DC activation involves activation of IKK and NFκB***

TLR signalling is known to activate various signalling mediators culminating in the activation of transcription factors such as NFκB and AP-1, which are involved in pro-inflammatory cytokine production. Therefore, we wanted to check the involvement of NFκB in OmpU-mediated activation of DCs. In the steady state, NFκB remains inactivated in the cytoplasm by inhibitor IκB protein which is degraded by the IκB kinase (IKK) upon stimulation leading to translocation of free NFκB subunit into the nucleus. We first probed whether IKK is involved in OmpU-mediated signalling using IKK inhibitor. We observed a significant decrease in OmpU-induced cytokine responses in the presence of the IKK inhibitor. Further, we observed a significant decrease in the levels of IκB protein in OmpU-activated DCs. All these data suggest that NFkB is involved in OmpU-mediated pro-inflammatory responses in DCs.

***MAP kinases (p38, JNK and ERK) are involved in OmpU-mediated activation of DCs***

Apart from IKK activation, TLR signalling could also activate the mitogen-activated protein kinase (MAPK) pathway, which has been known to play a role in inflammatory signalling cascades and lead to the activation of NFκB and AP-1 transcription factors. MAPK pathway is multi-tiered and includes MAP3K, MAP2K and MAPKs. Among the MAPKs, p38, JNK and ERK are implicated in pro-inflammatory responses. Therefore, we probed whether p38, JNK and ERK were involved in OmpU-mediated pro-inflammatory signalling in DCs. We observed increased levels of phosphorylated p38, JNK and ERK in OmpU-treated DCs, suggesting the activation of these MAPKs. Further, we obtained a significant decrease in cytokine production in the presence of p38, JNK and ERK inhibitors indicating their involvement in OmpU-mediated pro-inflammatory responses in DCs.

***Phosphoinositide-3-kinases* (*PI3K) and AKT are involved in the OmpU-mediated activation of DCs***

In addition to the MAPKs, other kinases such as phosphoinositide-3-kinases (PI3Ks) could also be activated downstream of TLRs and induce the transcription of genes involved in pro-inflammatory responses [9]. We observed an increased level of phosphorylated-PI3K (p-PI3K) in OmpU-treated DCs, indicating the activation of PI3K. Further, we probed whether PI3K activation plays any role in OmpU-induced pro-inflammatory cytokine production and observed diminished levels of IL-6 in the presence of PI3K inhibitor LY294002. PI3K is

comprised of three classes: Class I, Class II and Class III. To assess the specific PI3K class involved in OmpU-induced DC signalling, we used PI3K class I/II inhibitor, GDC-0941 and PI3K class III inhibitor, SAR405 and observed that PI3K class I/II plays a role in OmpU-mediated cytokine production but not PI3K class III.

It is known that PI3K signalling results in the phosphorylation and activation of AKT via PDK1. We observed increased phosphorylation levels of AKT in response to OmpU in DCs. Further, we observed a decrease in IL-6 production in the presence of AKT inhibitor.

***Protein kinase C (PKC) are involved in DC activation by OmpU***

PI3K signalling is known to activate PKC, which could mediate the inflammatory pathways in response to PAMPs. We observed increased phosphorylation levels of PKC in OmpU-treated DCs. Further, we observed a significant decrease in pro-inflammatory cytokine levels in the presence of PKC inhibitor. Inhibitor studies indicated the involvement of PKCα/γ in OmpU-mediated IL-6 cytokine production.

Generally, the calcium flux, along with PI3K signalling, is known to activate PKC. Therefore, along with PKC activation, we also checked whether OmpU induces calcium flux in DCs and observed an increased calcium influx in OmpU-treated BMDCs.

**AIM 2: To explore whether inflammasome complex is involved in OmpU-mediated DC activation.**

As we have observed that OmpU induces the release of IL-1β pro-inflammatory cytokine from DCs, we wanted to check the involvement of inflammasome. IL-1β is produced as pro-IL-1β, and it needs the activation of caspase-1 via the multi-subunit inflammasome complex for the maturation of IL-1β.

***Inflammasome complex is activated in DCs in response to OmpU***

Inflammasome complex induces the activation of caspase-1, which further leads to the proteolytic activation of IL-1β. A typical inflammasome assembly is made up of a sensor NLR, an adaptor protein (ASC) and pro-caspase-1. Therefore, to probe whether inflammasome is involved in OmpU-mediated IL-1β release, we first checked whether caspase-1 is activated in response to OmpU. For this, we used the caspase-1 inhibitor, Ac-YVAD-fmk and observed a significant decrease in IL-1β production in OmpU-treated DCs in the presence of inhibitor.

Further, we have checked the caspase-1 levels by western blotting and detected an increased level of active caspase-1 in OmpU-treated DCs.

***NLRP3 inflammasome is involved in IL-1β maturation in OmpU-activated DCs***

As there are different inflammasomes, we wanted to discern which inflammasome complex is involved in OmpU-activated DCs. In case of bacterial infection, majorly NLRP3 and NLRC4 are involved, and various signalling can cause NLRP3 activation; we first probed for the involvement of NLRP3 inflammasome. NLRP3 inflammasome activation in the cell requires two levels of stimulation; one is the transcriptional upregulation of components of the inflammasome complex induced by TLR signalling, and the second signal involves cleavage of pro-caspase-1 to active caspase-1. We observed an increase in the level of NLPR3 in the cell following OmpU stimulation. Further, we observed that NLRP3 is recruited to mitochondria following OmpU treatment, indicating its activation. Finally, we confirmed the involvement of NLRP3 inflammasome in OmpU-activated DCs by using $NLRP3^{-/-}$ transgenic mice.

***Mitochondrial ROS and calcium are involved in OmpU-mediated activation of NLRP3 inflammasome activation in DCs***

Generally, host-derived signals such as ion imbalances, including potassium efflux and calcium influx, loss of mitochondrial membrane potential (MMP), mitochondrial ROS, and lysosomal rupture, cause NLRP3 activation. Toward understanding how OmpU induces NLRP3 activation in DCs, we first explored the role of potassium efflux from the DCs. We added potassium chloride in the extracellular medium, which inhibits potassium efflux from the cells. We observed that IL-1β production was unaffected by inhibition of potassium efflux, suggesting it is not the cause.

Further, we probed whether calcium influx upon OmpU stimulation in DCs plays any role in NLRP3 activation, and we observed that in the presence of calcium chelator BAPTA-AM, the OmpU-induced IL-1β production was inhibited.

Over the years, mitochondria have evolved as a crucial platform for the assembly of NLRP3 inflammasome, and it has been shown that mitochondrial ROS (mitoROS) can trigger the NLRP3 inflammasome activation. We, therefore, checked whether mitoROS generation was involved in NLRP3 activation in DCs by OmpU. Towards this, we first checked if mitoROS is produced in OmpU-stimulated DCs using MitoSOX dye. We observed the production of mitoROS in OmpU-activated DCs, and by employing the mitoROS scavenger (MitoTEMPO),

we observed a decrease in IL-1β production, suggesting its involvement in NLRP3 activation in OmpU-activated DCs.

***Both calcium signalling and translocation of OmpU to the host-cell mitochondria induce the generation of mitoROS in OmpU-activated DCs***

Our study so far has led to the question what signal could be involved in mitoROS generation following OmpU stimulation in DCs. Earlier studies by Gupta et al. from our lab have shown that *V. cholerae* OmpU translocates to the host cell mitochondria (monocytes and epithelial cells) and induces caspase-independent programmed cell death [10]. Also, a previous report from our lab suggests that OmpU translocation to mitochondria triggers mitoROS generation in macrophages [8]. Based on these observations, we probed whether OmpU translocation to mitochondria of DCs is involved in triggering mitoROS. For this, we first checked whether OmpU is translocated to the mitochondria of DCs and observed that OmpU is present in the enriched mitochondrial fractions isolated from OmpU-treated DCs. Further, using cytochalasin D, we observed an inhibition of OmpU translocation to mitochondria and consequent attenuation of mitoROS generation in DCs.

Further, by chelating the calcium flux using BAPTA-AM, we observed a decrease in mitoROS generation, suggesting that OmpU-induced calcium influx also contributes to mitoROS production in DCs.

Thus, we concluded that both OmpU translocation to mitochondria and OmpU-induced calcium influx are involved in mitoROS generation in DCs.

**AIM 3: To investigate whether there is any role of ROS in OmpU-mediated DC activation.**

ROS has been widely studied as an inflammatory mediator and secondary messenger involved in the activation of pro-inflammatory responses. A previous study from our lab has shown that OmpU induces NOX2-mediated ROS in macrophages. Therefore, we probed whether OmpU induces ROS in DCs and the signalling involved in ROS generation in OmpU-activated DCs.

***OmpU induces NADPH oxidase (NOX2)-mediated ROS generation in DCs***

To determine whether OmpU-stimulated DCs can produce cytoplasmic ROS, we treated BMDCs with OmpU for various time points and assessed for ROS production. Using dichlorofluorescein diacetate (DCFDA), a cell-permeable ROS indicator, we observed that

OmpU triggers ROS generation in DCs. Further, we observed that in the presence of total ROS scavenger, N-acetylcysteine (NAC), there was inhibition of the OmpU-induced ROS production.

Next, we explored the source of OmpU-mediated ROS generation in DCs. Apart from mitoROS, NOX2 is one of the major sources of ROS generation in cells. As we have already explored the role of mitoROS generation in OmpU-treated DCs, we further investigated the role of NOX2-mediated ROS in response to OmpU. We detected that OmpU-induced ROS production was scavenged using NOX inhibitor, diphenylene iodonium (DPI), indicating that NOX2 might be involved in ROS generation in DCs. NOX2 is a multi-subunit complex consisting of gp91 and p22 on the cell membrane and cytoplasmic subunits p47, p67 and rac. Upon PAMP stimulation, the cytoplasmic subunits could be recruited to the membrane NOX complex leading to ROS generation. Therefore, to confirm the involvement of NOX2 in OmpU-mediated ROS generation, we checked for the translocation of cytoplasmic subunit p47 to the cell membrane following OmpU stimulation. We observed co-localisation of p47 with the plasma membrane marker $Na^+$-$K^+$ ATPase upon OmpU treatment, confirming the role of NOX2 complex in ROS production in DCs.

***Cytoplasmic ROS contributes to OmpU-mediated DC activation***

ROS has been known to contribute to the activation of inflammatory pathways leading to the production of pro-inflammatory cytokines. Therefore, we assessed whether OmpU-induced ROS was involved in cytokine production in DCs. We examined the levels of IL-6 in the presence of NAC as well as DPI in the OmpU-treated DCs and observed attenuation of IL-6 production. These results suggest the involvement of ROS in OmpU-mediated pro-inflammatory signalling.

***TLR2 is involved in OmpU-mediated NOX2 activation and cytoplasmic ROS generation in DCs***

It has been shown that different PRRs can induce the signal for assembly and activation of NOX2 in response to PAMPs. TLRs have been known to be involved in the activation of NOX2 in case of several bacterial ligands. As we have described previously that OmpU mediates the pro-inflammatory cytokine production via TLR2 in DCs; therefore, we checked if TLR2 was involved in OmpU-mediated ROS production. For this, we assessed the ROS generation in BMDCs from $TLR2^{-/-}$ transgenic mice and detected that ROS generation was negligible upon OmpU treatment in $TLR2^{-/-}$ BMDCs. Further, we observed that the recruitment of p47 to the

plasma membrane was inhibited in case of TLR2$^{-/-}$ transgenic mice confirming the role of TLR2 in NOX2 activation in DCs.

***In addition to TLR2, CD36 is also involved in OmpU-mediated NOX2 activation and cytoplasmic ROS generation in DCs***

Several studies suggest that scavenger receptor CD36 can also activate NOX2 complex. Also, a previous study from our lab by Prasad et al. reported the involvement of CD36 in OmpU-mediated ROS in macrophages [8]. Therefore, we explored whether CD36 also plays a role in ROS generation in DCs by OmpU. For this, we first checked whether OmpU interacts with CD36 in DCs. We observed that OmpU co-immunoprecipitated with CD36 in OmpU-treated DCs. Further, to check the involvement of CD36 in OmpU-mediated ROS generation, we determined the ROS production in BMDCs from CD36$^{-/-}$ transgenic mice upon OmpU treatment and observed that ROS levels were attenuated in absence of CD36. To confirm the role of CD36 in NOX2 activation in DCs, we checked the co-localisation of p47 with plasma membrane marker $Na^{+}$-$K^{+}$ ATPase in BMDCs from CD36$^{-/-}$ transgenic mice and observed considerably less co-localisation compared to the BMDCs from wildtype mice.

***JNK MAPK is involved in OmpU-mediated ROS generation***

The activation of PRRs upon PAMP recognition is known to induce downstream signalling, which could result in the activation of NOX2 complex and ROS generation. Therefore, we explored the signalling molecules that could contribute to ROS generation in DCs. A previous report from our lab has shown the involvement of src kinases downstream to CD36 for ROS production in macrophages [8]. As we observed that CD36 mediates the OmpU-induced ROS generation in DCs, we checked whether src kinases were involved in OmpU-mediated ROS generation. However, we observed that the ROS levels were unaffected in the presence of src kinase inhibitor.

Further, in literature, it has been shown that MAPKs can induce the activation of NOX2 complex. As we have observed the activation of MAPKs in OmpU-stimulated DCs, we, therefore, assessed whether MAPKs p38, JNK and ERK play any role in ROS generation in OmpU-treated DCs. Employing different pharmacological inhibitors, we observed that JNK could be involved in OmpU-induced ROS production but not p38 and ERK.

## Conclusion

In this study, we have established that *V. cholerae* OmpU activates DCs via MyD88-TLR2 dependent pathway. We further observed that the activation of TLR2 pathway leads to activation of MAPKs p38, JNK and ERK, culminating in the activation of NFκB transcription factor. We also observed that OmpU-mediated signalling in DCs involved PI3K-AKT pathway and induced PKC activation. Further, we demonstrated that OmpU induces NLRP3 inflammasome activation in DCs, which leads to the activation of caspase-1 and, consequently, the maturation and release of IL-1β from the cells.

We also explored the signalling mechanisms involved in NLRP3 assembly and activation. Our results established that mitochondria play a central role in OmpU-induced NLRP3 inflammasome activation. We showed that OmpU induces mitoROS production in DCs, which triggers the NLRP3 activation. Further, we elucidated that OmpU translocation to mitochondria of DCs and OmpU-induced calcium influx in DCs contribute to the mitoROS production in DCs, leading to NLRP3 activation.

Furthermore, we demonstrated that OmpU also triggers NOX2-mediated ROS in DCs. From our observations, we concluded that both TLR2 and CD36 are indispensable for ROS generation in DCs. We further elucidated that MAPK JNK is probably involved in OmpU-induced ROS generation but not p38 and ERK.

Altogether our study highlights the role of *V. cholerae* OmpU as a PAMP in DCs activating multiple PRRs, which can contribute to the inflammatory responses. We have also elaborated on the mechanism by which bacterial porins can activate the NLRP3 inflammasome in case of infection.

## References


1. Banchereau, J., et al., *Immunobiology of dendritic cells.* Annu Rev Immunol, 2000. **18**: p. 767-811.
2. Dalod, M., et al., *Dendritic cell maturation: functional specialization through signaling specificity and transcriptional programming.* EMBO J, 2014. **33**(10): p. 1104-16.
3. Provenzano, D., C.M. Lauriano, and K.E. Klose, *Characterization of the role of the ToxR-modulated outer membrane porins OmpU and OmpT in Vibrio cholerae virulence.* J Bacteriol, 2001. **183**(12): p. 3652-62.
4. Wibbenmeyer, J.A., et al., *Vibrio cholerae OmpU and OmpT porins are differentially affected by bile.* Infect Immun, 2002. **70**(1): p. 121-6.

5. Mathur, J. and M.K. Waldor, *The Vibrio cholerae ToxR-regulated porin OmpU confers resistance to antimicrobial peptides.* Infect Immun, 2004. **72**(6): p. 3577-83.
6. Sakharwade, S.C., P.K. Sharma, and A. Mukhopadhaya, *Vibrio cholerae porin OmpU induces pro-inflammatory responses, but down-regulates LPS-mediated effects in RAW 264.7, THP-1 and human PBMCs.* PLoS One, 2013. **8**(9): p. e76583.
7. Khan, J., P.K. Sharma, and A. Mukhopadhaya, *Vibrio cholerae porin OmpU mediates M1-polarization of macrophages/monocytes via TLR1/TLR2 activation.* Immunobiology, 2015. **220**(11): p. 1199-209.
8. Prasad, G., V. Dhar, and A. Mukhopadhaya, *Vibrio cholerae OmpU Mediates CD36-Dependent Reactive Oxygen Species Generation Triggering an Additional Pathway of MAPK Activation in Macrophages.* J Immunol, 2019. **202**(8): p. 2431-2450.
9. Lee, I.T., et al., *Cooperation of TLR2 with MyD88, PI3K, and Rac1 in lipoteichoic acid-induced cPLA2/COX-2-dependent airway inflammatory responses.* Am J Pathol, 2010. **176**(4): p. 1671-84.
10. Gupta, S., G.V. Prasad, and A. Mukhopadhaya, *Vibrio cholerae Porin OmpU Induces Caspase-independent Programmed Cell Death upon Translocation to the Host Cell Mitochondria.* J Biol Chem, 2015. **290**(52): p. 31051-68.

**Publications:**

- **Dhar V**; Gandhi S; Sakharwade SC; Chawla A; Mukhopadhaya A; *Vibrio cholerae* OmpU activates dendritic cells via TLR2 and NLRP3 inflammasome; ***Infection and Immunity*** *(2023)*, *e00332-22*, *DOI: 10.1128/iai.00332-22*
- Prasad GVRK, **Dhar V**, Mukhopadhaya A. *Vibrio cholerae* OmpU Mediates CD36-Dependent Reactive Oxygen Species Generation Triggering an Additional Pathway of MAPK Activation in Macrophages. **J Immunol**. 2019 Apr 15;202(8):2431-2450. doi: 10.4049/jimmunol.1800389. Epub 2019 Mar 13. PMID: 30867241.
- Kundu N, Verma P, Kumar A, **Dhar V**, Dutta S, Chattopadhyay K. N-Terminal Region of *Vibrio parahemolyticus* Thermostable Direct Hemolysin Regulates the Membrane-Damaging Action of the Toxin. **Biochemistry**. 2020 Feb 4;59(4):605-614. doi: 10.1021/acs.biochem.9b00937. Epub 2019 Dec 20. PMID: 31808340.